Advances in Mechanical Engineering

Natural Fiber Composites

Guest Editors: Hiroyuki Hamada, Johanne Denault,
Amar K. Mohanty, Yan Li, and Mohamed S. Aly-Hassan

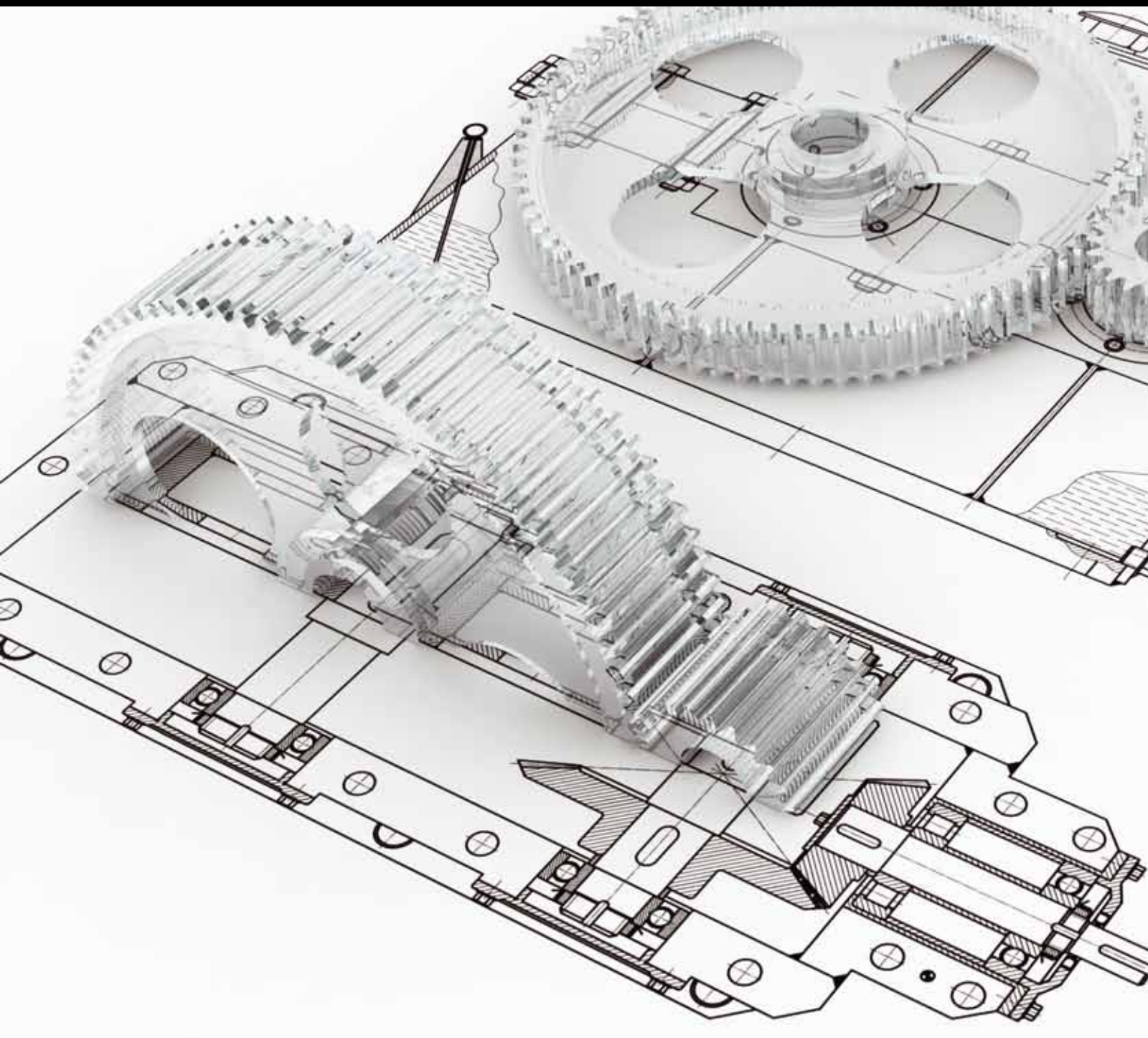

Natural Fiber Composites

Advances in Mechanical Engineering

Natural Fiber Composites

Guest Editors: Hiroyuki Hamada, Johanne Denault, Amar K. Mohanty, Yan Li, and Mohamed S. Aly-Hassan

Editorial Board

Contents

Hindawi Publishing Corporation
Advances in Mechanical Engineering
Volume 2013, Article ID 569020, 2 pages
http://dx.doi.org/10.1155/2013/569020

Editorial
Natural Fiber Composites

Hiroyuki Hamada,[1] Johanne Denault,[2] Amar K. Mohanty,[3] Yan Li,[4] and Mohamed S. Aly-Hassan[1]

[1] *Department of Advanced Fibro-Science, Kyoto Institute of Technology, Matsugasaki, Sakyo-Ku, Kyoto 606-8585, Japan*
[2] *Industrial Materials Institute, National Research Council of Canada, 75 de Mortagne Boulevard Boucherville, QC, Canada J4B 6Y4*
[3] *Department of Plant Agriculture, University of Guelph, 50 Stone Road. E., Guelph, ON, Canada N1G 2W1*
[4] *School of Aerospace Engineering and Applied Mechanics, Tongji University, 1239 Siping Road, Shanghai, China*

Correspondence should be addressed to Hiroyuki Hamada; hhamada@kit.ac.jp

Received 30 April 2013; Accepted 30 April 2013

Recently, the preservation of natural resources and the strict environmental regulations have forced the composite industry to find alternative fiber reinforcements and resin systems that are ecofriendly to produce compatible composites. Therefore, the need for natural fiber-reinforced composites has never been as prevalent as it currently is. Natural fibers offer renewability, biodegradability, abundance, cost savings, and low specific gravity when compared to synthetic fibers such as glass and carbon. Though the strength of natural fibers is not as great as glass or carbon, the specific properties are comparable. Currently natural fiber composites have two main issues that need to be addressed: resin compatibility and water absorption. Thus, natural fiber composites are the main subject in this special issue. The authors have focused on the following topics.

In the paper entitled "*Injection moulded biocomposites from oat hull and polypropylene/polylactide blend: fabrication and performance evaluation*" by J. P. Reddy et al., oat hull fibre reinforced polypropylene (PP)/polylactide (PLA) based biocomposites were fabricated; their process engineering and performances were evaluated. The effect of ethylene propylene-g-maleic anhydride (EP-g-Ma) compatibilizer on mechanical properties of 30 wt% oat hull reinforced PP/PLA (90/10) blend composites was investigated. Thermal degradation parameters of the oat hull fibre were determined using thermogravimetric analysis. The effect of fibre reinforcement on crystallinity of oat hull fibre reinforced PP/PLA composites was studied by differential scanning calorimetry (DSC). Thermomechanical properties of the composites were analyzed by dynamic mechanical analyzer (DMA). The interfacial bonding between the fibre and the matrix was examined using scanning electron microscope (SEM). Significant improvement in tensile strength (40%) and flexural strength (46%) was observed with the addition of EP-g-Ma compatibilizer. DSC analysis of oat hull fibre reinforced composites showed an increase in the crystallization temperature (Tc) due to the nucleation effect of oat hull fibre. DMA results revealed that the storage modulus of PP/PLA/oat hull fibre composites was higher compared to PP/PLA blend throughout the investigated range of temperature.

In the paper entitled "*Studies of moisture absorption and release behaviour of akund fiber*" by X. Yang et al., an effort has been made to study the moisture absorption and release behaviour of akund fiber and its mechanical performance at relative air humidity ranging from 0% to 100%. The gain and loss in moisture content in akund fiber due to water absorption and release were measured as a function of exposure time under the environment, in which temperature is 20°C and humidity is 65%. The regression equations of the absorption and release process were established. From the study, it was found that the water absorption curve of akund is similar with those of cotton and kapok, and its water absorption ability is better than those of cotton and kapok. According to the regression analysis and comparison with

cotton and kapok, the initial water absorption rate of akund fiber is a little lower, its balance moisture regain is bigger, and moisture releasing rate is faster. This feature shows that the akund fiber has less absorption moisture which is absorbed by hydroxyl directly and contains more indirectly absorbed moisture. This phenomenon may be decided by its chemical content, which has less cellulose content, and its big hollow structure.

In the paper entitled "*The processing design of jute spun yarn/PLA braided composite by pultrusion molding*" by A. Memon and A. Nakai, the fabrication of tubular jute spun yarn/PLA braided composite by pultrusion molding was presented. The intermediate materials were prepared by comingled technique. The braiding technique manufactured preform which had jute fiber diagonally oriented at certain angles with the glass fiber inserted into the braiding yarns along the longitudinal direction. The braided preformances were pulled through a heated die where the consolidation flow took place due to reduced matrix viscosity and pressure. The pultrusion experiments were done with jute/PLA comingled yarns and combined with glass fiber yarns to fabricate the tubular composite. Impregnation quality was evaluated by microscope observation of the pultruded cross-sections. The flexural mechanical properties of the pultruded were measured by four-point bending test.

The paper entitled "*Developing simple production of continuous ramie single yarn reinforced composite strands*" by H.-B. Kim et al. deals with long fiber-reinforced composite strands using continuous ramie yarns, in which polypropylene including Maleic anhydride grafted polypropylene (MA-PP) was used as a matrix material. The composite strands were fabricated by a new method called multipin-assisted resin impregnation (M-PaRI) process, for which the equipment was newly applied after conventional extrusion process. The composite strands were then pelletized and injection molded. Tensile strength and Young's modulus of the resultant short ramie/PP reinforced composites were investigated. Results show that this new process improved the mechanical properties of injection-molded specimens.

In the paper entitled "*Continuous natural fiber reinforced thermoplastic composites by fiber surface modification*" by P. Wongsriraksa et al., an intermediate material, which allows highly impregnation during molding, has been investigated for fabricating continuous fiber-reinforced thermoplastic composite by aligning resin fiber alongside reinforcing fiber with braiding technique. This intermediate material has been called "microbraid yarn (MBY)." Moreover, it is well known that the interfacial properties between natural fiber and resin are low; therefore, surface treatment on continuous natural fiber was performed by using polyurethane (PU) and flexible epoxy (FLEX) to improve the interfacial properties. The effect of surface treatment on the mechanical properties of continuous natural fiber-reinforced thermoplastic composites was examined. From these results, it was suggested that surface treatment by PU with low content could produce composites with better mechanical properties.

In the paper entitled "*Effect of red mud and copper slag particles on physical and mechanical properties of bamboo fiber reinforced epoxy composites*" by S. Biswas et al., series of bamboo-fiber-reinforced epoxy composites are fabricated by using red mud and copper slag particles as filler materials. Filler plays an important role in determining the properties and behavior of particulate composites. The effects of these two fillers on the mechanical properties of bamboo-epoxy composites are investigated. Comparative analysis shows that with the incorporation of these fillers, the tensile strength of the composites increases significantly, whereas the flexural strength and impact strength decrease with increase in filler content (red mud and copper slag fillers) in the epoxy-bamboo fiber composites. The density and hardness are also affected by the type and content of filler particles. It is found that the addition of copper slag filler improves the hardness of the bamboo-epoxy composites, whereas the addition of red mud filler reduces the hardness value of bamboo-epoxy composites. The study reveals that the addition of copper slag filler in bamboo-epoxy composites shows the better physical and mechanical properties as compared to the red mud filled composites.

In the paper entitled "*Mechanical, thermal degradation, and flammability studies on surface modified sisal fiber reinforced recycled polypropylene composites*" by A. K. Gupta et al., the effect of surface treatment of fiber on the mechanical, thermal, flammability, and morphological properties of sisal fiber (SF) reinforced recycled polypropylene (RPP) composites was investigated. The surface of sisal fiber was modified with different chemical processes such as silane, glycidyl methacrylate (GMA), and O-hydroxybenzene diazonium chloride (OBDC) to improve the compatibility with the matrix polymer. The experimental results revealed an improvement in the tensile strength to 11%, 20%, and 31.36% and impact strength to 78.72%, 77%, and 81% for silane, GMA, and OBDC treated sisal fiber-reinforced recycled polypropylene (RPP/SF) composites, respectively, as compared to RPP. The thermogravimetric analysis (TGA), differential scanning calorimeter (DSC), and heat deflection temperature (HDT) results revealed improved thermal stability as compared with RPP. The flammability behaviour of silane, GMA, and OBDC treated SF/RPP composites was studied by horizontal burning rate by UL-94. The morphological analysis through scanning electron micrograph (SEM) supports and improves surface interaction between fiber surface and polymer matrix.

Hiroyuki Hamada
Johanne Denault
Amar K. Mohanty
Yan Li
Mohamed S. Aly-Hassan

Hindawi Publishing Corporation
Advances in Mechanical Engineering
Volume 2013, Article ID 761840, 8 pages
http://dx.doi.org/10.1155/2013/761840

Research Article

Injection Moulded Biocomposites from Oat Hull and Polypropylene/Polylactide Blend: Fabrication and Performance Evaluation

Jeevan Prasad Reddy,[1] Manjusri Misra,[1,2] and Amar Mohanty[1,2]

[1] *Bioproducts Discovery and Development Centre (BDDC), Department of Plant Agriculture, University of Guelph, Guelph, ON, Canada N1G 2W1*
[2] *School of Engineering, Thornbrough Building, University of Guelph, Guelph, ON, Canada N1G 2W1*

Correspondence should be addressed to Amar Mohanty; mohanty@uoguelph.ca

Received 2 June 2012; Accepted 8 February 2013

Academic Editor: Hiroyuki Hamada

Oat hull fibre reinforced polypropylene- (PP-)/polylactide- (PLA-) based biocomposites were fabricated and their process engineering and performances were evaluated. The effect of ethylene propylene-g-maleic anhydride (EP-g-Ma) compatibilizer on mechanical properties of 30 wt% oat hull reinforced PP/PLA (90/10) blend composites was investigated. Thermal degradation parameters of the oat hull fibre were determined using thermogravimetric analysis. The effect of fibre reinforcement on crystallinity of oat hull fibre reinforced PP/PLA composites was studied by differential scanning calorimetry (DSC). Thermomechanical properties of the composites were analyzed by dynamic mechanical analyzer (DMA). The interfacial bonding between the fibre and the matrix was examined using scanning electron microscope (SEM). Significant improvement in tensile strength (40%) and flexural strength (46%) was observed with the addition of EP-g-Ma compatibilizer. DSC analysis of oat hull fibre reinforced composites showed an increase in the crystallization temperature (T_c) due to the nucleation effect of oat hull fibre. DMA results revealed that the storage modulus of PP/PLA/Oat hull fibre composites was higher compared to PP/PLA blend throughout the investigated range of temperature.

1. Introduction

Polymer composites are an important class of materials which are being used in a wide variety of applications. Synthetic fibre reinforced composites have found successful application in automotive, aerospace, and other such industries dealing with structural materials. However, due to increased environmental awareness and depleting petroleum resources, natural fibre composites have gained significant attention. Recent research has been focused on natural fibre composites mainly to find alternatives to replace synthetic fibres used in composites for some specific applications. Biodegradable nature, eco-friendly process, low-cost, and low density are some of the major advantages associated with the use of natural fibre as reinforcement for the polymer matrix composites. Extensive research has been conducted on natural fibre reinforced thermoplastics such as polypropylene (PP) and polyethylene (PE). Studies on identification and characterization of natural fibres from different origins like stem, leaf, and hull are also well established for the application of polymer composites [1].

Oat hull fibre is the outermost layer of the oat grain. The major chemical compositions of oat fibre are cellulose, lignin, and fewer amounts of polysaccharides [2]. Rodney et al. have evaluated the performance of PP composites reinforced with different bast fibers, leaf fibers and agricultural residues. They have reported that the mechanical properties of PP composites containing oat hull, wheat straw, kenaf core and oat straw were all similar [3].

Due to outstanding combination of inexpensive production cost and excellent physical properties, polypropylene is commonly used for widespread applications. Studies of

natural fibre reinforced polypropylene have been well established. Among the renewable polymers, PLA has attracted much attention because of its biodegradability and good mechanical properties [4]. In order to reduce brittleness and increase toughness, PLA has been blended with polyolefin [5, 6]. However, PLA/polyolefin blends are immiscible because of their difference in chemical nature and polarity. Studies on miscibility of PLA/PP blend have been reported previously [7]. Ying-Chen et al. [8] reported the fabrication of PLA/PP blend based biocomposites and the fibre matrix interaction have been improved by the use of maleic anhydride-grafted PP (MAH-g-PP).

It is generally accepted that the performance of the fibre reinforced polymer composites depends on many factors such as nature of the matrix, fibre volume or weight fraction, fibre aspect ratio, and fibre-matrix compatibility. Several methods have been used to improve the interfacial adhesion between the fibre and matrix of the natural fibre composites [9, 10]. The most prominent and useful method to reduce the polarity of a natural fibre is the surface modification which can help to improve the interfacial interaction with the nonpolar polymer matrix. Another method to improve the compatibility of natural fibre with the polymer matrix is to use compatibilizer which can react with the functional groups of both the fibre and matrix [11].

In this work, PP/PLA/Oat hull composite was processed by extrusion followed by injection moulding. The thermal degradation parameters of the oat hull fibre were analysed using thermogravimetric analysis, in order to find out the effective processing temperature of the composites. The effects of compatibilizer on tensile, flexural, and impact properties of the composites were studied. The thermomechanical properties such as storage modulus and heat deflection temperature of the composite were also evaluated. Crystallization studies of the composites were studied using differential scanning calorimetry (DSC). The interfacial adhesion of the composites was analysed by scanning electron microscope (SEM).

2. Experimental

2.1. Materials. Polypropylene 4220H (High impact coploymer) having a notched Izod impact strength ≥534 J/m (nonbreak) and MFI = 20 gm/10 min (@ 230°C, 2.16 kg load) was obtained from Pinnacle Polymers, USA. Poly-L-lactic acid (PLLA) was purchased from Biomer, Krailling, Germany (Biomer L 9000), henceforward referred to as PLA throughout the paper. Oat hull having fibre length of 3/8 inch was used for fabricating the composites. A-C ethylene-propylene-maleic anhydride copolymer (EP-g-Ma) compatibilizer was obtained from Honeywell, USA.

2.2. Fabrication of Composites. PLA and oat hull fibre were dried in a hot air oven at 80°C for 4 hours. The composite materials with different formulations were melt processed using DSM's (Netherlands) 15 cc twin screw microcompounder. A known proportion of PP, PLA, and oat hull was fed into the barrel, and the processing temperature was set at 190°C. The extruder was operated at a screw speed of 100 rpm, and the residence time was 2 min. The extrudate was collected and transferred into a preheated microinjection moulding machine. The mould temperature was maintained at 30°C, and the injection pressure was optimized for the biocomposites. Finally, the test specimens were conditioned according to ASTM standards prior to testing.

3. Characterization

3.1. Thermogravimetric Analysis (TGA). TGA of the dried oat hull fibre and the composites was measured in TA Q500 thermal analyzer. The samples were heated from 30°C to 600°C at a heating rate of 10°C/min.

3.2. Melt Flow Index (MFI). Melt flow index (MFI) of PP, PP/PLA, and PP/PLA/Oat hull composites was determined according to ASTM D1238. Melt Flow Indexer from Qualitest (model 2000A) was used to determine the MFI of the composites at 230°C with a load of 2.16 kg.

3.3. Mechanical Properties

3.3.1. Tensile and Flexural Properties. The tensile and flexural properties of the composites were tested in a UTM (universal testing machine), Instron 3382 instrument. The standard test methods ASTM D638 and ASTM D790 were used to measure the tensile and flexural properties of the composites, respectively.

3.3.2. Izod Impact Strength. Notched Izod impact property of the composite materials of various formulations was investigated in a TMI impact tester (model 43-02-01) employing ASTM standard D256.

3.4. Differential Scanning Calorimetry (DSC). DSC analysis of PP, PP/PLA blend, and PP/PLA/Oat hull composites was performed using a TA Instrument, DSC Q200 in a heat/cool/heat mode. The sample was heated from 30°C to 190°C at a heating rate of 10°C/min and cooled to −20°C at a heating rate of 5°C/min. The thermal parameters such as glass transition (T_g), crystallization (T_c), and melting (T_m) temperatures were analysed with the TA universal analysis software.

3.5. Dynamic Mechanical Analysis (DMA). The dynamic mechanical analysis of the composites was carried out in TA Instrument, Q800 DMA analyzer in dual cantilever mode. Specimens were tested with 1 Hz frequency at a temperature range of −30 to 140°C and at a heating rate of 4°C/min.

3.6. Heat Deflection Temperature (HDT). HDT of the PP/PLA blend and PP/PLA/Oat hull composites was tested as per ASTM D648 standard. The DMA (TA Q800) was used to determine the HDT of the composites specimen. The samples were heated from 30 to 140°C at a heating rate of 2°C/min. The HDT was reported as the temperature at which a deflection of 250 μm occurred.

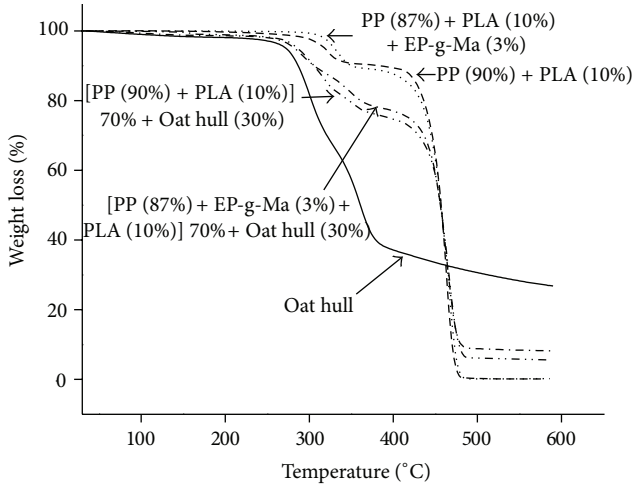

Figure 1: TGA analysis of oat hull fibre and PP/PLA/Oat hull composites.

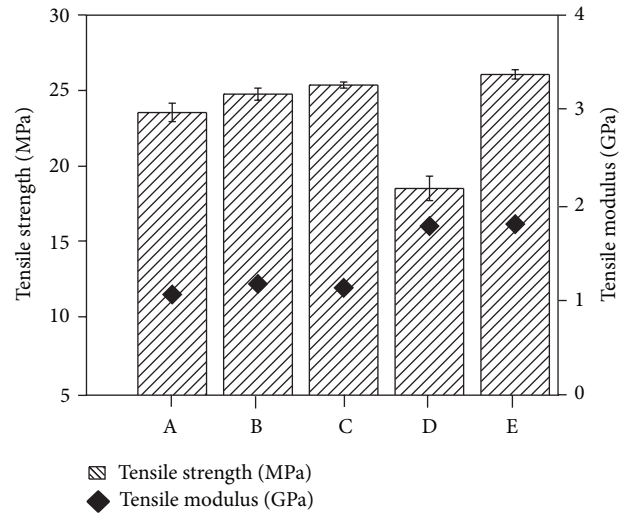

Figure 2: Tensile properties of PP, PP/PLA, and PP/PLA/Oat hull composites. (A) PP, (B) PP (90%) + PLA (10%), (C) PP (87%) + PLA (10%) + EP-g-Ma (3%), (D) [PP (90%) + PLA (10%)] 70% + Oat hull (30%), and (E) [PP (87%) + EP-g-Ma (3%) + PLA (10%)] 70% + Oat hull (30%).

3.7. SEM of Composites. The scanning electron micrographs of the tensile fractured composite specimens were recorded on FEI S 50 microscope. The composite samples were gold coated before recording the micrographs.

4. Results and Discussion

4.1. Thermogravimetric Analysis of Oat Hull Fibre. Figure 1 illustrates thermogravimetric analysis of dried oat hull fibre and the composites. Initial degradation temperature of the oat hull fibre observed from the thermogram was 241°C. The degradation that occurred in the temperature range between 50°C and 120°C was due to the elimination of moisture and other volatiles. The degradation temperatures at 5%, 25%, and 50% were 271, 310, and 353°C, respectively. Also, the final degradation temperature of the oat hull fibre was at 400°C. Generally the initial stage of natural fibre degradation is associated with degradation of the hemicellulose and some part of the lignin. The final stage of degradation observed is for cellulose and lignin [12]. Only 1.3 wt% of the fibre degraded between 150°C and 250°C. This suggested that within this temperature range oat hulls can be processed to make composites with polymers. Therefore, we selected 190°C, as a processing temperature for PP/PLA composites. The thermograms of the PP/PLA and PP/PLA/EP-g-Ma showed five percentage of weight loss at 317°C and 329.7°C, respectively. Also, the five percent weight loss of the PP/PLA/oat hull and PP/PLA/EP-g-Ma/oat hull composites occurred at 281°C and 287°C, respectively. It can be seen from Figure 1 that the composites were beginning to lose weight at lower temperatures compared to PP/PLA blend. This is due to the cellulosic and hemi-cellulosic components of the natural fibre in the composites.

4.2. MFI. The MFI values of virgin PP, PP/PLA, and PP/PLA/Oat hull composites are presented in Table 1. The MFI values of PP/PLA were higher than that of virgin PP. This increase could be attributed to the high MFI value of PLA in the blend. The MFI of biocomposites is less than that of the PP/PLA matrix. This is because the fibres were able to restrict the polymer melt flow which resulted in lower MFI than PP/PLA blend [13]. However, EP-g-Ma had no significant effect on MFI value of PP/PLA blend and the composites.

4.3. Mechanical Properties. The tensile properties of neat PP, PP/PLA blends, and PP/PLA/Oat hull composites with and without compatibilizer are presented in Figure 2. The tensile strength of the PP/PLA blend was almost the same as virgin PP. However, oat hull reinforced PP/PLA composite showed reduction in tensile strength compared to PP/PLA blends. Further with the addition of compatibilizer, the tensile strength of the composites improved and it is slightly higher than virgin PP. With the addition of 3% compatibilizer, the increment in tensile strength of the PP/PLA blend was low, whereas the PP/PLA/Oat hull composite strength was increased from 18 MPa to 26 MPa. This improvement in tensile properties of the composites was due to the improved stress transfer efficiency in the composites by the compatibilizer. In the composites with EP-g-Ma, the anhydride end of the compatibilizer can readily react with the hydroxyl groups of oat hull fibre, and the olefinic end of compatibilizer is more miscible with the PP (Figure 3). It is well known that the maleated PP improves the interface between the matrix and fibre thus improving the strength of the composites [14].

4.4. Stress-Strain Curves. The tensile strain versus tensile stress curves of the PP, PP/PLA, and PP/PLA/Oat hull composites are shown in Figure 4. The stress strain curves showed the necking extension for virgin PP. With the addition of PLA, a drop in stress occurred, and the area of the stress curve reduced due to the brittle nature of the PLA. However, the yield stress of the PP/PLA and compatibilized

Table 1: Differential scanning calorimetry of PP/PLA/Oat hull fibre composites.

Composites	T_g ˚C	T_c ˚C	T_m ˚C	ΔH_m J/g	MFI 230˚C, @ 2.16 kg
PP	12	133.6	166.5	59.04	19.8 ± 1.2
PLA	62.2	109.1	171	36.09	28.9 ± 102
PP (90%) + PLA (10%)	64.5	122.3	166.4	65.11	30 ± 0.7
PP (87%) + PLA (10%) + EP-g-Ma (3%)	64.6	118.4	167.9	64.2	28.9 ± 0.8
{PP (90%) + PLA (10%)} 70% + Oat hull (30%)	62.2	126.1	167.1	43.6	16.8 ± 1.3
{PP (87%) + PLA (10%) + EP-g-Ma (3%)} 70% + Oat hull (30%)	61.5	122.1	166.8	27.6	17 ± 0.8

T_c: crystallization temperature; T_m: melting temperature; ΔH_m: enthalpy of melting.

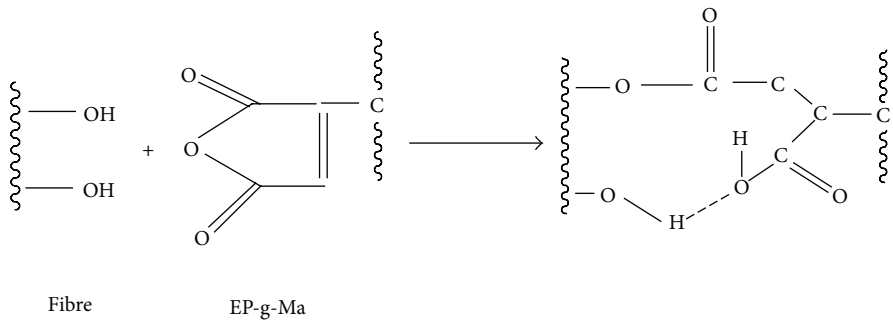

Figure 3: Chemical reaction mechanism of the oat hull fibre with EP-g-Ma.

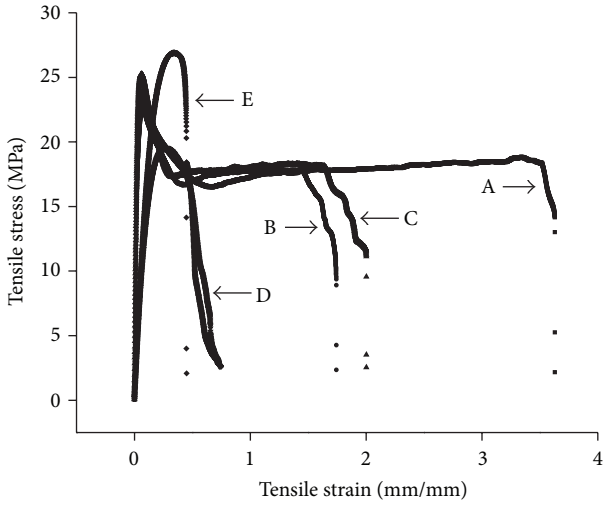

Figure 4: Tensile stress-strain curves of the biocomposites. (A) PP, (B) PP (90%) + PLA (10%), (C) PP (87%) + PLA (10%) + EP-g-Ma (3%), (D) [PP (90%) + PLA (10%)] 70% + Oat hull (30%), and (E) [PP (87%) + EP-g-Ma (3%) + PLA (10%)] 70% + Oat hull (30%).

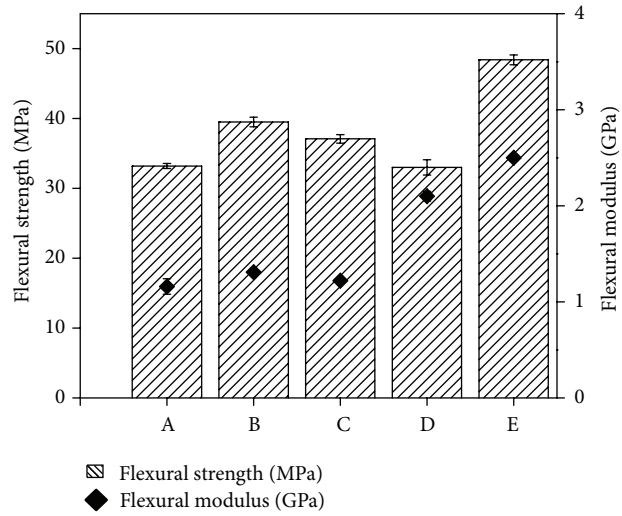

Figure 5: Flexural properties of PP and PP/PLA/Oat hull composites. (A) PP, (B) PP (90%) + PLA (10%), (C) PP (87%) + PLA (10%) + EP-g-Ma (3%), (D) [PP (90%) + PLA (10%)] 70% + Oat hull (30%), and (E) [PP (87%) + EP-g-Ma (3%) + PLA (10%)] 70% + Oat hull (30%).

PP/PLA blends was similar. The stress-strain curve of the PP/PLA/Oat hull composites clearly showed the reinforcing effect of the fibres through the increased stiffness [15]. The PP/PLA/Oat hull composites failed at lower strain values than the PP/PLA blend, but even at these strains, the stress levels of the composites were lower than the corresponding stress levels for the pure polypropylene and PP/PLA blend. The use of compatibilizer increased ultimate yield stress of the PP/PLA/Oat hull composite.

Figure 5 illustrates the flexural properties of PP, PP/PLA blend, and PP/PLA/Oat hull composites with and without compatibilizer. The performance of oat hull fibre reinforced PP/PLA composites without compatibilizer was compared with that of PP/PLA composites with compatibilizer. The addition of 30 wt% oat hull fibre into the PP/PLA blends decreased the flexural strength when compared to the control. However, the addition of EP-g-Ma compatibilizer significantly increased the flexural strength of the composites. Similar behavior has been observed previously after the addition of compatibilizer, that is, increment in flexural strength of the natural fibre reinforced composites [14]. The addition of

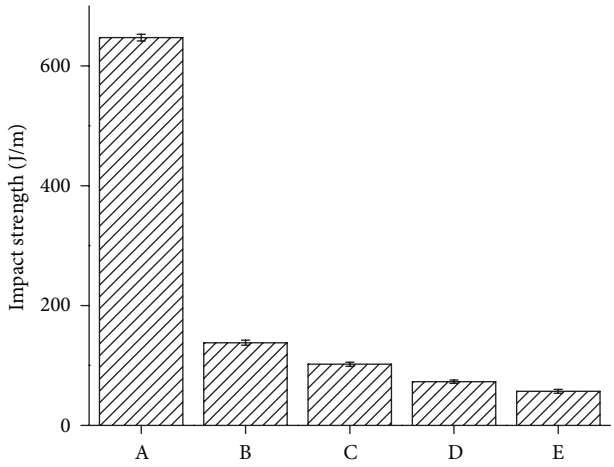

Figure 6: Impact strength of PP and PP/PLA/Oat hull composites. (A) PP, (B) PP (90%) + PLA (10%), (C) PP (87%) + PLA (10%) + EP-g-Ma (3%), (D) [PP (90%) + PLA (10%)] 70% + Oat hull (30%), and (E) [PP (87%) + EP-g-Ma (3%) + PLA (10%)] 70% + Oat hull (30%).

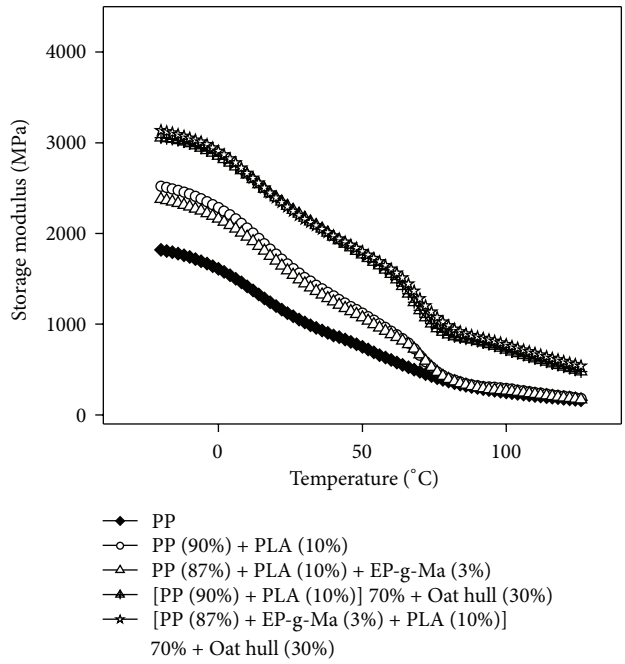

Figure 7: Storage modulus of PP and PP/PLA/Oat hull composites.

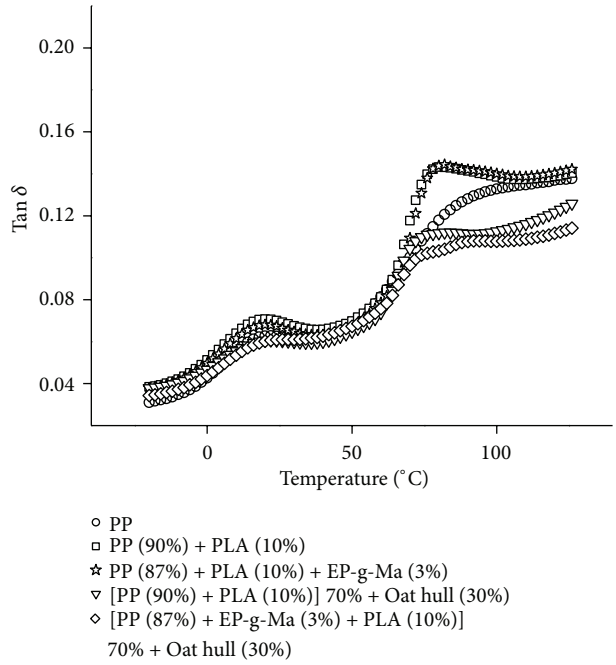

Figure 8: Tan δ values of PP/PLA/Oat hull composites.

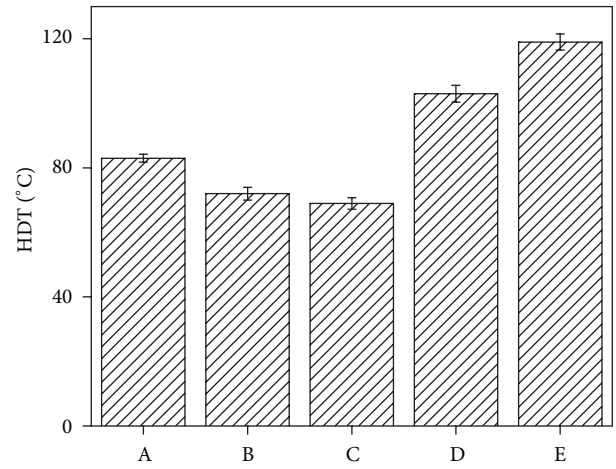

Figure 9: HDT of PP, PP/PLA, and PP/PLA/Oat hull composites. (A) PP, (B) PP (90%) + PLA (10%), (C) PP (87%) + PLA (10%) + EP-g-MA (3%), (D) [PP (90%) + PLA (10%)] 70% + Oat hull (30%), and (E) [PP (87%) + EP-g-MA (3%) + PLA (10%)] 70% + Oat hull (30%).

EP-g-Ma did not affect the tensile and flexural modulus, but it improved the tensile and flexural strength of the composite.

4.5. Impact Strength. Figure 6 illustrates the notched Izod impact strength of the PP, PP/PLA, and PP/PLA/Oat hull composites. PP has excellent impact strength, therefore it showed a nonbreak impact behavior (647 J/m) when tested for notched Izod impact strength. Due to the lower impact strength of PLA, PP/PLA blend showed reduced impact strength. The impact strength of PP/PLA blend without and with compatibilizer was 138 and 102 J/m, respectively. The impact strength of uncompatibilized and compatibilized composites is 73 and 57 J/m, respectively. From the previous results, it is clear that the impact strength of the PP/PLA blend was also affected by compatibilizer. The impact strength of the PP/PLA blend is mainly affected by the miscibility and the interphase separation and morphologies between PP and PLA [16]. With the addition of 3% EP-g-Ma, a reduction in impact strength of the PP/PLA and PP/PLA/Oat hull composites was observed. Khalid et al. [17] also observed similar behaviour for the PP/Cellulose composites, as the impact strength of the composite decreased by the addition of MA-PP compatibilizer.

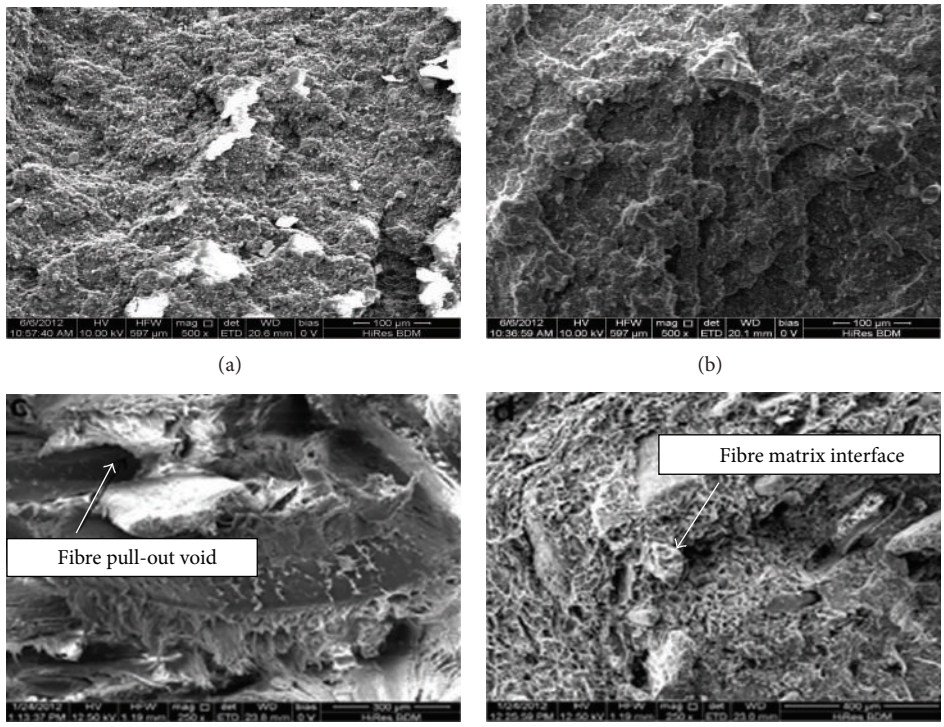

Figure 10: SEM of the tensile fractured surface of PP/PLA/Oat hull composites. (a) PP (90%) + PLA (10%), (b) PP (87%) + PLA (10%) + EP-g-MA (3%), (c) [PP (90%) + PLA (10%)] 70% + Oat hull (30%), and (d) [PP (87%) + EP-g-MA (3%) + PLA (10%)] 70% + Oat hull (30%).

4.6. Differential Scanning Calorimetry. Summary of DSC data on crystallization and melting behaviour of PP, PP/PLA blends and composites are presented in Table 1. The melting enthalpy of PP was increased from 59.04 to 65.11 J/g with the addition of PLA. Further, the melting enthalpies of uncompatibilized and compatibilized composites were observed to be 43.6 and 23.6 J/g. Incorporation of PLA increased the melting enthalpy of PP/PLA blends. This is probably due to the improved polymer segment mobility in the PP/PLA blend because of the incompatibility between PP and PLA [18]. With the addition of oat hull, the melting enthalpy of PP/PLA blends decreased due to poor melting kinetics. Further, the T_c value of PP/PLA/EP-g-Ma blend was enhanced by the addition of oat hull fibre. The oat hull fibre reinforced composite showed increased crystallization temperature (T_c). This improvement in crystallization temperature of the composite is due to the nucleation effect of oat hull fibre surface on to the polymer matrix [19].

4.7. Dynamic Mechanical Analysis. The storage modulus of the composites from −30 to 150°C temperature range is presented in Figure 7. It is clear from Figure 7 that the storage modulus of the PP/PLA blend is higher than PP. This was due to the higher storage modulus of PLA. The addition of compatibilizer had no effect on storage modulus of the PP/PLA blend and composite. The storage modulus of the 30% oat hull fibre reinforced composites was enhanced when compared to PP/PLA blend. The addition of filler or fibre into the matrix enhances the stiffness of the polymer and this improves the storage modulus of the composites [20]. Effective stress transfer at the fibre-matrix interface also resulted in increased storage modulus of PP/PLA/oat hull composites [21].

Tan δ value represents the viscoelastic nature of a material. Temperature dependence of tan δ of PP, PP/PLA, uncompatibilized, and compatibilized composites is presented in Figure 8. From Figure 8, it is clear that there are two distinct peaks observed at 12°C and 65°C. This belongs to the glass transition regions of PP and PLA, respectively. These peaks clearly showed the formation of biphasic structure. The peak intensity of PP/PLA is higher than PP because the damping was affected in association with the additional viscoelastic energy dissipation in the blend [7]. However, in oat hull fibre reinforced composite, the damping was affected in the presence of fibres that reduced the peak intensity of the composites. The addition of stiff filler like natural fibre and other reinforcing agents will reduce the damping property of PP/PLA matrix that implies a reduction of the tan δ peak in the glass transition temperature range [21].

4.8. Heat Deflection Temperature. Heat deflection temperature (HDT) of the specimens is shown in Figure 9. Heat deflection temperature is the relative heat resistance of a polymeric material. The HDT of PP is 83°C and PLA is 65°C. With the addition of compatibilizer a slight reduction in HDT was observed. The maleated ethylene-propylene

copolymer affects the stiffness at higher temperature, hence, a slight reduction in HDT was observed. However, the HDT is directly proportional to the flexural modulus; thus, the results are in good agreement with the flexural data. Improvement in HDT with the natural fibre reinforced composites has been reported by several other researchers [22].

4.9. Morphology. Figure 10 shows the tensile fractured surface of PP/PLA, PP/PLA/EP-g-Ma, and PP/PLA/EP-g-Ma/oat hull reinforced composite. From the micrographs, it is clear that a smooth fracture surface was observed for the EP-g-MA compatibilized PP/PLA blends (Figure 10(b)). The micrographs indicated that the EP-g-MA forms an interphase between PP and PLA. Figure 10(c) shows the fracture surfaces of the composite without compatibilizer. SEM micrographs revealed traces of pulled-out oat hull fibre which indicated poor adhesion between the matrix and the fibre. Also, the gaps between the fibre and the matrix suggested poor interfacial adhesion. The composite with 3% EP-g-Ma (Figure 10(d)) exhibited fibre pullout, but the fibres were still covered by residual amount of matrix. This indicated improved interfacial adhesion between oat hull fibre and matrix [23]. These results are in good agreement with the tensile and flexural properties of the composites. With the addition of compatibilizer, the tensile and flexural properties of the composite improved when compared to uncompatibilized composite.

5. Conclusion

The oat hull fibre reinforced PP/PLA composites were successfully fabricated by melt processing method. Thermogravimetric analysis of the oat hull fibre clearly showed that the processing temperature of 190°C was acceptable. The assessment of mechanical properties revealed that the PP/PLA blend has slightly improved tensile and flexural properties compared to PP. Oat hull fibre reinforced composites showed the reduction in tensile and flexural properties when compared to the PP/PLA blend. The tensile and flexural properties of the composites significantly improved in the presence of compatibilizer. HDT of the composites improved 43% over the PP/PLA blend. Composites with the 30 wt% oat hull loading showed improved storage modulus for both uncompatibilized and compatibilized systems. SEM analysis of the composites showed that the interfacial adhesion of the fibre and matrix was improved by the compatibilizer.

Acknowledgment

The authors would like to acknowledge the financial support from NSERC AUTO21 NCE, Canada, to carry out this research work.

References

[1] A. K. Bledzki and J. Gassan, "Composites reinforced with cellulose based fibres," *Progress in Polymer Science*, vol. 24, no. 2, pp. 221–274, 1999.

[2] A. M. Stephen, W. J. Dahl, D. M. Johns, and H. N. Englyst, "Effect of oat hull fiber on human colonic function and serum lipids," *Cereal Chemistry*, vol. 74, no. 4, pp. 379–383, 1997.

[3] E. Rodney Jacobson, R. M. Rowell, D. E. Caulfield, and A. R. Sanadi, "Property improvement effects of agricultural fibers and wastes as reinforcing fillers in polypropylene-based composites: by the forest products society," in *Woodfiber-Plastic Composites*, pp. 211–219, 1996.

[4] B. Bax and J. Müssig, "Impact and tensile properties of PLA/Cordenka and PLA/flax composites," *Composites Science and Technology*, vol. 68, no. 7-8, pp. 1601–1607, 2008.

[5] D. Li, B. Shentu, and Z. Weng, "Morphology, rheology, and mechanical properties of Polylactide/Poly(Ethyleneco-octene) blends," *Journal of Macromolecular Science B*, vol. 50, no. 10, pp. 2050–2059, 2011.

[6] H. Balakrishnan, A. Hassan, and M. U. Wahit, "Mechanical, thermal, and morphological properties of polylactic acid/linear low density polyethylene blends," *Journal of Elastomers and Plastics*, vol. 42, no. 3, pp. 223–239, 2010.

[7] C. Priyanka, M. Smita, S. K. Nayak, and U. Lakshmi, "Poly(L-lactide)/polypropylene blends: evaluation of mechanical, thermal, and morphological characteristics," *Journal of Applied Polymer Science*, vol. 121, no. 6, pp. 3223–3237, 2011.

[8] Z. Ying-Chen, W. Hong-Yan, and Q. Yi-Ping, "Morphology and properties of hybrid composites based on polypropylene/polylactic acid blend and bamboo fiber," *Bioresource Technology*, vol. 101, no. 20, pp. 7944–7950, 2010.

[9] N. Reddy and Y. Yang, "Natural cellulose fibers from switchgrass with tensile properties similar to cotton and linen," *Biotechnology and Bioengineering*, vol. 97, no. 5, pp. 1021–1027, 2007.

[10] S. Kalia, B. S. Kaith, and K. Inderjeet, "Pretreatments of natural fibers and their application as reinforcing material in polymer composites: a review," *Polymer Engineering and Science*, vol. 49, no. 7, pp. 1253–1272, 2009.

[11] A. S. Herrmann, J. Nickel, and U. Riedel, "Construction materials based upon biologically renewable resources-from components to finished parts," *Polymer Degradation and Stability*, vol. 59, no. 1–3, pp. 251–261, 1998.

[12] B. Wielage, T. H. Lampke, G. Marx, K. Nestler, and D. Starke, "Thermogravimetric and differential scanning calorimetric analysis of natural fibres and polypropylene," *Thermochimica Acta*, vol. 337, no. 1-2, pp. 169–177, 1999.

[13] P. V. Joseph, G. Mathew, K. Joseph, G. Groeninckx, and S. Thomas, "Dynamic mechanical properties of short sisal fibre reinforced polypropylene composites," *Composites A*, vol. 34, no. 3, pp. 275–290, 2003.

[14] A. R. Sanadi and D. F. Caulfield, "Transcrystalline interphases in natural fiber-PP composites: effect of coupling agent," *Composite Interfaces*, vol. 7, no. 1, pp. 31–43, 2000.

[15] S. Oza, R. Wang, and N. Lu, "Thermal and mechanical properties of recycled high density polyethylene/hemp fiber composites," *International Journal of Applied Science and Technology*, vol. 1, no. 5, pp. 31–36, 2011.

[16] E. Wojciechowska, J. Fabia, C. Ślusarczyk, A. GawThlowski, M. Wysocki, and T. Graczyk, "Processing and supermolecular structure of new iPP/PLA fibres," *Fibres and Textiles in Eastern Europe*, vol. 5, no. 53, pp. 126–128, 2005.

[17] M. Khalid, S. Alil, L. C. Abdullah, C. T. Ratnam, and S. Y. Thomas Choong, "Effect of MAPP as coupling agent on the mechanical properties of palm fibre empty fruit bunch and cellulose polypropylene biocomposites," *International Journal of Engineering and Technology*, vol. 3, no. 1, pp. 79–84, 2006.

[18] K. S. Anderson and M. A. Hillmyer, "The influence of block copolymer microstructure on the toughness of compatibilized polylactide/polyethylene blends," *Polymer*, vol. 45, no. 26, pp. 8809–8823, 2004.

[19] K. S. Anderson and M. A. Hillmyer, "Melt preparation and nucleation efficiency of polylactide stereocomplex crystallites," *Polymer*, vol. 47, no. 6, pp. 2030–2035, 2006.

[20] Y. Tao, L. Yan, and R. Jie, "Preparation and properties of short natural fiber reinforced poly(lactic acid) composites," *Transactions of Nonferrous Metals Society of China*, vol. 19, no. 3, pp. s651–s655, 2009.

[21] E. Lezak, Z. Kulinski, R. Masirek, E. Piorkowska, M. Pracella, and K. Gadzinowska, "Mechanical and thermal properties of green polylactide composites with natural fillers," *Macromolecular Bioscience*, vol. 8, no. 12, pp. 1190–1200, 2008.

[22] S. S. Ahankari, A. K. Mohanty, and M. Misra, "Mechanical behaviour of agro-residue reinforced poly(3-hydroxybutyrate-co-3-hydroxyvalerate), (PHBV) green composites: a comparison with traditional polypropylene composites," *Composites Science and Technology*, vol. 71, no. 5, pp. 653–657, 2011.

[23] A. Nourbakhsh, V. K. Bouhuslav, A. Ashori, and J. L. Ahmad, "Effect of a novel coupling agent, polybutadiene isocyanate, on mechanical properties of wood-fiber polypropylene composites," *Journal of Reinforced Plastics and Composites*, vol. 27, no. 16-17, pp. 1679–1687, 2008.

Hindawi Publishing Corporation
Advances in Mechanical Engineering
Volume 2013, Article ID 685104, 6 pages
http://dx.doi.org/10.1155/2013/685104

Research Article

Continuous Natural Fiber Reinforced Thermoplastic Composites by Fiber Surface Modification

Patcharat Wongsriraksa,[1] Kohsuke Togashi,[2] Asami Nakai,[3] and Hiroyuki Hamada[1]

[1] *Kyoto Institute of Technology, Matsugasaki, Sakyo-ku, Kyoto 606-8585, Japan*
[2] *Komatsu Seiren Co., Ltd., Nu-167 Hama-machi, Nom, Ishikawa Prefecture 929-0124, Japan*
[3] *Gifu University, 1-1 Yanagido, Gifu 501-1193, Japan*

Correspondence should be addressed to Patcharat Wongsriraksa; w.patcharat@gmail.com

Received 1 June 2012; Accepted 1 March 2013

Academic Editor: Johanne Denault

Continuous natural fiber reinforced thermoplastic materials are expected to replace inorganic fiber reinforced thermosetting materials. However, in the process of fabricating the composite, it is difficult to impregnate the thermoplastic resin into reinforcement fiber because of the high melt viscosity. Therefore, intermediate material, which allows high impregnation during molding, has been investigated for fabricating continuous fiber reinforced thermoplastic composite by aligning resin fiber alongside reinforcing fiber with braiding technique. This intermediate material has been called "microbraid yarn (MBY.)" Moreover, it is well known that the interfacial properties between natural fiber and resin are low; therefore, surface treatment on continuous natural fiber was performed by using polyurethane (PU) and flexible epoxy (FLEX) to improve the interfacial properties. The effect of surface treatment on the mechanical properties of continuous natural fiber reinforced thermoplastic composites was examined. From these results, it was suggested that surface treatment by PU with low content could produce composites with better mechanical properties.

1. Introduction

The current emphasis is to develop materials that are renewable, degradable, ecofriendly, and recyclable, better known as "green materials," as alternative to the petroleum or mineral-based material [1, 2]. Natural fiber-reinforced thermoplastic composites are becoming more and more commonplace by the development of new production techniques and processing equipment. Compared with the traditional synthetic fibers, natural fibers present lower density, lower cost, and they are renewable and biodegradable [3].

The continuous natural yarns were used as reinforcement to enhance the mechanical properties of thermoplastic composites. The problem with producing continuous natural fiber-reinforced thermoplastic composite, however, is the difficulty to impregnate the thermoplastic resin into the fibers due to the high melt viscosity. In these circumstances, intermediate material, which allows high impregnation during molding, has been developed for fabricating continuous fiber-reinforced thermoplastic composite by aligning resin fiber alongside reinforcing fiber with braiding technique [4, 5]. This intermediate material has been called "microbraided yarn (MBY)" as shown in Figure 1. Since resin fibers are located close to the reinforcement fiber bundle, the impregnation state is excellent [6].

Since the interfacial properties between natural fiber and polymer matrix are low, surface treatment on jute fibers was required. In this study, polyurethane (PU) and flexible epoxy (FLEX) were used to improve the thermal resistance and interfacial properties of jute fiber. Polyurethane (PU) is one of the most rapidly developing branches in polymer technology with a wide variety of applications, such as foams, coatings, elastomers, resins, and medicine. PU was used for the improvement of the wear resistance and mechanical properties. Epoxy resins are a class of high performance thermosetting polymers widely used as matrix resins for advanced composite materials for application in the automotive, construction, and aerospace industries. Flexible

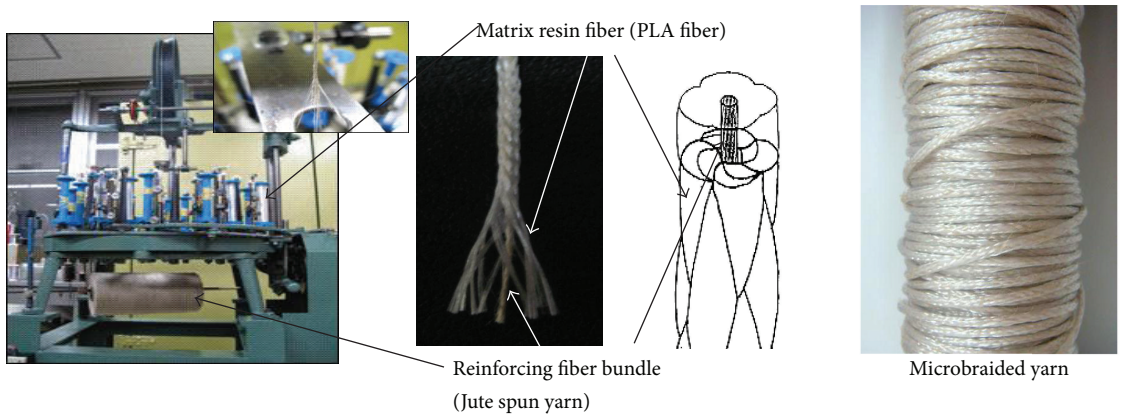

Figure 1: Microbraided yarn (MBY).

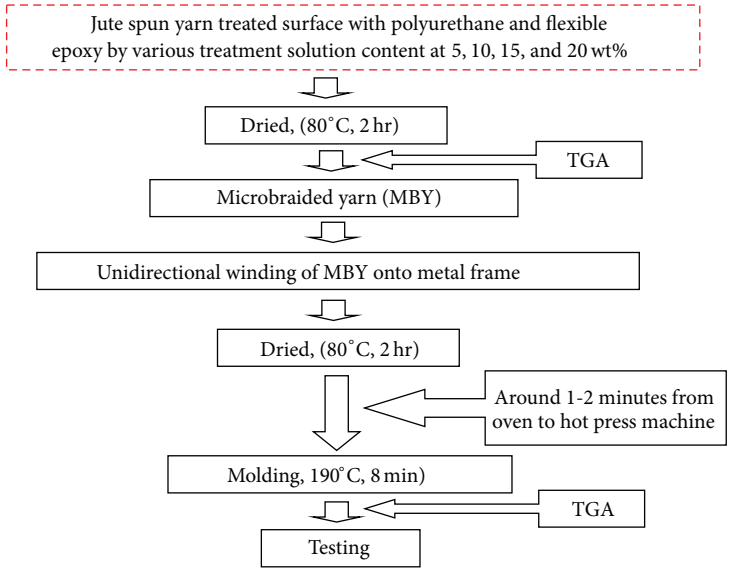

Figure 2: Processing flow chart of jute spun yarn untreated and treated with PU or FLEX/PLA composite.

epoxy resin (FLEX) was used to create flexible interphase and improve thermal degradation resistance. Smith Thitithanasarn, et al. shows that thermal resistance of jute fiber was improved by coating with flexible epoxy resin [7]. The objective of this study was to investigate the effect of surface treatment on the mechanical properties of continuous natural fiber-reinforced thermoplastic composites.

2. Experimental Details

2.1. Materials. The materials used in this study were jute spun yarn as the reinforcement and biodegradable polylactic acid (PLA) fibers that will become the matrix after compression molding. Jute yarns of 400 tex fineness were supplied by Bangladesh Janata Jute Mills Ltd., while PLA fibers (Lactron) were supplied by Unitika Ltd. Polyurethane (PU) and flexible epoxy (FLEX) were used as a surface treatment for the jute spun yarn to improve interfacial adhesion between jute and PLA matrix. PU was supplied by Nicca Chemical Co., Ltd., and FLEX was supplied by Daicel Chemical. Co., Ltd.

2.2. Sample Preparation. Figure 2 shows the processing flow chart of jute spun yarn untreated and treated with PU or FLEX/PLA composite. The method for PU or FLEX treatment is shown in Figure 3; the jute spun yarn was treated by using PU and FLEX with various contestations at 0, 5, 10, 15, and 20 wt%. The jute spun yarns were immersed into PU or FLEX bath for 10 minutes and then dried in an oven at 80°C for 2 hours. Untreated and PU or FLEX treated jute yarns were braided with PLA fibers to yield jute yarn and PLA MBY, which was later used to prepare composites. A tubular braiding machine was used for fabricating MBY as an intermediated material for producing unidirectional continuous natural fiber-reinforced plastic composites [8]. Jute yarns as the reinforcement fibers were aligned vertically and braided with PLA fibers to yield jute/PLA MBY by using a technique known as microbraiding. The MBYs were wound onto a steel frame to obtain an unidirectional alignment of 18 yarns side by side. The steel frame had a spring mechanism to adjust the tension caused by the thermal shrinkage of fiber during processing shown in Figure 4. The wound frame was then dried

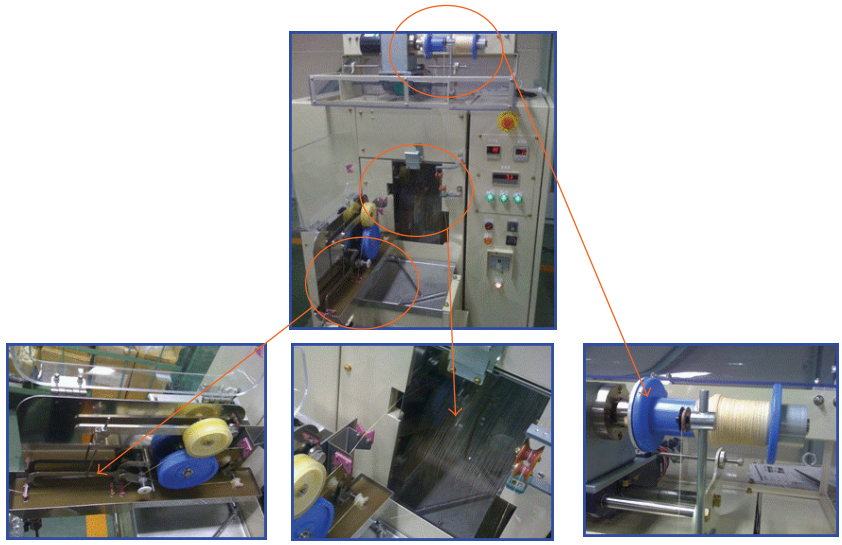

Figure 3: Method for PU and FLEX treatment.

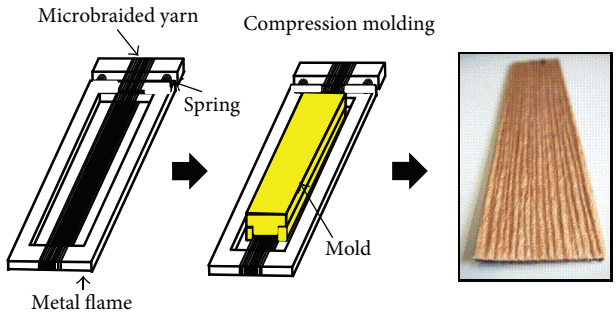

Figure 4: Fabrication method of composites.

in the oven at 80°C with drying times of 2 hours. The frame was then placed into a heated mold with size of 20 × 200 mm concave geometry and compressed at 200°C with a molding pressure of 1.33 MPa for 8 minutes. Cooling was subsequently performed by running water through the mold while keeping the specimens under constant pressure. The time taken to transfer the steel frame from the oven to the compression molding machine was approximately 1-2 minutes, because the natural fiber itself is "hygroscopic" and easily absorbs moisture. From previous study, the moisture absorption rate was increased with increasing exposure time, and the percentage of moisture absorption at 1-2 min was about 0.02%.

2.3. Testing Method. Thermal resistance of jute spun yarn and composites was investigated by thermogravimetric analyzer (TGA2950, TA Instruments) at heating rate of 20°C/min from 30°C to 600°C in air atmosphere. The weight change in a material was determined by TGA as a function of temperature (or time) under a controlled atmosphere. Measurements are used primarily to determine the composition of materials and to predict their thermal stability at temperatures up to 600°C. The technique can characterize materials that exhibit weight loss or gain due to decomposition, oxidation, or dehydration.

Tensile properties of the composite (JIS, K 7165) was tested on the INSTRON universal testing machine (model 4206). The specimen size was 200 mm in length, 20 mm in width, and 0.8~1 mm in thickness, and aluminum tabs (thickness 0.5 mm, width 20 mm, and length 50 mm) were put on both ends. The span length was 100 mm and the crosshead speed was 1 mm/min.

For interfacial properties (JIS, K 7017), 3-point bending test of unidirectional composites in 90 and 0 degree direction was performed by using an INSTRON universal testing machine (model 4206). The specimen size was 50 mm in length, 15 mm in width, and 1.5~1.8 mm in thickness. The span length was 25 mm, and the test speed was 1 mm/min, and the reinforcing fibers were oriented parallel to the loading bars.

For the cross-sectional observation, the cross-section of jute/PLA composites were polished and observed by using an optical microscope OLYMPUS-PME3 (IC5).

3. Results and Discussion

Figure 5 shows the relationship between thermal resistances of jute spun yarn treated with PU and FLEX and content of surface treatment. In the case of jute spun yarn treated with PU, thermal resistance was increased at PU 5 wt% and slightly decreased with increase in surface treatment content. Meanwhile, in the case of jute spun yarn treated with FLEX, thermal resistance was increased with increasing surface treatment content. The jute spun yarn treated with FLEX exhibited higher thermal resistance as compared to the PU.

Figures 6 and 7 show the impregnation state by cross-sectional photographs of composites by varying surface treatment content of PU and FLEX. Specimens untreated and

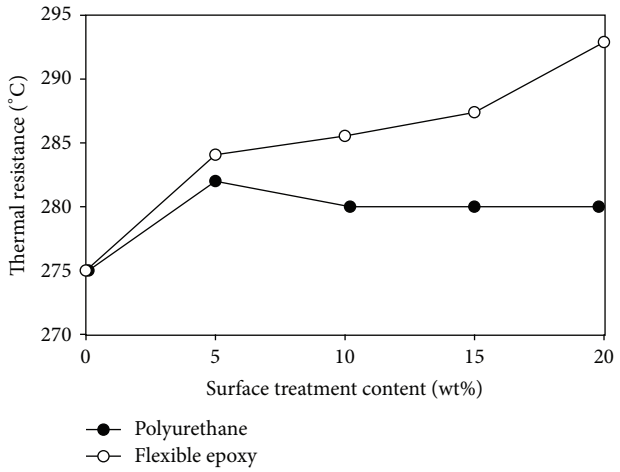

Figure 5: Relationship between thermal resistances of jute spun yarn treated with PU and FLEX and content of surface treatment.

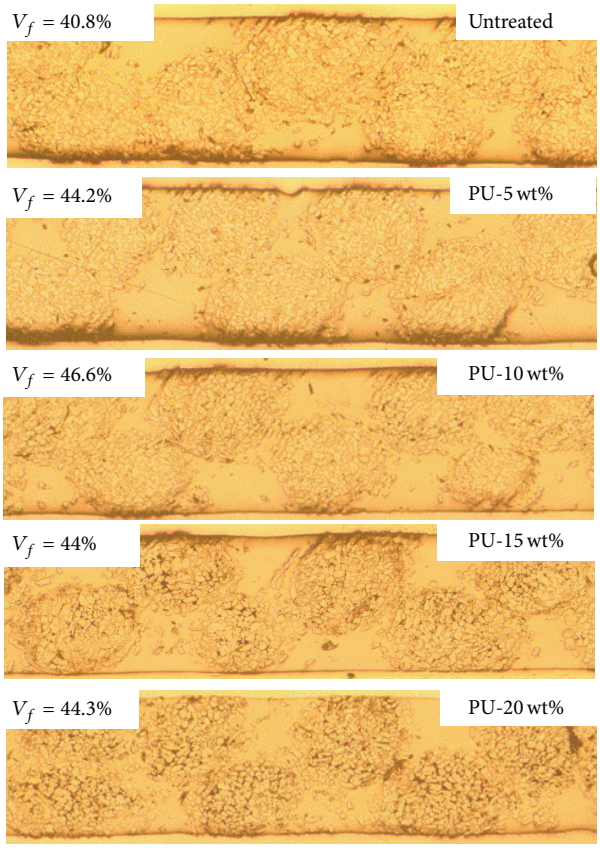

Figure 6: Cross-sectional photographs of composites by varying surface treatment content of PU.

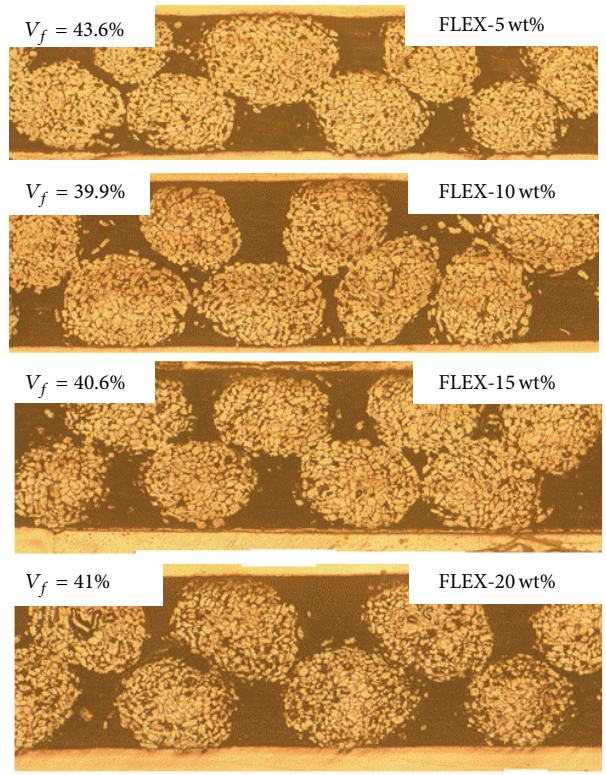

Figure 7: Cross-sectional photographs of composites by varying surface treatment content of FLEX.

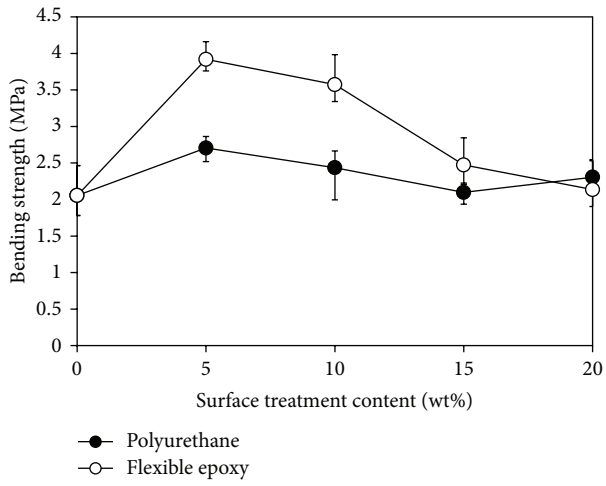

Figure 8: 90 degree bending strength (MPa) of composites varying surface treatment content of PU and FLEX.

treated with 5 wt% of PU and FLEX provided more impregnated amount of PLA resin into the jute fiber bundle than the specimens treated with 10, 15, and 20 wt%. Meanwhile, at the specimens treated with PU, the PLA resin appeared in the jute fiber bundle more than in specimens treated with FLEX because the specimens treated with FLEX inhibited the impregnation of matrix resin. Therefore, it is suggested that PLA was well impregnated into jute fiber bundle with low content surface treatments of PU.

The interfacial properties of the composites were examined by 90 degree bending test conducted parallel to the alignment of jute fibers, and the results are shown in Figure 8. The bending strength of jute spun yarn/PLA composites was measured with varying the content of surface treatment of PU

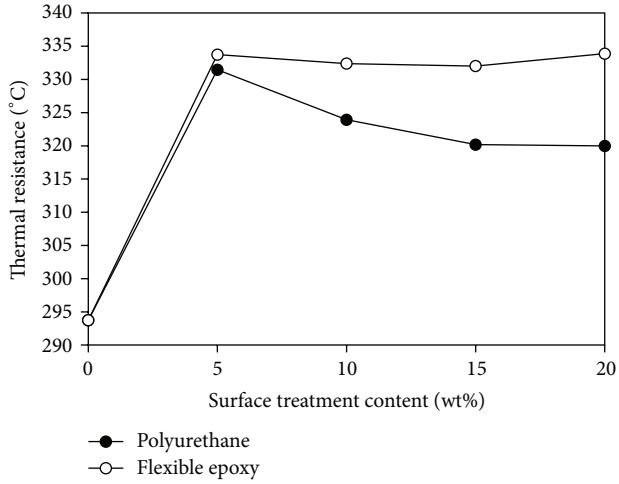

Figure 9: Relationship between thermal resistances of composites by treated with PU and FLEX and content of surface treatment.

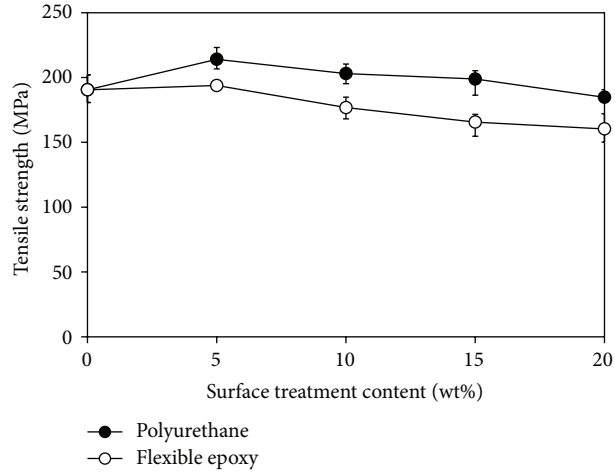

Figure 11: Tensile strength (MPa) of composites by varying surface treatment content of PU and FLEX.

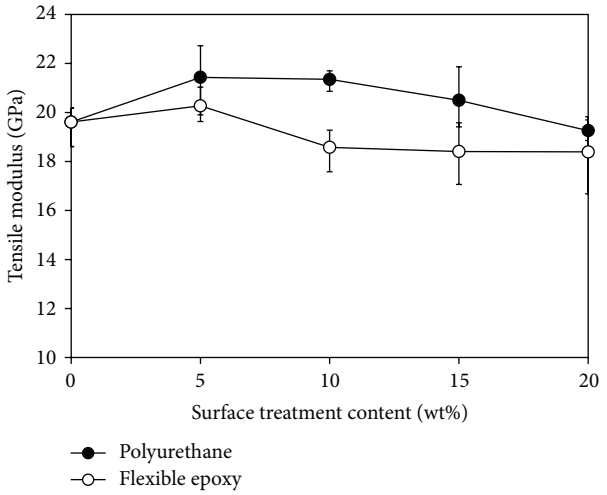

Figure 10: Tensile modulus (GPa) of composites by varying surface treatment content of PU and FLEX.

and FLEX; the bending strength of jute spun yarn/PLA composites showed the highest value at surface treatment content of 5 wt% both for PU and FLEX and slightly decreased with increase in surface treatment content. Specimen treated with PU showed higher strength than the specimens treated with FLEX. This indicates that FLEX was able to improve the interfacial between fiber-matrix interfacial adhesions.

Figure 9 shows the relationship between thermal resistances of composites treated with PU and FLEX and content of surface treatment. In the case of jute spun yarn/PLA composites treated with PU, thermal resistance was increased at PU 5 wt% and slightly decreased with increasing surface treatment content. Meanwhile in the case of jute spun yarn/PLA composites treated with FLEX, thermal resistance was slightly increased with increasing surface treatment content. The jute spun yarn/PLA composites treated with FLEX exhibited higher thermal resistance as compared to the PU.

Figures 10 and 11 show tensile modulus and strength of jute spun yarn/PLA composites with varying the content of surface treatment of PU and FLEX. The tensile modulus and strength of jute spun yarn/PLA composites showed the highest value at surface treatment content of 5 wt% both for PU and FLEX and slightly decreased with increase in surface treatment content. Specimen treated with PU showed higher tensile modulus and strength than the specimens treated with FLEX, because it had good impregnation of PLA into the jute fibers bundle.

From these results, impregnation state was decreased with increase in the surface treatment content, especially for FLEX. On the other hand, it is considered that the interfacial properties were improved by surface treatment especially with PU. Therefore, it was found that the optimum content of surface treatment was 5 wt% with PU to achieve higher mechanical properties.

4. Conclusion

It was established that surface treatment by PU with low content could produce composites with better mechanical properties. This indicates that surface treatment by PU was effective in the impregnation state and the interfacial properties.

References

[1] U. S. Ishiaku, X. Y. Yang, Y. W. Leong, H. Hamada T Semba, and K. Kitagawa, "The effects of fiber content and alkali treatment on the mechanical and morphological properties of PLA/PCL blend jute fiber filled biodegradable composites," *Biobased Materials and Bioenergy*, vol. 1, pp. 78–86, 2007.

[2] K. Goda and Y. Cao, "Research and development of fully green composites reinforced with natural fibers," *Journal of Solid Mechanics and Materials Engineering*, vol. 1, pp. 1073–1084, 2007.

[3] D. Nwabunma and T. Kyu, *Polyolefin Composites*, John Wiley & Sons, 2008.

[4] O. A. Khonder, U. S. Ishikaku, A. Nakai, and H. Hamada, "Fabrication mechanical properties of unidirectional Jute/PP composites using Jute Yarns by film stacking method," *Journal of Polymer and Enviroment*, vol. 13, no. 2, pp. 115–126, 2005.

[5] Y. Takai, N. Kawai, A. Nakai, and H. Hamada, "Effect of resins on crack propagation of long-fiber reinforced thermoplastic composites," in *Design, Manufacturing and Applications of Composites*, pp. 196–202, 2006.

[6] X. Liu and G. Dai, "Impregnation of thermoplastic resin in jute fiber mat," *Frontiers of Chemical Engineering in China*, vol. 2, pp. 145–149, 2008.

[7] S. Thitithanasarn, Y. W. Leong, K. Yamada, H. Nishimura, and H. Hamada, "Effect of natural fiber surface treatment on thermal and mechanical properties of bagasse and nylon 11 composites," *SPE-ANTEC Technical Papers*, vol. 57, pp. 537–540, 2011.

[8] M. Sakaguchi, A. Nakai, H. Hamada, and N. Takeda, "The mechanical properties of unidirectional thermoplastic composites manufactured by a micro-braiding technique," *Composites Science and Technology*, vol. 60, no. 5, pp. 717–722, 2006.

Hindawi Publishing Corporation
Advances in Mechanical Engineering
Volume 2013, Article ID 816513, 8 pages
http://dx.doi.org/10.1155/2013/816513

Research Article

The Processing Design of Jute Spun Yarn/PLA Braided Composite by Pultrusion Molding

Anin Memon[1] and Asami Nakai[2]

[1] *Department of Advanced Fibro-Science, Kyoto Institute of Technology, Matsugasaki, Sakyo-ku, Kyoto 606-8585, Japan*
[2] *Department of Mechanical Engineering, Gifu University, 1-1 Yanagido, Gifu 501-1193, Japan*

Correspondence should be addressed to Anin Memon; anin_rmutt@hotmail.com

Received 4 June 2012; Revised 27 December 2012; Accepted 8 February 2013

Academic Editor: Hiroyuki Hamada

Prevalently, the light has been shed on the green composite from the viewpoint of environmental protection. Jute fibers are natural fibers superior due to light weight, low cost, and being environmentally friendly corresponding to the green composite materials. Meticulously, fibers of polylactic acid (PLA) thermoplastic biopolymer were used as the resin fibers. In this study, the fabrication of tubular jute spun yarn/PLA braided composite by pultrusion molding was presented. The intermediate materials were prepared by commingled technique. The braiding technique manufactured preform which had jute fiber diagonally oriented at certain angles with the glass fiber inserted into the braiding yarns along the longitudinal direction. The braided preforms were pulled through a heated die where the consolidation flow took place due to reduced matrix viscosity and pressure. The pultrusion experiments were done with jute/PLA commingled yarns and combined with glass fiber yarns to fabricate the tubular composite. Impregnation quality was evaluated by microscope observation of the pultruded cross-sections. The flexural mechanical properties of the pultruded were measured by four-point bending test.

1. Introduction

Many of common composite production methods are unsuitable for mass production. One exception is the pultrusion process; it is possible to maintain a continuous production of straight profile with constant cross-sections. Pultrusion is a manufacturing process in which reinforcing fibers impregnation with matrix is pulled through a die to form composites of a constant cross-section. Generally, the unidirectional fibers are impregnated with low viscosity thermosetting resins before passing through a series of dies for shaping and curing during pultrusion process [1–3]. While thermoset pultrusion is a well-known and commercially established manufacturing method, there is less knowledge about the thermoplastic pultrusion. In contrast to thermosets, thermoplastic matrix is generally polymerized, no further chemical reaction is necessary; therefore the processing is reduced to first melting the matrix, then shaping the composite under pressure, and finally cooling it to preserve the new shape. Thermoplastic resins contain very high melt viscosities which difficultly make the melt matrix resin impregnated into the reinforcement fiber. For this reason, various intermediate materials have been developed to overcome these problems such as microbraided yarn, commingled yarn, and parallel configuration yarn as shown in Figure 1. The schematic of tubular braiding fabric was showed in Figure 2, all fiber bundles are diagonally oriented, and the angle (θ) of the fiber bundle to the longitudinal direction can be adjusted freely. Also, the fiber bundle called the middle end yarn (MEY) can be inserted into the braiding yarns (BY) along the longitudinal direction. For this reason, the braiding technique can control the anisotropic of pultrusion molding.

In the early stage, jute fiber reinforced PLA resin has been made with good impregnation quality and mechanical properties using compression of microbraided yarns [4, 5]. The thermoplastic braided composite by pultrusion molding with various forms of materials has been widely studied. The method combines the braiding technique of the pultrusion process to produce multiaxially reinforced continuous beam were successful with using PP/Glass fiber [6]. The braiding

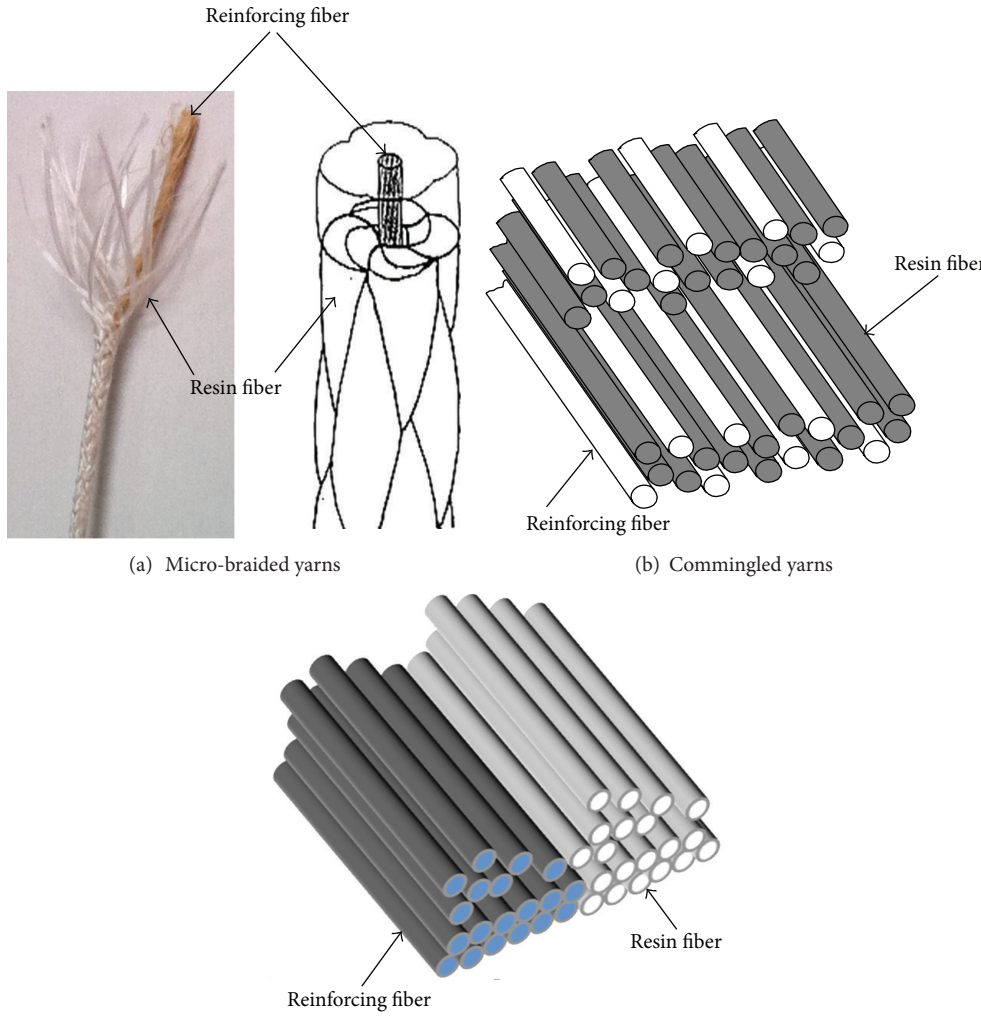

(a) Micro-braided yarns

(b) Commingled yarns

(c) Pararlle yarns

Figure 1: The schematic of intermediate material.

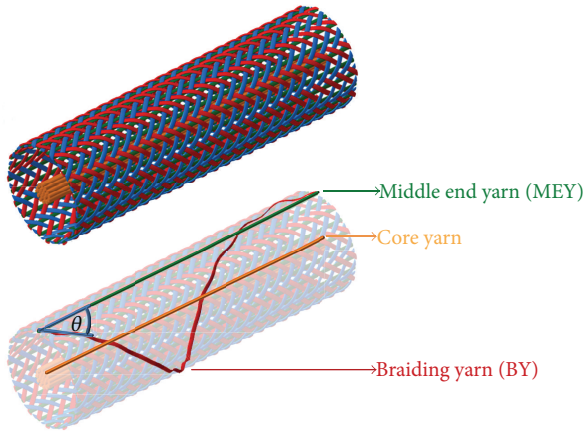

Figure 2: The schematic of tubular braiding fabric.

technique was developed for pultrusion of the continuous fiber reinforced thermoplastic tube which commingled yarn carbon fibers and PA66 which were used as intermediate materials [7]. The pultrusion technique was used to manufacture the continuous composite using flax fiber reinforced PP which offers good opportunities as the reinforcement material for composite, good mechanical properties and the ecological and environment advantages [8].

The use of natural fibers derived from annually renewable resource as reinforcement in thermoplastic matrix composite provides the positive environment benefit with respect to ultimate disposability and raw materials utilization [9–11]. The biocomposites, using natural fibers compounded with natural matrices, could diminish the impact of plastic waste on the environment. Jute fibers are natural fibers superior due to light weight, low cost, and being environmentally friendly corresponding to the green composite materials. PLA is biodegradable aliphatic polyester derived from renewable resources, such as cornstarch, tapioca, or sugarcanes. PLA can be processed like most thermoplastics into fiber or film. Previously, jute fiber reinforced PLA resin has been made with good impregnation quality and mechanical properties using compression of microbraided yarns. In this study, the

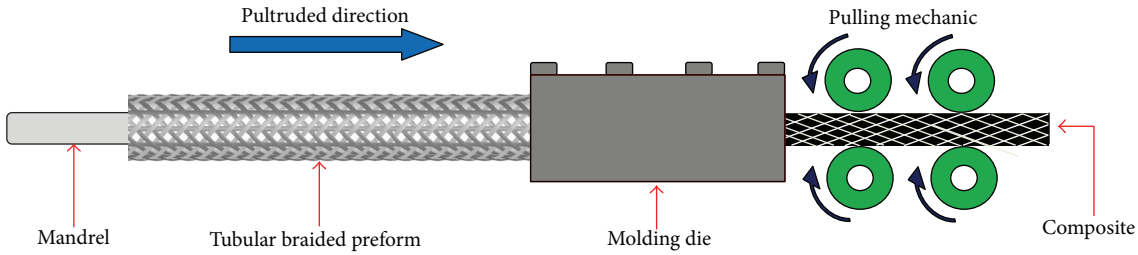

Figure 3: The schematic of pultrusion process of braided composite.

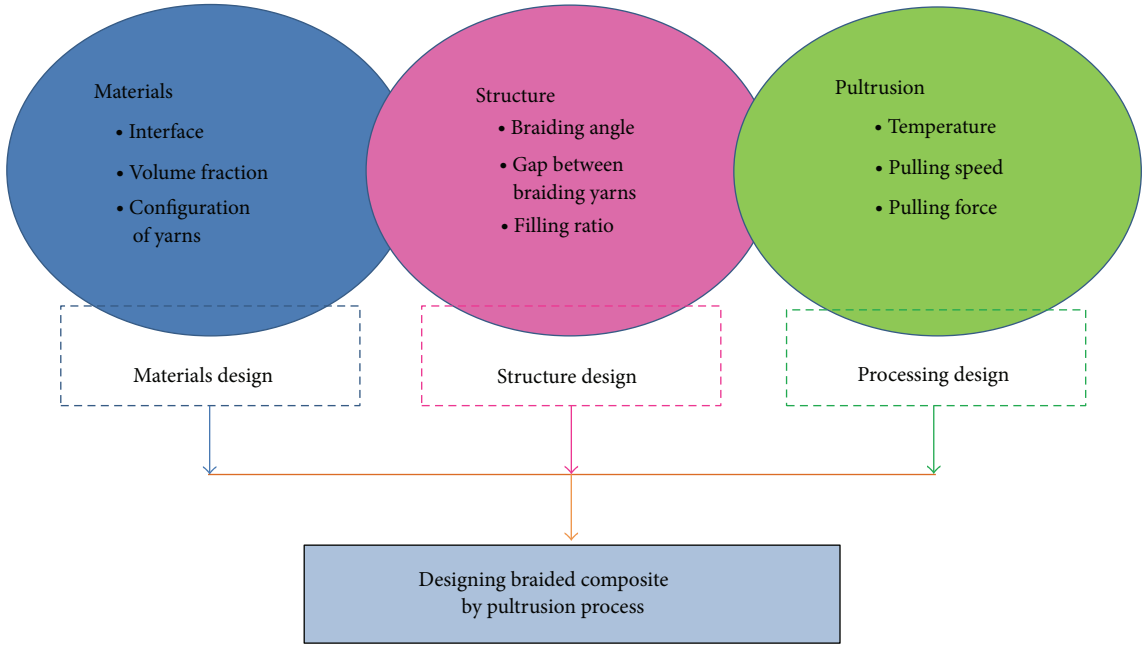

Figure 4: Design concept of braided composite by pultrusion molding.

commingled yarus were used as intermediate materials (as shown in Figure 2(b)).

The advantages of pultrusion process are threefold. Firstly, it is suitable to produce the continuous composite with uniform cross-sections. Secondly, it also has mass production and low cost. Finally, the composite contains high mechanical properties due to the continuous fiber. The objective of this investigation was to demonstrate the fabrication of the tubular jute spun yarn/PLA braided composite by pultrusion molding. The jute spun yarn was used as reinforcement, and PLA was used as the matrix resin corresponding to the green composite materials. Figure 3 shows the schematic of pultrusion process of braided composite in this study. The commingled yarns were used as intermediate materials to prepare the pultrusion preform by braiding technique. The fabrication quality of pultrusion process was evaluated by cross-section observation and mechanical properties evaluated by four-point bending test.

2. Materials and Experiment

2.1. Design Concept. In this paper, the designed concept of braided composite by pultrusion molding is described. The designed concept involves the materials design, structure design, and processing design as shown in Figure 4. Material designs consisted of interface such as surface treatment on reinforcement fiber, volume fraction, and configuration of yarn on intermediate materials. Braiding angle, gap between braiding yarns, and filling ratio are the important parameters of the structure design. Meanwhile, the processing designs consisted of pultrusion temperature, pulling speed, and pulling force.

2.2. Materials. In the previous study, the intermediate materials were prepared by microbraided yarn and parallel configuration yarn. Successful tubular braided composite was realized using glass fiber for middle end yarns in the braided structure. It was found that successful tubular braided composite was realized using glass fiber 1,150 tex for middle end yarns in the braiding structure. The highest bending strength and modulus were found in the specimen using parallel yarn configuration. Meanwhile, the region of unimpregnation areas is seen inside reinforced fiber, and macrovoids are seen outside the fiber [12].

Following the designed concept in this study, jute fiber tows were commingled with PLA fiber. Figure 5 showed the commingled technique for mixing the resin fiber with reinforced fiber. The jute fibers tow having a fineness of ~400

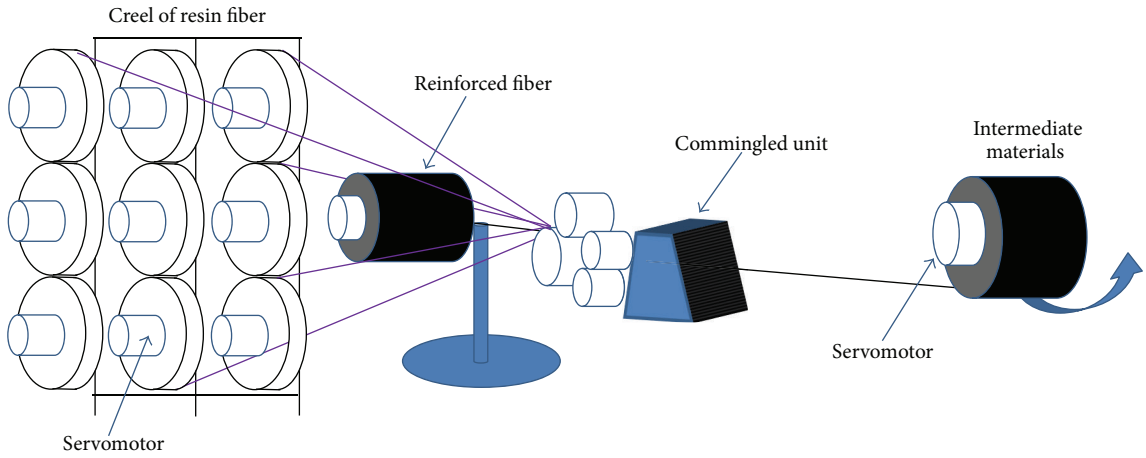

Figure 5: Commingled technique.

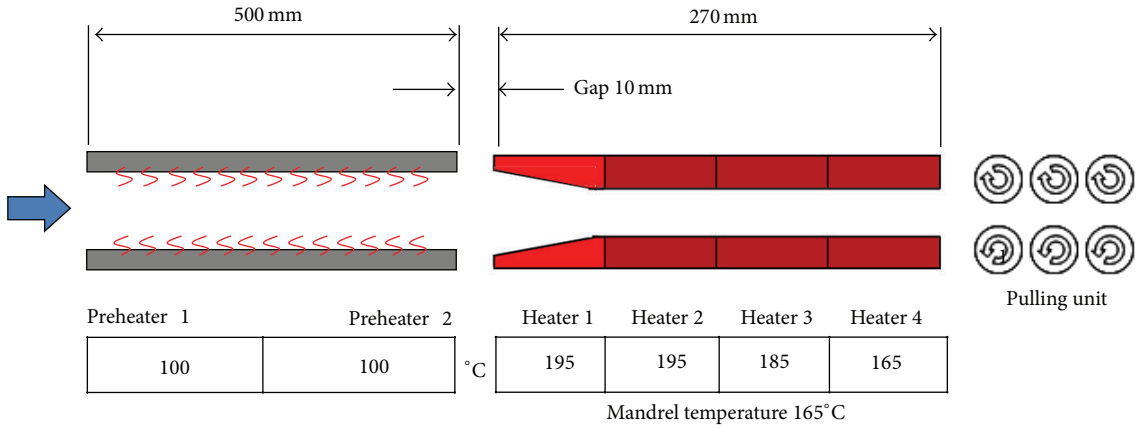

Figure 6: Schematic of the pultrusion system.

tex were used as reinforcement fibers. The continuous PLA fibers in a tow configuration were used as resin fibers, having a fineness of ~56 tex. Glass fiber (GF) yarns having a fineness of 1150, 720, 600, and 520 tex were used as MEYs. They were used to enhance the strength of braided fabric. The braided fabric preforms for pultrusion were fabricated using 48 BY and 24 MEYs in a tubular braiding machine with 48 carriers (Murata Machinery). The braided preforms were done using braiding ring with diameter of 30 mm and mandrel with diameter of 20 mm, and the braiding angle was 30–38 degrees. The layer of braided fabric was 2 layers. Table 1 lists the four tubular braided preforms with different GFs as MEYs.

Generally, glass fiber had strength around 1.5 GPa, jute fiber had strength around 207 MPa, and PLA fibers had strength around 48 MPa. The strength of materials was used to estimate the limited force for pultrusion molding. In the estimation, the fibers in braided preform were assumed in parallel configuration (braiding angle equal to 0 degree). The estimated limited pulling forces of preforms were 20.52, 22.82, 26.28, and 38.66 kN, respectively.

2.3. Molding. Figure 6 shows the schematic of the tubular pultrusion molding assembly, consisting of the preheater and the pultrusion die. The tubular molding die had outside

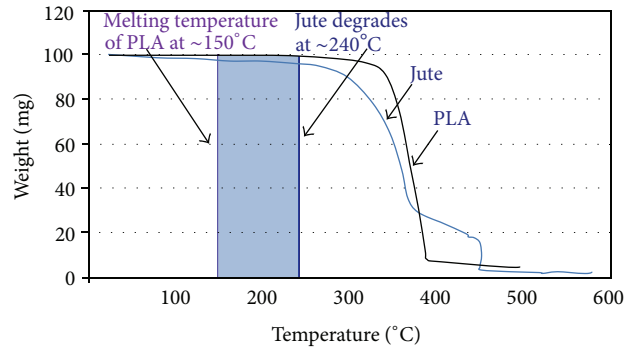

Figure 7: The TGA data of jute and PLA.

diameter of 23 mm and inside diameter of 20 mm (mandrel). The length of the molding die was 270 mm. The preheater had length 500 mm, and the entrance side of the die was large and gradually reduced in taper region 50 mm until a constant cross-section of the die. According to the TGA data of jute and PLA (Figure 7), the thermal resistance of the jute degrades at ~240°C and PLA degrades at ~320°C. Meanwhile the melting temperature of PLA was ~175°C. Therefore, the

Table 1: Lists of the four different tubular braided preforms.

Preform number	Braiding angle (degree; °)	Vf of composite (%)	Vf of jute (%)	Vf of GF (%)	Filling ratio (%)
(1) GF520	38	43.26	33.41	9.85	101
(2) GF600	38	46.18	32.58	13.60	101
(3) GF720	35	46.27	32.58	13.69	101
(4) GF1150	30	52.60	30.81	21.80	104

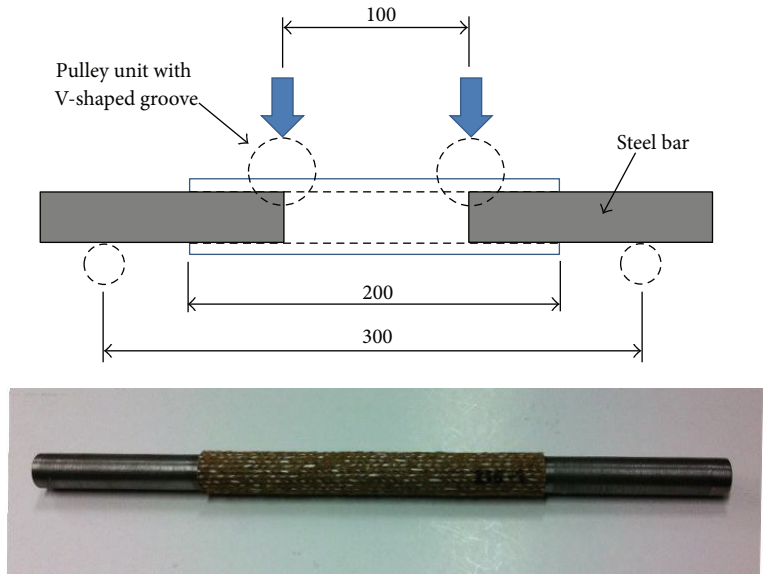

Figure 8: The schematic of four-point bending test.

Table 2: Pultrusion temperature.

Preform number	Pultrusion temperature (°C)	Pulling speed (mm/min)
1	195	18
2	205	18
3	215	18
4	225	18
5	235	18

*The temperature is changed in molding die zones 1 and 2.

processing window of pultrusion temperature could be ~175–240°C. In this study, the pultrusion temperature was designed at 195–235°C. Prior to pultrusion, the preforms were dried at 80°C in convection oven for 2 hours. The preheater was set to 100°C. The molding die had four separate heating zones, and the temperature at each zone was set, respectively, at 195, 195, 185, and 165°C from entrance side of the die. The temperature of mandrel inside the molding die was set to 165°C. The braided preforms were pulled through the molding die by a pulling mechanic at a speed of 18 mm/min. Generally, GF was used as MEY to enhance the strength of tubular braided preform for pultrusion molding. This study will select the preform which uses the small amount of glass fibers in braided preform to examine the effect of molding temperature. After that the five specimens were produced by changing the pultrusion temperature in molding die zone 1 and zone 2 with constant molding speed. The pultrusion temperature is shown in Table 2. The pultruded specimens were cut and polished in a direction perpendicular to longitudinal direction for the cross-section observation in order to investigate the internal state of the molding by using optical microscope.

2.4. Experiments. The mechanical properties were performed by four-point bending test. It was performed by using the pulley unit and the metal solid bar as shown in Figure 8. The pulley unit and steel bar are capable of decreasing the stress concentration generated at the point for support and loading nose. The bending test was performed by using an INSTRON universal testing machine with a span length of 300 mm and cross-head speed of 1 mm/min.

3. Result and Discussion

The pultrusion of preform with GF520 and GF600 was interrupted due to the MEY breakage inside the pultrusion die. The preform with GF720 and GF1150 was fabricated without problem because it had enough strength for pultrusion. The tubular composite jute/PLA with GF1150 had rougher surface than using GF720. From these results, the preforms which had limited pulling force lower than 26.28 kN

(a) Tubular composite jute/PLA with GF 1150 (b) Tubular composite jute/PLA with GF 720

Figure 9: The tubular braided composite.

(a) Specimens No.1—195°C

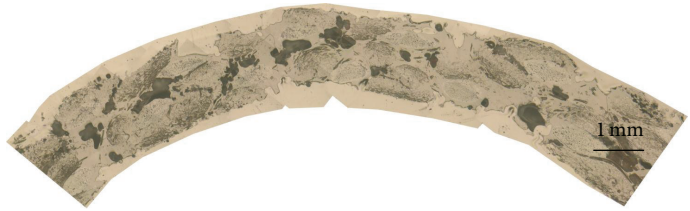

(b) Specimens No.2—205°C

(c) Specimens No.3—215°C

(d) Specimens No.4—225°C

Figure 10: The cross-section observation of specimens.

were unsuccessful for pultrusion molding. The preform with GF720 was successfully pultruded and had minimized usage of glass fiber and good surface quality as shown in Figure 9. Therefore, it was selected for the experiment with the different pultrusion temperature.

From Table 3, specimens no. 5 could not be successfully fabricated because the jute fibers of specimens were burned due to high temperature. The specimens with molding temperature of 195, 205, 215, and 225°C were successfully pultruded. The result from four-point bending test was

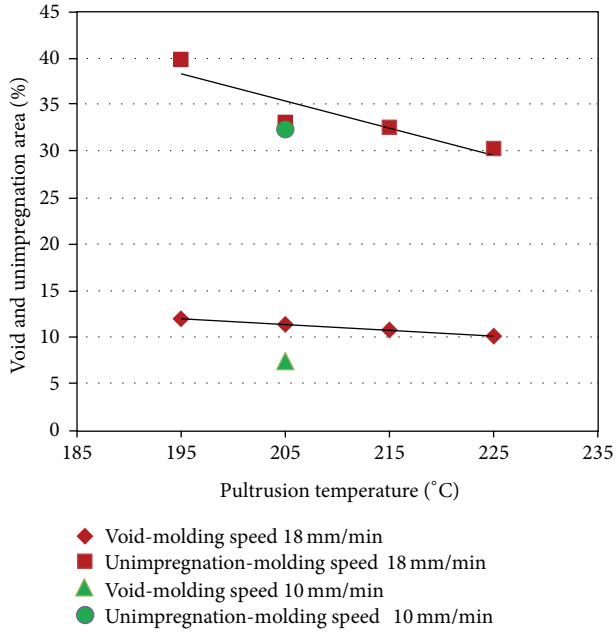

Figure 11: Relationship between void, unimpregnation, and molding temperatures.

Table 3: The result from four-point bending test.

Specimens number	Pultrusion temperature (°C)	Modulus		Strength	
		(GPa)	S.D.	(MPa)	S.D.
1	195	8.95	0.73	29.04	1.88
2	205	9.64	0.78	29.96	1.29
3	215	9.26	0.47	29.00	3.12
4	225	8.80	1.64	24.52	3.31
5	235	Unsuccessful		Unsuccessful	

shown in Table 3. The highest bending modulus of 9.64 GPa and strength of 29.96 MPa were obtained in specimens no. 2. Meanwhile, specimens no. 4 had the lowest modulus and strength because the temperature was higher than others.

The characteristic of commingled yarn in this study shows the higher mechanical properties compares to the previous study with the similar filling ratio because the resin fibers were mixed with jute spun yarns using blow air. In the previous study, microbraiding yarn and parallel yarn configuration were used as braiding yarns for fabricating the preforms. The cross-section photographs of specimens are shown in Figure 10. From the photograph, the dark regions between the fiber bundles indicate macrovoid and the dark regions inside of fiber bundles indicate unimpregnation area. The relationship between void, unimpregnation, and molding temperature is shown in Figure 11. Consequently, it was clarified that void and unimpregnation area was decreased with increasing the molding temperature. Moreover, it was found that void and unimpregnation area was decreased with decreasing the molding speed. Figure 12 shows the cross-section photographs of specimens with temperature 205°C, and pulling speed was decreased to 10 mm/min. The void area was 7.47% and un-impregnation area was 32.36% (as shown in the comparison in Figure 11).

From these results, the impregnation quality was increased when the molding temperature increased because the matrix viscosity was reduced at higher temperature. The matrix resin was easily impregnated into the jute spun yarn and GF. Meanwhile, with increasing molding temperature the modulus and strength were decreased due to the high temperature affecting the degradation of jute spun yarns. Therefore, the molding temperature of 205°C is the optimum temperature for fabrication of the tubular jute spun yarn/PLA braided composite. Moreover the impregnation quality was improved by decreasing the pulling speed.

4. Conclusion

Pultrusion molding is one technique for manufacturing the continuous composite with uniform cross-sections. In this study, the processing design of tubular braided composite using jute spun yarns reinforced PLA by pultrusion molding was performed. The commingled technique mixed the resin fiber and jute spun yarn which were used as intermediate materials. The effects of processing design such as the

Figure 12: The cross-section observation of specimens with pulling speed 10 mm/min.

molding temperature and the molding speed are effects on the impregnation quality and mechanical properties of tubular braided composite. It was clarified that the impregnation quality increased with increasing the molding temperature and decreasing the molding speed. While the temperature increased, the mechanical properties decreased. The pultrusion of jute spun yarn/PLA tubular braided composite in this study is an important step towards the economically viable production of high performance of the biocomposite products.

References

[1] G. Bechtold, S. Weidmer, and K. Friedrich, "Pultrusion of thermoplastic composite—new delopement and modeling studies," *Thermoplastic Composite Materials*, vol. 15, pp. 443–465, 2002.

[2] A. Carlsson and B. Tomas Åström, "Experimental investigation of pultrusion of glass fibre reinforced polypropylene composites," *Composites Part A*, vol. 29, no. 5-6, pp. 585–593, 1998.

[3] D. H. Kim, W. I. Lee, and K. Friedrich, "A model for a thermoplastic pultrusion process using commingled yarns," *Composites Science and Technology*, vol. 61, no. 8, pp. 1065–1077, 2001.

[4] N. Shikamoto, P. Wongsriraksa, A. Ohtani, Y. W. Leong, and A. Nakai, "Processing and mechanical properties of jute reinforced PLA composite," in *Proceedings of the 52nd International SAMPE Symposium: Material and Process Innovations: Changing our World (SAMPE '08)*, May 2008.

[5] O. A. Khondker, U. S. Ishiaku, A. Nakai, and H. Hamada, "A novel processing technique for thermoplastic manufacturing of unidirectional composites reinforced with jute yarns," *Composites Part A*, vol. 37, no. 12, pp. 2274–2284, 2006.

[6] W. Michaeli and D. Jürss, "Thermoplastic pull-braiding: pultrusion of profiles with braided fibre lay-up and thermoplastic matrix system (PP)," *Composites Part A*, vol. 27, no. 1, pp. 3–7, 1996.

[7] Y. Tanaka, N. Shikamoto, A. Ohtani, A. Nakai, and H. Hamada, "Development of pultrusion system for carbon fiber reinforced thermoplastic composite," in *Proceedings of the 17th International Conference on Composite Materials*, 2009.

[8] K. Van De Velde and P. Kiekens, "Thermoplastic pultrusion of natural fibre reinforced composites," *Composite Structures*, vol. 54, no. 2-3, pp. 355–360, 2001.

[9] A. K. Mohanty, M. A. Khan, and G. Hinrichsen, "Surface modification of jute and its influence on performance of biodegradable jute-fabric/Biopol composites," *Composites Science and Technology*, vol. 60, no. 7, pp. 1115–1124, 2000.

[10] P. J. Herrera-Franco and A. Valadez-González, "Mechanical properties of continuous natural fibre-reinforced polymer composites," *Composites Part A*, vol. 35, no. 3, pp. 339–345, 2004.

[11] P. Wambua, J. Ivens, and I. Verpoest, "Natural fibres: can they replace glass in fibre reinforced plastics?" *Composites Science and Technology*, vol. 63, no. 9, pp. 1259–1264, 2003.

[12] A. Memon and A. Nakai, "Structure and processing design of jute spun yarns/PLA composite by pultrusion molding," in *Proceedings of the ANTEC*, Orlando, Fla, USA, 2012.

Hindawi Publishing Corporation
Advances in Mechanical Engineering
Volume 2013, Article ID 496274, 7 pages
http://dx.doi.org/10.1155/2013/496274

Research Article

Developing Simple Production of Continuous Ramie Single Yarn Reinforced Composite Strands

Hyun-Bum Kim,[1] Koichi Goda,[2] Junji Noda,[2] and Kenji Aoki[3]

[1] *Graduate School of Science and Engineering, Yamaguchi University, Yamaguchi, Ube 755-8611, Japan*
[2] *Department of Mechanical Engineering, Yamaguchi University, Yamaguchi, Ube 755-8611, Japan*
[3] *Product Management Division, Kayaku Akzo Co., Ltd., Yamaguchi, Sanyo-Onoda 755-0002, Japan*

Correspondence should be addressed to Hyun-Bum Kim; r501wc@yamaguchi-u.ac.jp

Received 2 June 2012; Revised 28 December 2012; Accepted 20 January 2013

Academic Editor: Amar Mohanty

This paper deals with long fiber-reinforced composite strands using continuous ramie yarns, in which polypropylene including MA-PP (maleic anhydride-grafted polypropylene) was used as a matrix material. The composite strands were fabricated by a new method called multi-pin-assisted resin impregnation (M-PaRI) process, for which the equipment was newly applied after conventional extrusion process. The composite strands were then pelletized and injection molded. Tensile strength and Young's modulus of the resultant short ramie/PP reinforced composites were investigated. Results show that this new process improved the mechanical properties of injection-molded specimens.

1. Introduction

Glass fiber, a representative reinforcement for polymer matrix composites, has many excellent physical and mechanical properties such as low density, heat resistance, wear resistance, and high specific strength, and stiffness. Glass fiber-reinforced composites have thus been investigated for many years because of huge demand for their use in industry. They also have disadvantage such as difficulty in disposal after their lifetime. Important recent concerns are environmental problems such as global warming caused by petroleum-based materials and energy. These concerns have shifted the focus to producing alternative materials and energy from biomass resources commonly throughout the world. In December, 2010, the Japanese government made a cabinet decision to administer a plan called The Master Plan for the Promotion of Biomass Utilization [1]. By this plan, additional research and development of the utilization of herbaceous plants and woods were demanded.

Plant-based natural fibers are abundant, biodegradable, and renewable. Moreover, they have similar specific strength and stiffness to those of glass fiber [2–5]. On the other hand, plant-based natural fibers also have disadvantages such as poor compatibility with hydrophobic polymer matrices [6–8], flammability, and thermal instability [9–11]. Despite those drawbacks, increasing attention has been devoted to improvement of natural fibers as reinforcement of polymer matrix composites that can be substituted for petroleum-based fibers [12, 13]. Ramie, a well-known plant-based natural fiber, can be used as a textile fiber because of low lignin content [14]. It has advantages of high tenacity, silk-like luster, and resistance to bacteria. Ramie is also a popular reinforcement material used for polymer matrix composites [15].

During the last two decades, various attempts have been made to develop various methods for producing complete composites using reinforcements such as glass/natural fibers and thermoplastic resins. The main problem is that the fibers often break, resulting in shorter fiber length than the critical one [16] because the fibers were inserted directly into the extrusion machine. In order to maintain appropriate mechanical properties of the composites, the fiber length must be longer than the critical value. One method is to use pultrusion technique developed by ICI for the manufacture of Verton long fiber molding materials [17, 18]. The impregnation devices applied in the past are simple in form, as used in the processing of thermoset resin. Thomason [19] also introduced a coating process using jute yarns to

Table 1: Physical and chemical properties of ramie fibers.

Density (g/cm^3)	Cell diameter (μm)	Cell length (mm)	Microfibril angle (°)	Moisture content (wt%)	Chemical composition (wt%)					
					Cellulose	Lignin	Hemicellulose	Pectin	Wax	Refrence
1.50	—	—	7.5	8.0	68.6–76.2	0.6-0.7	13.1–16.7	1.9	0.3	[22]
	40–50	154	7.5–1.2	—	80–85	0.5	3-4	—	—	[23]

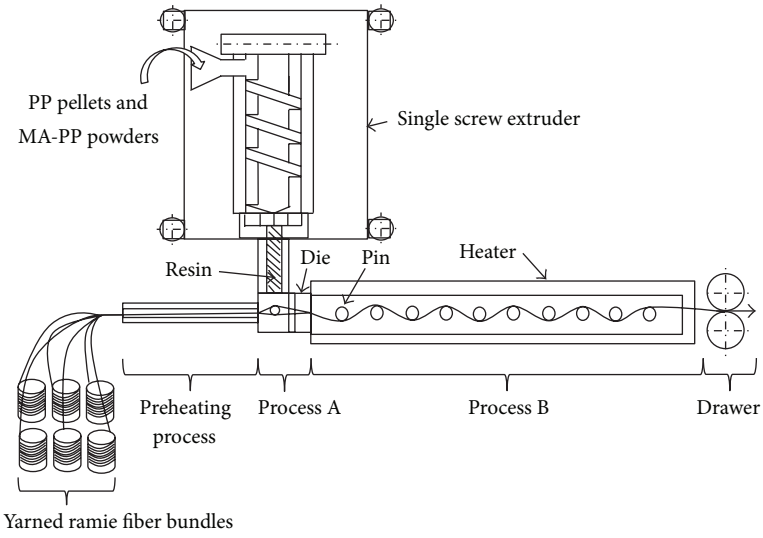

Figure 1: Schematic view of the present fabrication system. (Process A: resin-coating process, Process B: multi-pin-assisted resin impregnation (M-PaRI) process).

produce thermoplastic resin matrix composite strands. However, poor performance of tensile properties on injection-molded composite materials was reported. Bledzki et al. [20] used a two-step extrusion process for the combination of natural fiber yarns and polylactic acid (PLA) to improve impregnation into interfibers. Recently, a new technology for production of jute-twisted yarn-reinforced composites was reported by Tanaka and Hirano [21], in which both complete impregnation and long fiber length were achieved. Results showed that the resultant composites yielded much better mechanical properties than those of short fiber-reinforced composites, while the disadvantage of this technology is that the fabrication procedures are complicated.

In this study, thus, a continuous ramie single yarn reinforced polypropylene (PP) composite strand was developed using a new and simple combined technique. The strands were chopped to pellets for injection-molding, and tensile properties of the molded specimens were investigated.

2. Experimental

2.1. Materials. Continuous ramie single yarns, having fineness of 95 tex, Type no. 16 (Tosco Co., Ltd., Japan) and polypropylene (Prime Polymer Co. Ltd., Japan) were used as reinforcement and matrix material, respectively. Physical and chemical properties of ramie fibers are listed in Table 1 [22, 23]. According to [22, 23], although cellulose contents vary widely from 65% to 85%, both data are in an agreement in terms of low lignin contents. The cross-sectional area of ramie fibers is not circular, but rather elliptical as shown later. The major axis is approximately 30 μm. The degree of microfibrillar angle of ramie fibers is one of the smallest classes among plant-based natural fibers.

It is known that high adhesion between hydrophilic fibers and hydrophobic resin by chemical bonding is induced by available OH groups on the fiber surface. The resin adheres to the fiber surface through molecular chain entanglement. During this reaction, maleic anhydride-grafted polypropylene (MA-PP) works as a coupling agent to realize such chemical bonding [24]. In this study also, MA-PP (Kayaku Akzo Co., Ltd., Japan) was used to promote a chemical interaction between the fiber and matrix.

2.2. Fabrication Procedures. Figure 1 shows a schematic of the present fabrication system. Continuous ramie single yarn/PP composites were produced through a new combined technique proposed in this study, which consists of resin coating and multi-pin-assisted resin impregnation (M-PaRI) processes, as shown in Processes A and B of Figure 1. The continuous ramie single yarns were first delivered via preheating process into a cross-head die attached to a ϕ15 mm single screw extruder (Musashino Kikai Co., Ltd., Japan), into which PP pellets and MA-PP powders were fed at the same time. The mixed resin was coated onto the ramie yarns in the die at Process A (resin-coating process). Subsequently, it was impregnated into interfibers through the multi-pin system, as shown in Process B (M-PaRI) of Figure 1. The number and diameter of pins used here were 22 and 5 mm, respectively.

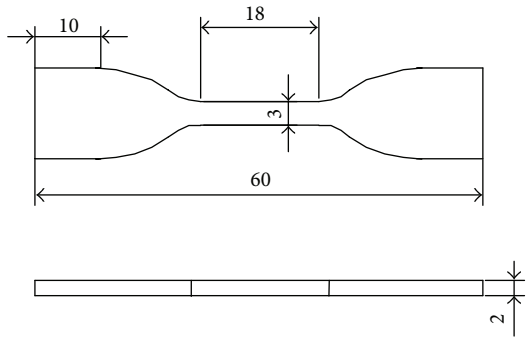

Figure 2: Shape and dimensions of small-sized tensile specimen.

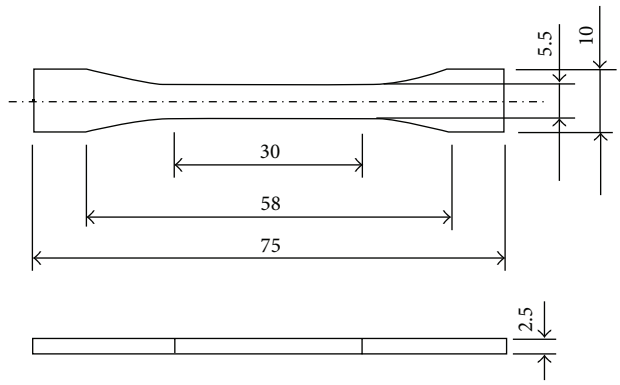

Figure 3: Shape and dimensions of medium-sized tensile specimens.

Temperatures of the single screw extruder were all set at 190°C with a screw speed of 7.0 rpm. A motor was set to draw the composite strand with a screw speed of 45.0 rpm.

The continuous composite strands containing six ramie yarns were chopped to pellets of 2 mm length. The set temperature(s) was 190°C at Process A, and was changed in the 160–225°C range for Process B. The pellets were molded into specimen dies of two types on an injection molding machine (Shinko Sellbic Co., Ltd.). Then small- (Japanese Industrial Standards, JIS K 7162, Type 5B) and medium-sized (JIS K 7162, Type 1BA) tensile specimens were obtained, as shown in Figures 2 and 3, respectively. The temperatures were set at 180–185°C for injection molding. Fiber contents of small- and medium-sized specimens were adjusted to 30 wt% and 10–50 wt%, respectively.

2.3. Tensile Test. Tensile tests were conducted using a universal testing machine (Desktop type universal testing machine, LSC-1/30, JT Toshi Co., Ltd.) for small-sized specimens, and tensile and compression testing machine (Minebea Co., Ltd.) for medium-sized specimens at a crosshead speed of 10 mm/min and 17 mm/min, respectively. The mean cross-section area of small- and medium-sized specimens was measured on three locations along the longitudinal direction, using a micrometer and then taking an average. Five specimens were evaluated to obtain an average value. Ultimate stress (MPa), stiffness (GPa, linear region between strain 0.05 and 0.25), and strain (%) were determined from the stress-strain curves for each test.

3. Results and Discussion

3.1. Degree of Continuous Strand Impregnation by the Proposed Combine Technique. Microscopic cross-section images of ramie/PP composite strands are shown in Figure 4, in which the temperature of Process B was set at 195°C. The strand was taken out of the fabrication system after it was stopped intentionally. Its several cross-sections before or inside Process B were observed. It is apparent from Figure 4(a) that many voids exist among fibers before Process B, although resin is locally infiltrated. Bledzki et al. [20] carried out a two-step extrusion process, in which abaca/PLA strands obtained firstly by yarn coating process were pelletized and secondly inserted into a single extruder. It is guessed that the second process was conducted because such voids might not be removed in the first-step process. Figures 4(b) and 4(c) show images after the 11th and 15th pins, respectively. They show almost no void. The final product in Figure 4(d) shows that the cross-section contains the resin completely infiltrated among fibers with no void. It is well verified that the attached multi-pin system assists in impregnating the resin into interfibers. This system does not need any additional extrusion process. The mechanism of this impregnation is estimated such that continuous contact and rubbing between resin-coating yarns and pins flattens the yarns and widens the interfiber spaces. Consequently, the resin can be impregnated easily among fibers.

Tanaka and Hirano [21] achieved complete resin impregnation for jute-twisted yarn. They also widened the interfiber spaces through an untwisted yarn process. Although this process can control the magnitude of the spaces by changing the number of untwists, it has to be prepared for each yarn. It demands complicated and expensive facilities. On the other hand, the composite process proposed herein can be widened among fibers by a simple process, as mentioned previously. It is concluded that, thereby, the composite strands can be produced successfully and more easily through such a combined technique: a conventional resin-coating process (Process A) followed by M-PaRI process (Process B).

3.2. Tensile Properties

3.2.1. Stress-Strain Behavior. Figure 5 shows the effect of temperature during Process B on the tensile stress-strain behavior of the composites specimens containing 30 wt% fibers. The size of specimen was a small type in Figure 2. All of the stress-strain curves show nonlinearity at around 2-3%, but the stress levels during deformation of composite specimens are much higher than that of PP. The level of composite stress also depends on the temperature at Process B. Composite specimens produced at low temperatures during Process B, that is, 160°C and 185°C, exhibit less stress, while composite specimens produced at 195°C, 205°C, and 225°C show higher stress and almost identical stress-strain behavior, especially at the initial stage. However, composite specimens produced at 160°C, 185°C, and 195°C exhibit a similar strain at break,

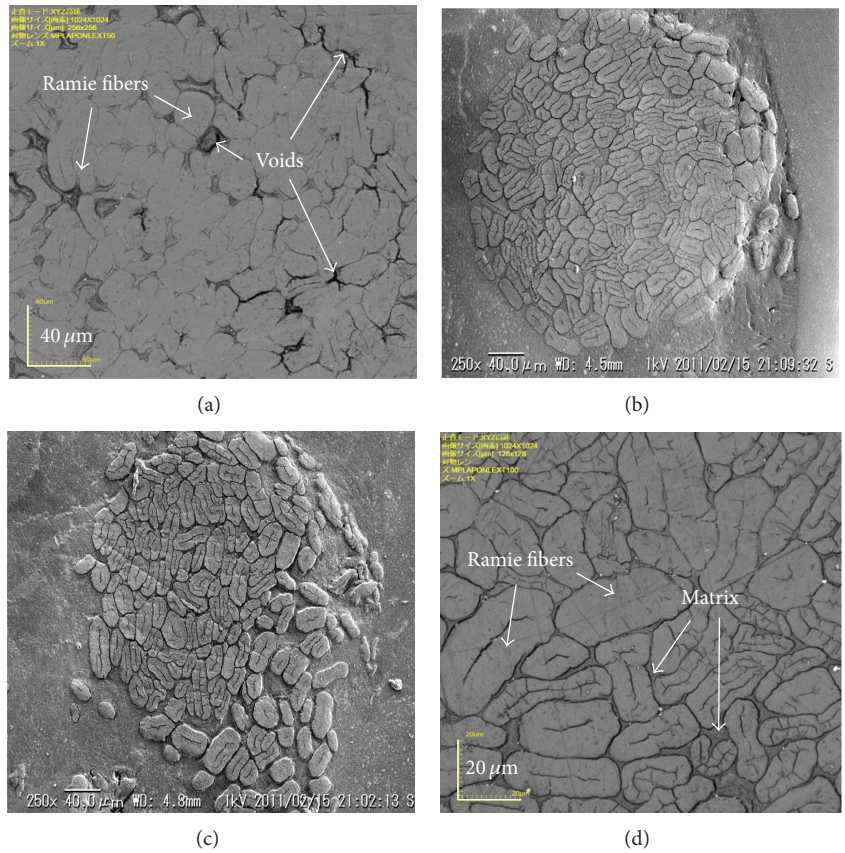

Figure 4: Cross-sectional images of ramie/PP composite strands—(a) before M-PaRI process, (b) after 11th pin, (c) after 15th pin, and (d) final product. Images in (a) and (d) are obtained using 3D laser measuring microscopy. Images in (b) and (c) were obtained using scanning electron microscopy.

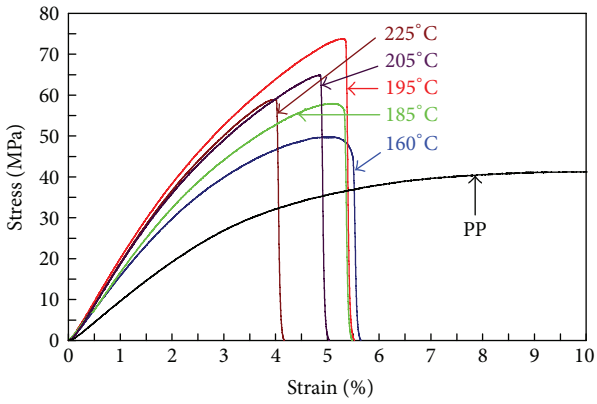

Figure 5: Typical stress-strain curves of short ramie/PP reinforced composites produced at different temperatures during Process B.

Table 2: Tensile properties of short ramie/PP composites.

Material	T_{rip} °C	Young's modulus (GPa)	Tensile strength (MPa)	Fracture strain (%)
PP (0 wt%)	—	1.04 (0.071)	42.4 (0.027)	>200
Composites	160	1.45 (0.11)	50.6 (0.053)	5.65 (0.083)
	185	1.64 (0.080)	55.1 (0.066)	5.32 (0.077)
	195	1.94 (0.072)	69.2 (0.046)	5.37 (0.040)
	205	1.72 (0.12)	67.7 (0.032)	5.26 (0.039)
	225	1.72 (0.086)	53.1 (0.086)	4.04 (0.093)

T_{rip}: temperature at multi-pin-assisted resin impregnation (M-PaRI) process.
Numbers in parentheses denote coefficients of variation.

whereas those produced at 205°C and 225°C show less fracture strain. In other words, less fracture energy is brought from thermal exposure higher than 195°C during Process B.

3.2.2. Tensile Strength and Young's Modulus. Table 2 shows averages and coefficients of variation of the tensile properties of the small-sized PP and composite specimens. It can be seen that tensile strength and Young's modulus increase with increasing temperature over the whole 160–195°C range. Eventually, in the composites specimens of 195°C, not only did tensile strength improved 1.63 times higher than that

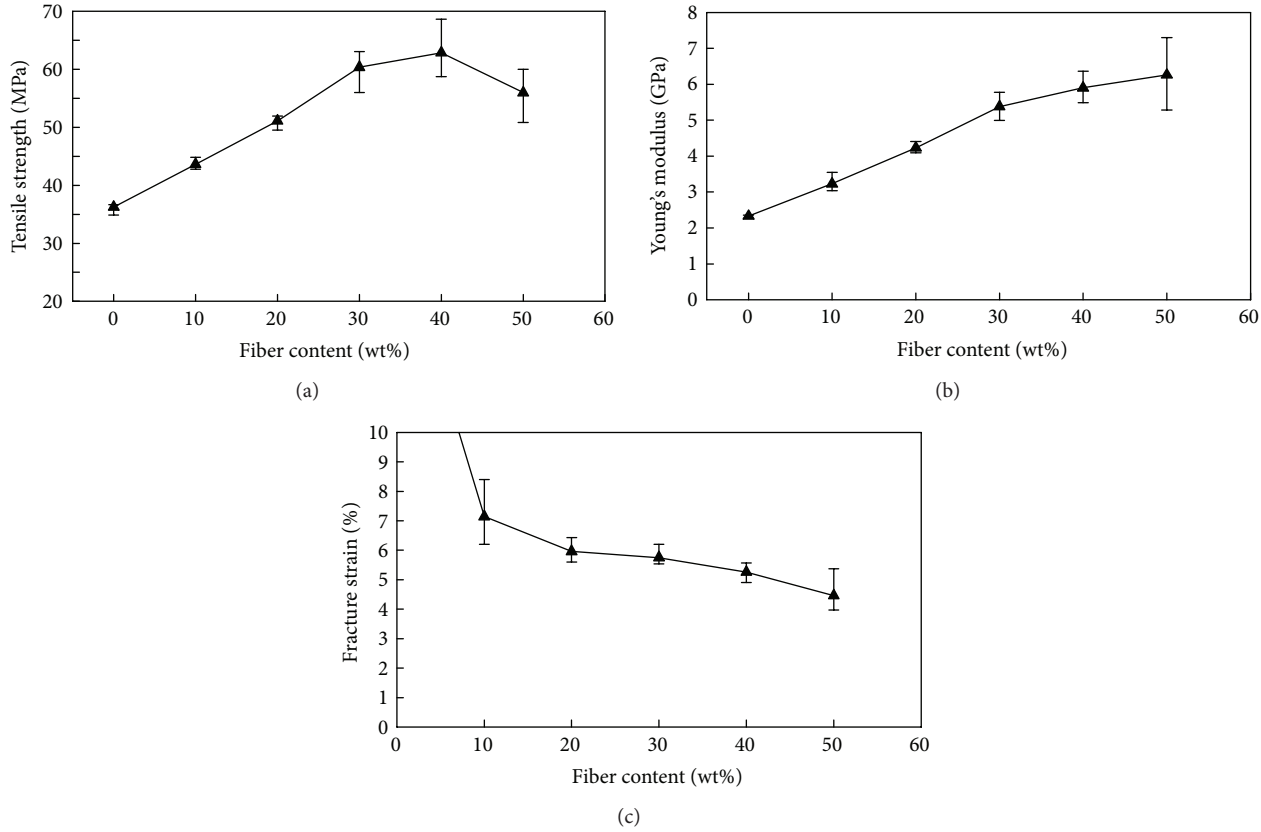

Figure 6: Effect of fiber content on tensile properties of short ramie/PP reinforced composites produced at 195°C during Process B—(a) tensile strength, (b) Young's modulus, and (c) fracture strain.

of PP specimens, but also Young's modulus increased 1.87 times. However, a slight decrease in tensile strength in the specimens of 205°C is found with a subsequent dramatic decrease of 225°C. From the above, the maximum properties of composites could be obtained at 195–205°C in the present fabrication system.

It was observed that voids did not disappear, similar to Figure 4(a), when the composite strands were produced at 160°C and 185°C. That is to say, the resin was not impregnated completely into interfibers even after Process B. The remaining voids decreased tensile strength and Young's modulus, as well as the whole stress level. It is inferred that, for the composite specimens of 205°C and 225°C, overheating causes degradation of ramie fibers during Process B. It is considered that such a thermal degradation of fibers induces premature fracture of the composite specimens.

3.2.3. Effects of Fiber Content. Figure 6 presents effects of fiber content on tensile properties of composite specimens. The size of the specimens was medium size of a type in Figure 2. For the specimens, the pellets produced at 195°C during Process B were used. It is apparent in Figure 6(a) that the tensile strength increases with increasing fiber content. This trend reaches a maximum level at 40 wt%. Tensile strength of 40 wt% increased 1.73 times higher than PP specimens. Above this level of fiber content, the tensile strength starts to decrease. As can be seen in Figure 6(b), a continuous increase in Young's modulus occurs as the fiber content increases. That of 50 wt% specimens increased 2.17 times higher than the PP specimen. Results for fracture strain are shown in Figure 6(c). It is seen that fracture strain is decreased almost linearly between 4.0 and 7.0%. Consequently, although it exists between 30–50 wt%, it can be said that the weight fraction of fiber content giving the best tensile properties is about 40 wt%.

3.3. Fiber Dispersion and Fiber Length Distribution. Figure 7 shows a polished view of transverse section in a small-sized specimen produced at 195°C during Process B. The fiber content in Figure 7 is 30 wt%. The black bar-like areas show marks of ramie fibers separated from matrix during the polishing process. White dots denote cross-sectional area of ramie fibers. As presented from Figure 7, a higher proportion of white dots is visible. Such a phenomenon can also be observed on glass fiber-reinforced composite specimens [25, 26]. This means that short ramie/PP reinforced composites have a high degree of fiber orientation to the flow direction.

Figure 8 shows a magnified view of Figure 7. Results show that individual fibers after injection molding are well dispersed, despite the fact that high-density fiber bundles were obtained after M-PaRI process, as shown in Figure 4(d). When being strongly bonded, it is known that the bundles act

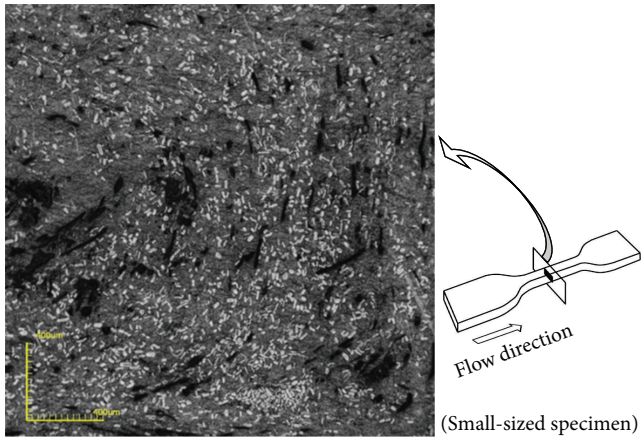

Figure 7: Laser micrograph of transverse section of short ramie/PP reinforced composites produced at 195°C during Process B.

Figure 8: Laser micrograph of transverse section of short ramie/PP reinforced composites produced at 195°C during Process B.

Figure 9: SEM micrograph of extracted fibers from short ramie/PP reinforced composites produced at 195°C during Process B.

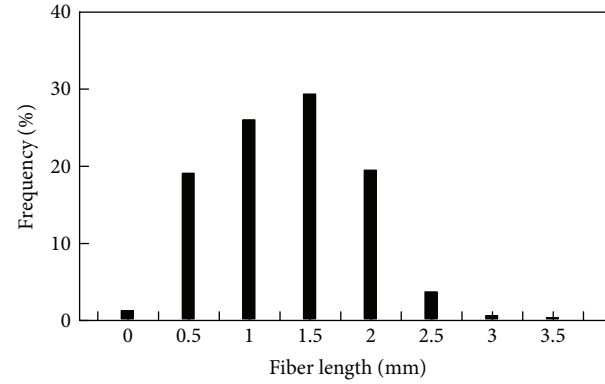

Figure 10: Fiber length distribution of extracted fibers from short ramie/PP reinforced composites produced at 195°C during Process B.

as a reinforcing unit, which means that pull-out of bundles occurs at much lower stresses [26]. Consequently, it should be noted that much higher interfacial stress can be yielded on the surface of the fibers.

To confirm the change in fiber length after the applied fabrication processes, small-sized composite specimens produced at 195°C during Process B were dissolved in boiling xylene for 24 hr to remove PP resin. Then, extracted ramie fibers were dried at 100°C for 2 hr. Figure 9 shows an SEM micrograph of ramie fibers. Although partial microfibril detachment is observed, the single fibers maintain their original structure even after Processes A and B with subsequent injection molding processing applied.

Fiber length distribution of the specimens dissolved above is presented in Figure 10. The total number of measured fibers was 780. Average fiber length was 1.56 mm and the standard deviation was 0.61 mm. It is necessary for short fiber-reinforced composites to be longer than the critical fiber length. According to an earlier report [27], the critical fiber length of ramie fiber is 0.47 mm. It can be clearly seen that over 98% of ramie fibers are longer than the critical length in this study. This brings sufficiently high stress to composite specimens because the matrix transfer mechanism does not cause low fiber stress.

4. Conclusions

A new combination technique of resin-coating and multi-pin-assisted resin impregnation (M-PaRI) processes was introduced to produce a continuous ramie single yarn/polypropylene (PP) reinforced composite strand. By addition of M-PaRI process, we found that the resin can be impregnated completely into the yarn interfibers. Furthermore, tensile tests of injection-molded composites were conducted using strands produced at different temperatures of M-PaRI process. Results show that the maximum mechanical properties of composites could be obtained between 195 and 205°C. The fiber content giving the best tensile properties was about 40 wt%.

The new process presented in this study demonstrates marked improvements of mechanical properties on composites in comparison with conventional methods, in which fibers are inserted directly during the extrusion process. A fascinating point is the simplification of production for long natural fiber-reinforced composites. The composite strands

obtained here are expected for use as a semifinished material for injection and compression molding products.

References

[1] Official homepage of The Ministry of Agriculture, Forestry and Fisheries, Japan, http://www.maff.go.jp/j/biomass/b_kihonho/pdf/keikaku.pdf.

[2] A. K. Bledzki and J. Gassan, "Composites reinforced with cellulose based fibres," *Progress in Polymer Science*, vol. 24, no. 2, pp. 221–274, 1999.

[3] K. Goda and Y. Cao, "Research and development of fully green composites reinforced with natural fibers," *Journal of Solid Mechanics and Materials Engineering*, vol. 1, no. 9, pp. 1073–1084, 2007.

[4] S. Kalia, B. S. Kaith, and I. Kaur, "Pretreatments of natural fibers and their application as reinforcing material in polymer composites-a review," *Polymer Engineering and Science*, vol. 49, no. 7, pp. 1253–1272, 2009.

[5] H. Ku, H. Wang, N. Pattarachaiyakoop, and M. Trada, "A review on the tensile properties of natural fiber reinforced polymer composites," *Composites B*, vol. 42, pp. 856–873, 2011.

[6] M. U. de la Orden, C. G. Sánchez, M. G. Quesada, and J. M. Urreaga, "Effect of different coupling agents on the browning of cellulose-polypropylene composites during melt processing," *Polymer Degradation and Stability*, vol. 95, pp. 201–206, 2010.

[7] A. Awal, G. Cescutti, S. B. Ghosh, and J. Müssig, "Interfacial studies of natural fibre/polypropylene composites using single fibre fragmentation test (SFFT)," *Composites A*, vol. 42, no. 1, pp. 50–56, 2011.

[8] A. Arbelaiz, B. Fernández, G. Cantero, R. Llano-Ponte, A. Valea, and I. Mondragon, "Mechanical properties of flax fibre/polypropylene composites. Influence of fibre/matrix modification and glass fibre hybridization," *Composites A*, vol. 36, no. 12, pp. 1637–1644, 2005.

[9] G. Dores, A. Taguet, L. Ferry, and J. M. Lopez-Cuesta, "Thermal and fire behavior of natural fibers/PBS biocomposites," *Polymer Degradation and Stability Xxx*, pp. 1–9, 2012.

[10] F. Yao, Q. Wu, Y. Lei, W. Guo, and Y. Xu, "Thermal decomposition kinetics of natural fibers: activation energy with dynamic thermogravimetric analysis," *Polymer Degradation and Stability*, vol. 93, no. 1, pp. 90–98, 2008.

[11] L. B. Manfredi, E. S. Rodríguez, M. Wladyka-Przybylak, and A. Vázquez, "Thermal degradation and fire resistance of unsaturated polyester, modified acrylic resins and their composites with natural fibres," *Polymer Degradation and Stability*, vol. 91, no. 2, pp. 255–261, 2006.

[12] H. L. Bos, M. J. A. Van Den Oever, and O. C. J. J. Peters, "Tensile and compressive properties of flax fibres for natural fibre reinforced composites," *Journal of Materials Science*, vol. 37, no. 8, pp. 1683–1692, 2002.

[13] P. R. Hornsby, E. Hinrichsen, and K. Tarverdi, "Preparation and properties of polypropylene composites reinforced with wheat and flax straw fibres: part II Analysis of composite microstructure and mechanical properties," *Journal of Materials Science*, vol. 32, no. 4, pp. 1009–1015, 1997.

[14] S. K. Batra, M. Lewin, and E. M. . Pearce, "MEds and Marcel Deker," in *Handbook of Fiber Science and Technology*, vol. 1, pp. 727–803, 1985.

[15] S. Nam and A. N. Netravali, "Green composites. II. Environment-friendly, biodegradable composites using ramie fibers and soy protein concentrate (SPC) resin," *Fibers and Polymers*, vol. 7, no. 4, pp. 380–388, 2006.

[16] H. L. Bos, J. Müssig, and M. J. A. van den Oever, "Mechanical properties of short-flax-fibre reinforced compounds," *Composites A*, vol. 37, no. 10, pp. 1591–1604, 2006.

[17] F. N. Cogswell, D. J. Hezzell, and P. J. Williams, "Fibre reinforced compositions and methods for producing such compositions," US Patent No. 4559262, 1985.

[18] A. G. Gibson and J. A. Månson, "Impregnation technology for thermoplastic matrix composites," *Composites Manufacturing*, vol. 3, no. 4, pp. 223–233, 1992.

[19] J. L. Thomason, "Dependence of interfacial strength on the anisotropic fiber properties of jute reinforced composites," *Polymer Composites*, vol. 31, no. 9, pp. 1525–1534, 2010.

[20] A. K. Bledzki, A. Jaszkiewicz, and D. Scherzer, "Mechanical properties of PLA composites with man-made cellulose and abaca fibres," *Composites A*, vol. 40, no. 4, pp. 404–412, 2009.

[21] T. Tanaka and Y. Hirano, "Long fiber pellet production plants and their application to natural fiber composites (eco-composites)," *Kobe Steel Engineering Reports*, vol. 51, no. 2, pp. 62–66, 2001.

[22] K. Goda, M. S. Sreekala, A. Gomes, T. Kaji, and J. Ohgi, "Improvement of plant based natural fibers for toughening green composites-Effect of load application during mercerization of ramie fibers," *Composites A*, vol. 37, no. 12, pp. 2213–2220, 2006.

[23] K. G. Satyanarayana, J. L. Guimarães, and F. Wypych, "Studies on lignocellulosic fibers of Brazil. Part I: source, production, morphology, properties and applications," *Composites A*, vol. 38, no. 7, pp. 1694–1709, 2007.

[24] G. W. Beckermann and K. L. Pickering, "Engineering and evaluation of hemp fibre reinforced polypropylene composites: fibre treatment and matrix modification," *Composites A*, vol. 39, no. 6, pp. 979–988, 2008.

[25] W. H. Bowyer and M. G. Bader, "On the re-inforcement of thermoplastics by imperfectly aligned discontinuous fibres," *Journal of Materials Science*, vol. 7, no. 11, pp. 1315–1321, 1972.

[26] D. Hull, *An Introduction to Composite Materials*, Cambridge University Press, Cambridge, UK, 1st edition, 1981.

[27] L. G. Angelini, A. Lazzeri, G. Levita, D. Fontanelli, and C. Bozzi, "Ramie (*Boehmeria nivea* (L.) Gaud.) and Spanish Broom (*Spartium junceum* L.) fibres for composite materials: agronomical aspects, morphology and mechanical properties," *Industrial Crops and Products*, vol. 11, no. 2-3, pp. 145–161, 2000.

Hindawi Publishing Corporation
Advances in Mechanical Engineering
Volume 2012, Article ID 356548, 4 pages
doi:10.1155/2012/356548

Research Article

Studies of Moisture Absorption and Release Behaviour of Akund Fiber

Xue Yang, Liqian Huang, Longdi Cheng, and Jianyong Yu

Key Laboratory of Textile Science and Technology, Ministry of Education, Donghua University, Shanghai 201620, China

Correspondence should be addressed to Xue Yang, 2100108@mail.dhu.edu.cn

Received 27 May 2012; Revised 2 December 2012; Accepted 3 December 2012

Academic Editor: Mohamed S. Aly-Hassan

Akund fiber is a new type of natural cellulose fiber. Because of its excellent properties, akund fiber has become one of the new ecological materials which have huge development potential. Recently natural fibers have shown great promise in a variety of applications that were previously dominated by synthetic fibers due to their important aspects of biocompatibility, possible biodegradation, nontoxicity, and abundance. Moisture absorption and release behaviour of natural fiber plastic composites is one major concern in their outdoor applications. So the knowledge of the moisture content and the moisture absorption and release rate is very much essential for the application of akund fiber as an excellent reinforcement in polymers. An effort has been made to study the moisture absorption and release behaviour of akund fiber and the mechanical performance of it at relative air humidity from 0% to 100%. The gain and loss in moisture content in akund fiber due to water absorption and release were measured as a function of exposure time under the environment, in which temperature is 20°C and humidity is 65%. The regression equations of the absorption and release process were established.

1. Introduction

Akund fiber, also called calotropis fiber, is a new type natural cellulose fiber and is obtained from *Calotropis procera* and *Calotropis gigantea*, belonging to the *Apocynaceae* family. As one type of natural cellulose fiber, akund fiber has good touch to skin like cotton and beautiful luster like silk. Akund fiber has a large hollow structure with a thin wall that looks like an air-filled pipe. It is about 2 to 4 cm long and 12 to 42 microns in diameter. Because of its excellent properties, akund fiber has become one of the new ecological materials which have huge development potential [1].

With enhancement of environment protection consciousness of people recently, natural fibers have shown great promise in a variety of applications that were previously dominated by synthetic fibers due to their important aspects of biocompatibility, possible biodegradation, non-toxicity, and abundance. Currently, automotive and construction industries have been interested in composites reinforced with natural plant fibers as alternative materials for glass-fiber reinforced composites in structural applications with modest demands on strength reliability [2, 3]. It has been known that the high level of moisture absorption by natural fibers, the poor wettability, and the insufficient adhesion between the untreated fibers and the polymeric matrix lead to bonding failure with age [4]. Moreover, the absorbed moisture has many detrimental effects on the mechanical performance of these fibers. Therefore, an understanding of the hygroscopic properties of natural fibers is very important to improve the long-term performance of composites reinforced with these fibers [5]. In this paper, an effort has been made to study the hygroscopic properties of akund fiber and the mechanical performance of it at relative air humidity ranging from 0% to 100%. The gain and loss in moisture content in akund fiber due to water absorption and release were measured as a function of exposure time under the environment, in which temperature is 20°C and humidity is 65%. The regression equations of the absorption and release process were established. As akund fiber belongs to the plant fiber, which is similar with cotton and kapok fiber, and both cotton and kapok fiber are used to composite reinforce fiber, therefore, in order to explain the akund fiber's absorption

Table 1: Composition and structural parameters of samples [6].

Sample	Diameter (μm)	Length (mm)	Cellulose content (%)	Lignin content (%)
Akund fiber	20.63	30.36	55.45	16.15
Cotton	15.35	35.19	93.82	4.62
Kapok	19.28	19.08	43.73	11.36

and release moisture ability clearly, whole the analysis is according to the comparison with cotton and kapok fiber.

2. Experimental

2.1. Materials. Akund fiber and kapok fiber were collected from Yunnan province, China. The cotton fiber was collected from Xinjiang province, China. The compositions and structural parameters of samples studied in this work are listed in Table 1. All the test fiber was put in the constant temperature and humidity room, whose temperature was 20°C and relative air humidity was 65% for 24 hours.

2.2. Instruments. Y802A type eight basket constant temperature oven, AUY120 type electronic balance (uncertainty = ±0.0001 g), HHS2100 L type constant temperature and humidity test case, and XQ-2 single fiber strength and elongation test instrument were used.

2.3. Experimental Process [7, 8]

2.3.1. Moisture Absorption Experiment. In the case of the moisture absorption methods, each sample having a mass of 1.0 g was dried in the Y802A type eight basket constant temperature oven at 60°C for one hour. The dried samples were placed in the constant temperature and humidity room (the temperature was 20°C and relative air humidity was 65%) and weighed on the electronic balance (uncertainty = 0.0001 g) every 5 minutes, until the fibers reached to moisture absorption balance. The samples after reaching to absorption balance were dried in the constant temperature oven at 105°C to achieve a constant mass. The moisture content Mc at time "t" was calculated using

$$\mathrm{Mc} = \left[\frac{M_w - M_d}{M_d} \times 100\right]\%, \quad (1)$$

where M_d and M_w are, respectively, the mass of the dried smaple (in g) and the mass of the wet sample after time t (in g). In all cases, the mean ± standard deviation data from three repeated experiments were taken to ensure reliability of the results.

2.3.2. Moisture Release Experiment. In the case of the moisture release methods, each sample having a mass of 1.0 g was put in a 60 × 30 weighing bottle. The open weighing bottle was placed in a constant temperature and humidity test case for 48 hours in which the temperature was 20°C and the relative air humidity was (98 ± 2)%. Then the weighing bottle was closed; the sample was removed to the constant temperature and humidity room (the temperature is 20°C, and the humidity is 65%), and weighing bottles were opened. Every 5 minutes, the samples were weighed, until the fibers reach to moisture release balance. Then the samples were dried in a constant temperature oven at 105°C to achieve a constant mass. The moisture content Mc at time "t" was calculated using

$$\mathrm{Mc} = \left[\frac{M_h - M_d}{M_d} \times 100\right]\%, \quad (2)$$

where M_d is the mass of the sample after drying to a constant mass (in g) and M_h is the mass of the humidified sample (in g). In all cases, the mean ± standard deviation data from three repeated experiments were taken to ensure reliability of the results.

Table 2: The moisture content of absorption balance and desorption balance and the moisture absorption hysteresis property.

Samples	Moisture content of absorption balance/%	Moisture content of release balance/%	Moisture absorption hysteresis/%
Akund	10.44	12.21	1.77
Cotton	7.75	8.70	0.95
Kapok	9.86	12.14	2.28

2.3.3. Fiber Strength Test in Different Humidity. In the case of the fiber strength test methods, each sample having a mass of 1.0 g was put in a 60 × 30 weighing bottle. The open weighing bottle was placed in a constant temperature and humidity test case for 48 hours in which the temperature was 20°C and the relative air humidity, respectively, were 0%, 30%, 60%, 80%, and (98 ± 2)%. Then the weighing bottle was closed; the sample was removed to the constant temperature and humidity room (the temperature is 20°C, and the humidity is 65%). And according to the GB/T 14337-2008 methods of testing the fiber strength, 50 fibers were tested in each test.

3. Results and Discussion

3.1. The Moisture Absorption and Release Curve. The moisture absorption and release curves of akund fiber, cotton, and kapok are shown in Figures 1 and 2, and the experiment data are listed in the Table 2.

From Table 2, it can be seen that the moisture content of akund fiber in standard state is about 10.44% and akund fiber has the same moisture absorption hysteresis quality as cotton and kapok, in which the moisture content in absorption balance is smaller than that in release balance. The moisture hysteresis of akund fiber is 1.77%, which is bigger than that of the cotton fiber and smaller than that of the kapok fiber. From Figures 1 and 2, it can be found that during the process of moisture absorption and release, akund fiber takes longer time to equilibrate than the others, and it has a higher equilibrate moisture content than the others. The moisture content of akund fiber has a fluctuation of up and down. The general shape of the water absorption and

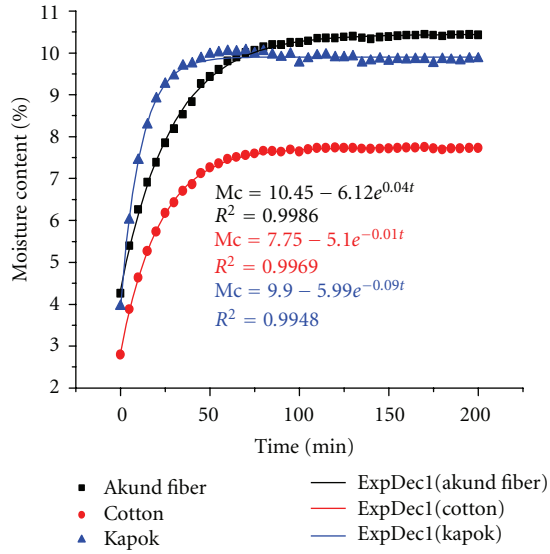

Figure 1: Moisture absorption fitting curve.

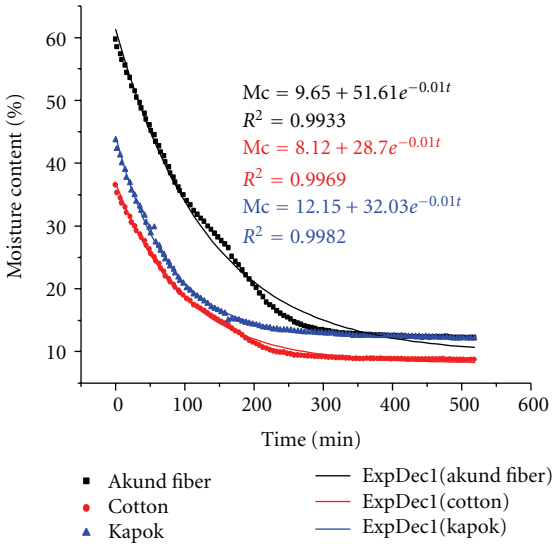

Figure 2: Moisture release fitting curve.

release curves for akund fiber is similar to those of cotton and kapok. The moisture content of akund fiber changes from 4.25% to 9.98% in the first 60 min, the changes is only from 10% to 10.44% in the following 100 min, and in the last 20 min, there are almost no changes in the moisture content. These results exhibit the two-stage absorption and release behaviour of akund fiber. The first stage occurred very rapidly having a linear uptake to 60% of absorption and release. The second stage of absorption and release began very slowly and proceeded up to complete balance.

3.2. Establishment of the Regression Equation of Moisture Absorption and Release Process. It is well accepted in the literature [7, 8] that the theoretical curve of the fibers' moisture absorption and release process is an exponential

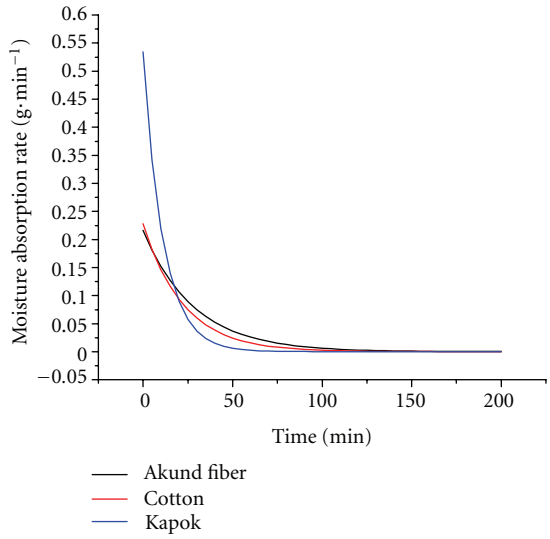

Figure 3: The moisture absorption rate.

curve, so the regression equation of moisture content (M) versus exposure time (t) can be expressed using

$$M = a + be^{-ct}, \tag{3}$$

where a, b, and c are all constants.

Taking (3) as a function, the regression equation can be established from the test data by custom function fitting of the moisture content (Mc) versus the exposure time (t) using data analysis software, Origin Pro 7.5. The fitting curves and the regression equations are shown in Figures 1 and 2.

From Figures 1 and 2, it could be found that the fitting curves of the moisture absorption and release are similar to the original data, and the coefficients of determination (R^2) of the regression equations are all above 0.98. Therefore, the regression equations can effectively express the relation between the moisture content (Mc) and the exposure time (t) during the moisture absorption and desorption process.

3.3. Establishment of the Regression Equation of the Moisture Absorption and Release Rate. The moisture absorption and release rate of fibers can be expressed by the weight of moisture absorption and release of unit quality fiber at instant time. So the differential equation of (3) is the regression equation of the rate of moisture absorption and release, which is shown

$$V = \left| bce^{-ct} \right|. \tag{4}$$

According to the regression equation of the moisture absorption and release rate of akund fiber, cotton, and kapok, the regression curves of the moisture absorption and release rate of the three kind of fibers could be determined, which are shown in Figures 3 and 4.

From Figures 3 and 4, it can be seen that the initial moisture absorption rate of akund fiber is similar with that of cotton in standard state and much lower than that of kapok. And the initial moisture release rate of akund fiber is similar

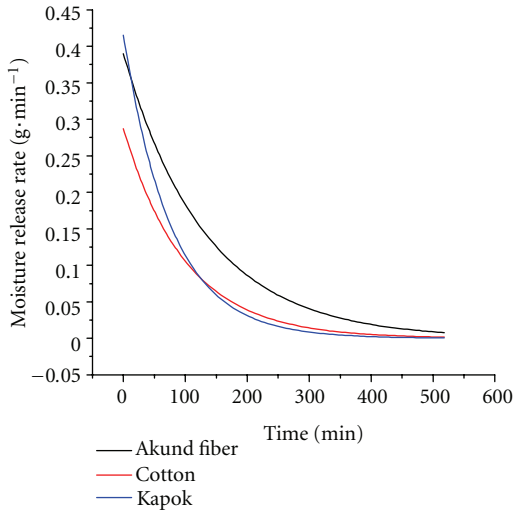

Figure 4: The moisture release rate.

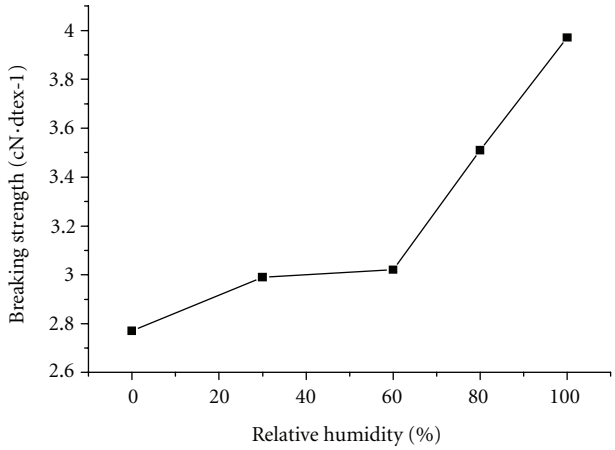

Figure 5: The breaking strength of akund fiber at different relative air humidity values.

with that of kapok, and higher than that of cotton. The rate of moisture absorption and release of the three fibers reduces gradually over time. The rate decrement of the moisture absorption and release of kapok is the fastest. Kapok reaches the moisture absorption and desorption balance first, the cotton is next to the kapok and the akund fiber is the slowest. So it can be concluded that akund fiber has a quick moisture release and slow moisture absorption performance.

3.4. The Mechanical Performance of Akund Fiber at Different Relative Humidity. In order to determine the environmental factor of the utility of akund fiber, the breaking strength of akund fiber was determined at different humidity values and the results are shown in Figure 5.

From Figure 5, it is evident that with an increase in the relative air humidity, the breaking strength of akund fiber increases. This is attributed to the possible changes in the interaction between the large molecular chains as a result of water entering into the fiber interior. The water absorption of akund fiber leads to the improvement of unevenness of macromolecular force and the increase in the number of the fracture molecular chain. And it is interesting to note that the samples have an approximately 4.3% increase in breaking strength from the low-humidity condition (0%) to the high-humidity condition (100%).

4. Conclusions

According to the above results and discussion, we can draw the following conclusions.

(1) The moisture content of akund fiber in standard state is a little more than that of kapok. The ability of moisture absorption and release of akund fiber is similar with that of kapok.

(2) Akund fiber has a quick moisture release and slow moisture absorption performance. The initial rate of moisture release of akund fiber is much higher than that of cotton, and similar to kapok. But its initial speed of moisture absorption is the slowest, and closest to cotton.

(3) The mechanical performance of akund fiber changes as the relative air humidity changes. Its breaking strength increases gradually with the increase of relative humidity. The wet strength of akund fiber is much higher than the dry strength.

References

[1] X. Yang, L. D. Cheng, L. Q. Huang, and W. H. Fan, "New materials and processes," *Advanced Materials Reserch*, vol. 476–478, pp. 1934–1938, 2012.

[2] D. Saikia, "Investigations on structural characteristics, thermal stability, and hygroscopicity of sisal fibers at elevated temperatures," *International Journal of Thermophysics*, vol. 29, no. 6, pp. 2215–2225, 2008.

[3] D. Saikia, "Studies of water absorption behavior of plant fibers at different temperatures," *International Journal of Thermophysics*, vol. 31, no. 4-5, pp. 1020–1026, 2010.

[4] D. Saikia, "The effect of heat on structural characteristics and water absorption behavior of agave fibers," in *Proceedings of the 4th National Conference on Thermophysical Properties (NCTP '07)*, pp. 48–52, September 2007.

[5] D. Saikia and M. N. Bora, "Study of hygroscopic properties of some plant fibres under thermal condition," *Indian Journal of Pure and Applied Physics*, vol. 41, no. 6, pp. 484–487, 2003.

[6] X. Yang, L. Q. Huang, and L. D. Cheng, "Study on the structure and the properties of akund fiber," *Applied Mechanics and Materials*, vol. 217–219, pp. 617–621, 2012.

[7] Y. Q. Wan, L. L. Wu, and J. Y. Yu, *Journal of Textile Research*, vol. 25, no. 3, pp. 14–16, 2004.

[8] Y. P. Liu and J. H. Wu, *CottonTextile Technology*, vol. 36, no. 3, pp. 23–26, 2008.

Hindawi Publishing Corporation
Advances in Mechanical Engineering
Volume 2012, Article ID 418031, 13 pages
doi:10.1155/2012/418031

Research Article

Mechanical, Thermal Degradation, and Flammability Studies on Surface Modified Sisal Fiber Reinforced Recycled Polypropylene Composites

Arun Kumar Gupta, Manoranjan Biswal, S. Mohanty, and S. K. Nayak

Laboratory for Advanced Research in Polymeric Materials (LARPM), Central Institute of Plastics Engineering and Technology (CIPET) Bhubaneswar, Orissa 751024, India

Correspondence should be addressed to S. K. Nayak, drsknayak@gmail.com

Received 10 April 2012; Accepted 12 November 2012

Academic Editor: Yan Li

The effect of surface treated sisal fiber on the mechanical, thermal, flammability, and morphological properties of sisal fiber (SF) reinforced recycled polypropylene (RPP) composites was investigated. The surface of sisal fiber was modified with different chemical reagent such as silane, glycidyl methacrylate (GMA), and O-hydroxybenzene diazonium chloride (OBDC) to improve the compatibility with the matrix polymer. The experimental results revealed an improvement in the tensile strength to 11%, 20%, and 31.36% and impact strength to 78.72%, 77%, and 81% for silane, GMA, and OBDC treated sisal fiber reinforced recycled Polypropylene (RPP/SF) composites, respectively, as compared to RPP. The thermogravimetric analysis (TGA), differential scanning calorimeter (DSC), and heat deflection temperature (HDT) results revealed improved thermal stability as compared with RPP. The flammability behaviour of silane, GMA, and OBDC treated SF/RPP composites was studied by the horizontal burning rate by UL-94. The morphological analysis through scanning electron micrograph (SEM) supports improves surface interaction between fiber surface and polymer matrix.

1. Introduction

With the international governmental policies, ecological risks and increasing global energy crises have been the driving force behind the more and more research interest owing to their potential of serving as alternative for natural fiber reinforced thermoplastics composites [1–7]. Accordingly, extensive studies on the attractiveness of a plant based fiber reinforcement materials come from its low abrasion, multifunctionality, low density, unlimited availability, ecofriendliness, high specific mechanical performance, and renewability [8–16]. These properties have made fibers very attractive candidate material for many applications such as automotive, building, construction, and aerospace. In spite of the advantages, natural fibers are hydrophilic in nature as they are derived from lignocellulose, which contain strongly polarized hydroxyl groups. These fibers, therefore, are inherently incompatible with hydrophobic thermoplastics, such as recycled polypropylene; the main difficulty with using natural fiber arises due to improper adhesion with hydrophobic polymer matrix and formation of agglomerates during processing [17–23]. This has resulted in an increasing demand towards improving the adhesion between the fiber and matrix by the modification of the fiber and/or polymer matrix using chemical methods. Fiber modifications include mercerization, acetylation, silanation and treatment with strontium titanate ($SrTiO_3$), glycidyl methacrylate (GMA) & O-hydroxybenzene diazonium chloride (OBDC) by different authors for enhancing better surface interaction towards polymer matrix [15, 19, 24–31].

In the age of "going green" it is becoming easier and easier to recycle. A sustainable polymer product cannot be land filled but has to be recycled. Polymer recycling is classified into four distinct categories depending on the level of conservation of the polymer chemical structure. Recycling of polymeric material has been practiced for many years by industries without any great accuracy. The new environmental, economic, and petroleum crises have

induced the scientific community to deal with polymer reprocessing and sustainability. Recycled polypropylene (PP) is of great interest, particularly for the automotive industry. One problem with recycled resins is that tensile toughness and impact strength usually decrease during recycling and restoration requires additives. Polypropylene is an economical material that offers a unique combination of excellent physical, chemical, mechanical, thermal, and electrical properties which is not found in any other thermoplastic [32].

Again, PP is one of the most versatile thermoplastics polymers as a consequence of its recyclability and its capability low processing cost for massive production. The use of recycled polypropylene (RPP) obtained from the above application is not as easy as virgin one due to the inconsistent material properties in presence of impurities. To overcome this limitation several methods have already been developed but reinforcement with natural fiber are yet to be studied [33].

The sisal fibers used in this investigation is one of the most widely used natural fibers extracted from the leaves of the plant *Agave sisalana*. This was originated from Mexico and is now mainly cultivated in East Africa, Brazil, Haiti, India, and Indonesia. The name "sisal" comes from a harbor town in Yucatan, Maya, Mexico. It means cold water. Agave plants were grown by the Maya Indians before the arrival of the Europeans. They prepared the fibers by hand and used it for ropes, carpets, and clothing. Some clothes were called "nequen," and this is where the present name of Mexican agave, henequen, probably originates from. The outstanding mechanical properties of SF associated with high cellulose content and low microfibrillar angle have been taken into consideration for enhancing strength and performance characteristics in the current study. However, its hydrophilic character has been the main cause of poor compatibility between natural fibers and polymers matrix, which leads to unsatisfactory mechanical and thermal properties of reinforced composites [34, 35].

The interaction between the natural fiber and the matrix can be further improved by surface modification of the fibers using chemical treatment techniques, such as acetylation, benzylation, plasma treatment, and mercerization. Mechanical properties of natural fiber-reinforced composites can be further influenced by adhesion characteristics of the fiber-matrix interface. Similar investigation was carried out by Singleton et al. in his work on "On the mechanical properties, deformation and fracture of a natural fibre/recycled polymer composite" [8].

In this study, an attempt has been made to study the effect of chemically treated sisal fiber on mechanical, thermal, morphological, and flammability properties of fiber reinforced recycled polypropylene composites.

2. Experimental

2.1. Materials. Recycled polypropylene (RPP), obtained from M/s. Cargil Dow (Bair, US-NE), was used as a matrix material. The MFI for RPP is between 1 and 12 g/10 min (230°C, 2.16 kg), and density is 0.9 g/cc. Sisal fibers (*Agave sisalana*) obtained from M/s Sheeba fibers and handicrafts, Poovancode, Tamilnadu, India, with a density of 1.5 g/cc were used as reinforcement. Surface modifiers: 3-aminopropyltriethoxysilane (APS), a product of M/s Evonik Degussa (China) Co., Ltd. supplied by Aroma Chemical Agencies (India) Pvt. Ltd. and bis-(3-triethoxy silyl propyl) tetrasulfane (Si69) from M/s Sigma Aldrich. Co., Germany, were used as modifying agents. Common chemicals such as sodium hydroxide, acetic acid, acetic anhydride, and sulphuric acid were collected from Merck Specialities Pvt. Ltd., Mumbai, India.

2.2. Methods

2.2.1. Fiber Surface Modification. Prior to chemical treatment bundles of sisal fiber were cut in to a length of 13–15 cm and scoured in mild detergent solution at 60°C for 2 hrs to remove dust and other impurities. Finally the fibers were washed in distilled water and dried in air for 2 days.

NaOH Treatment (Mercerization). Mercerization of the fibers was carried out by immersing the fibers in 1 N sodium hydroxide (NaOH) solution for 1 hr at room temperature. Then the fibers were washed with distilled water containing few drops acetic acid, followed by washing under continuous stream of water until the complete removal of NaOH residue. Subsequently, the mercerized fibers were dried at room temperature for 24 hrs and then in a vacuum oven at 80°C for 12 hrs.

Acetylation. The fiber bundles were immersed in the mixture of acetic acid/acetic anhydride of ratio 1 : 1 along with 1 mL of conc. sulphuric acid as a catalyst. Then the fiber was drained from the mixture, washed with distilled water until the complete removal of unreacted reagents, and then finally dried in a oven for 24 hrs at 80°C.

Silane Treatment. The detergent washed fibers were dipped in 5 wt% silane solution in alcohol water mixture (60 : 40) for 1 hr at room temperature. Bis-(3-triethoxysilylpropyl) and 3-amino propyltriethoxysilane (APS) were used as coupling agents. The pH of the solution was maintained to 4 with acetic acid. Then the fibers were washed in distilled water and dried.

Strontium Titanate ($SrTiO_3$) Treatment. The fibers were dipped in 5 wt% alcoholic solution (ethanol) for 30 min in presence of 2% strontium titanate ($SrTiO_3$) as a coupling agent. The pH of the solution was maintained between 4.5 to 5.5 with the addition of ethanoic acid; further the fiber was washed with ethanol and dried in oven for 2 hrs.

Glycidyl Methacrylate (GMA) Treatment. Detergent washed sisal fiber was reacted at 90°C with 60 mL of glycidyl methacrylate solution. Hydroquinone (2% by weight of GMA) was added to minimize the free radical reaction at the unsaturated end of GMA molecules. After 2 hrs, the modified fibers were separated through filtration and rinsed

with acetone. The residual solvent was removed with excess of acetone and finaly dried under vacuum at 90°C for 24 hrs.

O-Hydroxybenzene Diazonium Chloride (OBDC) Treatment. O-hydroxybenzene diazonium chloride solution was prepared by the addition of O-hydroxyaniline (dissolved in HCl) with $NaNO_2$ in an ice bath temperature ≤5°C. The prepared solution was mixed with water in the ratio of 10 : 90. Then the fibers were dipped into the solution. After treatment the fibers were washed with distilled water followed by drying in oven for 4 hrs.

All the treated fibers were chopped using an electronic fiber cutting machine in to short fiber short fiber of length 2-3 mm. The surface treatments of sisal fiber have been confirmed using FTIR spectroscopy.

2.3. Fourier Transformation Infrared Spectroscopy (FTIR). FTIR spectra of untreated and treated sisal fiber were recorded using Nicolet 6700, USA spectrometer. Each spectrum was obtained by adding 64 consecutive scans with a resolution of 4 cm^{-1} within the range of 500–4000 cm^{-1}.

2.4. Fabrication of Composites. RPP/SF composites were prepared by melt mixing in a batch mixer (Haake Rheomex 600, Germany) at various percentages of fiber loading from 10, 20, and 30 to 40 wt%, respectively. The mixing was carried out at 180°C with a rotor speed of 40 rpm for 10 mins. The melt mixer obtained was cooled to room temperature, granulated, and conditioned at 80°C for 2 hrs prior to specimen preparation. Finally molded sheets of 3 ± 0.1 mm thickness were prepared using a 100 T compression press (M/s Delta Malikson, Mumbai) at 190°C, 80 kg/cm^2 pressure over a total cycle time of 15 min. Further, specimens were prepared from these sheets as per various ASTM standards using a count ceast copy milling machine (M/s ceast, Italy).

2.5. Mechanical Testing. Tensile properties were measured as per ASTM-D 638 with gauge length of 50 mm, at a cross head speed of 50 mm/min by using the Universal Testing Machine (3382 Instron, UK). Notched izod impact strength of the specimens was evaluated using an impactometer (Tinius olsen, USA) as per ASTM-D 256 with a notch depth of 2.54 mm and notch angle of 45°.

2.6. Thermal Characterization. The melting, crystallization, and thermal stability of RPP and RPP/SF composites have been studied using differential scanning calorimetry (DSC Q 20, TA Instruments, USA) and TGA (TGA Q 50, TA Instruments, USA), respectively. DSC analysis was carried out using 5–10 mg of samples at a scanning rate of 10°C/min with a temperature range of 30–200°C under nitrogen atmosphere. Similarly TGA of 5–10 mg samples were carried out from 30 to 600°C at a heating rate of 10°C under nitrogen atmosphere. An HV-2000A-C3, GOTech, (Taiwan) analyzer was used to measure the heat-deflection temperature (HDT) of the composites.

2.7. Flammability Study. Flammability of the samples was studied by a horizontal burning test as per UL-94. In the horizontal burning test, the sample was held horizontally and a flame fuelled by natural gas was applied to light one end of the sample. The time for the flame to reach from the first reference mark (25 mm from the end) to the second reference mark, which is at 100 mm from the end, was measured.

2.8. Morphological Analysis: Scanning Electron Microscopy (SEM). The SEM of impact fractured composite specimens was carried out using EVO MA 15, Carl zeiss SMT (Germany). The samples were sputtered with platinum and were dried for half an hour at 70°C in vaccum, before study.

3. Result and Discussion

3.1. FTIR Analysis. Untreated and treated Sisal fiber were investigated by FTIR analysis as shown in Figure 1 from wave number 4000 to 450 cm^{-1} and the possible reaction mechanism represented in Figure 2. Peaks in the region of 1030–1150 cm^{-1} are mainly due to the C–O–C and C–O symmetric stretching of primary and secondary hydroxyl group in the cellulose, lignin, and their glycoside linkages. Peak near to the 1654 cm^{-1} corresponds to –C=O stretching due to the presence of aliphatic carboxylic acid in cellulose chain, whereas ketonic groups indicate –OH stretching peak at around 3400 cm^{-1}. The peak area around 1600 cm^{-1} reveals absorbed moisture content in SF. In addition, –C–H stretching absorption around 2900 cm^{-1} also can be seen in the SF spectra.

Surface modification of SF exhibits the absence of characteristic peaks at 1643 and 1156 cm^{-1}, accompanied with reduction in peak intensity at 1425 cm^{-1}. This is because of the decomposition of hemicellulose and partial leaching out of lignin by sodium hydroxide [7]. The disappearance of the peak at 1643 cm^{-1} is due to the dissolution of a portion of uranic acid, a constituent of hemicelluloses xylan. The shift of the peak from 2900 cm^{-1} to 2515 cm^{-1} indicates participation of some free hydroxyl groups in the chemical reaction [24].

Similarly, acetylation of SF also leads to changes in the appearance or increment in absorbance peak in the region around 1735–1737 cm^{-1}. The appearance of peak at around 1500 cm^{-1} is associated with the bending of aromatic C–H bond, present in lignin. The peak corresponding to 1735–1737 cm^{-1} is due to the esterification of the hydroxyl groups, which results in an increased stretching vibration of the carbonyl (C=O) group present in the ester bonds. The spectrum of fibers near to 1732 cm^{-1} is primarily assigned to the C=O stretching vibration of the carboxyl and acetyl groups in "xylan" of hemicelluloses. The appearance of the peak at around 2372 cm^{-1} for the acetylated SF confirms formation of ester linkage between the acetyl and hydroxyl groups in the fibres [25].

Silane treated SF introduces organosiloxy group to the fiber surface. The expected change in FT-IR spectra with silane treatment of SF is symmetric –(Si–O) and (–C–Si) stretching frequencies and asymmetric O–Si–O– and

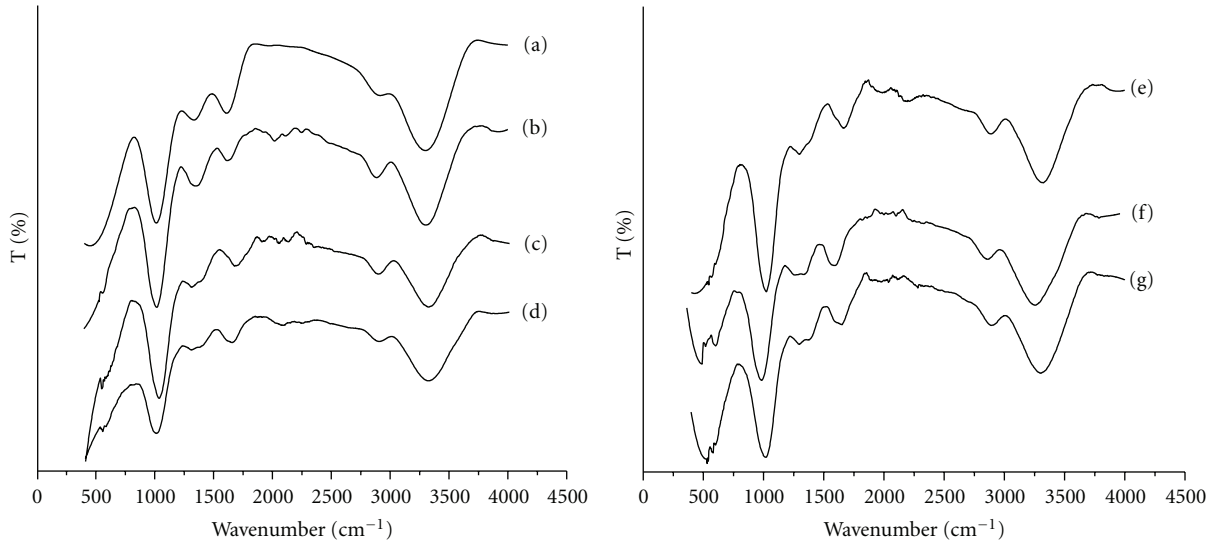

Figure 1: FTIR spectra of (a) untreated, (b) NaOH, (c) Acty, (d) Si, (e) $SrTiO_3$, (f) GMA, and (g) OBDC treated sisal fiber.

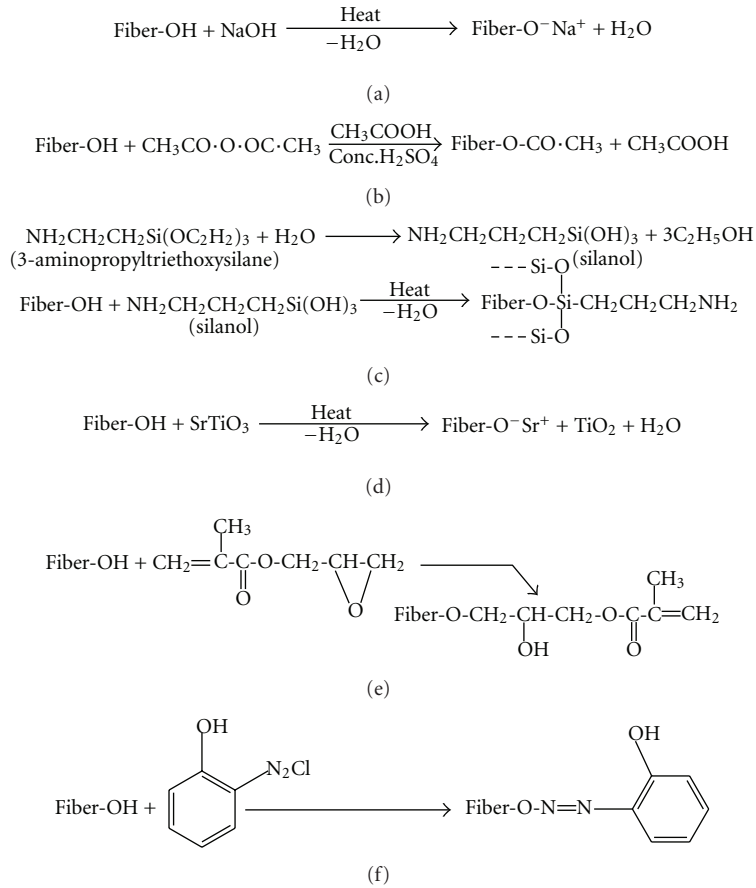

Figure 2: Mechanism of chemical treatments (a) NaOH, (b) acetylation, (c) Silanation, (d) $SrTiO_3$ treatment, (e) GMA treatment, and (f) O-hydroxybenzene diazonium chloride (OBDC) treatment.

–Si–O–C– stretching frequency in a region around 510–1160 cm^{-1}. Thus the peaks around 825 cm^{-1} and 1020 cm^{-1} are attributed to the Si–C symmetric stretching also contributes a peak around 891 cm^{-1} of the spectra. The asymmetric stretching frequencies of (–Si–O–C–) are due to the condensation reaction between the Silane and SF. These condensed Siloxanes also contribute to the Si–O–Si symmetric stretching frequency. In addition the above general characteristics peaks of Siloxane like C–N stretching frequencies around 2187 cm^{-1} can also have been observed [24, 25].

Treatment of SF by $SrTiO_3$ shows the disappearance of peak in the region of around 1630–1750 cm^{-1} conforming the partial dissolution of hemicelluloses group to carbonyl functionalities. The –OH stretching band becomes broad in a region around 2800–2900 cm^{-1} indicating the presence of increased number of hydroxyl group occurs due to the reaction of cellulosic group with sensitive $SrTiO_3$ [20].

Whereas treatment of SF by GMA shows a remarkable absorption peak in the carbonyl region at around 1728 cm^{-1} and peaks at 1418 and 1595 cm^{-1}, which are associated with the methacrylic ester bond and C=C group of GMA. The peak intensity in the modified samples increased with the reaction time, thus supporting a high reaction extent of the epoxide groups of GMA with the OH groups on the fiber surface [26].

However treatment with OBDC indicates absorption band at around 1700–1600 cm^{-1} and 1400–1000 cm^{-1} for N–O and C–O stretching, respectively; thus the result gives a clear indication of chemical modification of SF with O-hydroxybenzene diazonium chloride [15].

3.2. Mechanical Properties

3.2.1. Effect of Untreated Sisal Fiber Loading on Mechanical Properties of RPP/SF Composites. Figure 3 represents the mechanical properties of RPP/SF composites at a variable percentage of fiber loading from 10 to 40 wt%. Test results indicate that RPP has tensile strength, tensile modulus, and impact strength of 18.90 MPa, 1204.61 MPa, and 16.31 j/m respectively. Incorporation of SF into the RPP matrix reduces the tensile strength to about 41.57% at 30 wt% of fiber loading as compared with RPP. Likewise the percentage in tensile strain at break is found to be decreased confirming the discontinuity of dispersion in polymer matrix [28]. However tensile modulus and impact strength are found to be increased to small extent at 30 wt% of SF loading due to the reinforcing effect of fiber where stress is transfer from the matrix to the fiber. The results imply that untreated fiber does not have better interaction with the polymer matrix due to the presence of surface impurities. At higher fiber content the agglomeration of fiber is found to be more, which further results in deterioration in mechanical properties at 40 wt% of fiber loading [24]. The quality of a fiber reinforced composites depends considerably on the fiber matrix interface because only a well form interface allows better stress transfer from matrix to the fiber. Therefore good interfacial adhesion between the matrix and fiber is essential to improve the mechanical strength of composites.

3.2.2. Effect of Compatibilizer (MA-g-PP) on Mechanical Properties of RPP/SF Composites. The hydroxyl acid and the polar groups located in the branched heteropolysaccharide present in the Sisal fiber are active sites of water absorption, which results in incompatibility with hydrophobic RPP matrix. This incompatibility leads to weak interface and poor mechanical properties. With the addition of compatibilizer (MA-g-PP) in RPP/SF composites at 3–7 wt% of MA-g-PP loading result in significant improvement in mechanical properties, represented in Figure 4. Here addition of MA-g-PP acts as a dispersing agent between the polar fibers and the nonpolar matrix resulting in improved interfacial adhesion, which contributes towards enhanced stress transfer from the matrix to the fiber [6, 14].

As the RPP/SF composite at 30% fiber loading shows increased tensile modulus and impact strength, so this composition has been taken for preparation of RPP/SF/MA-g-PP composites for further characterization studies. Incorporation of MA-g-PP at 5 wt% shows increased tensile strength of 28.22% and tensile modulus of 2.11% as compared to RPP/SF composites without compatibilizer, which is as per the strength observed in case of RPP. This behaviour primarily attributed to the fact that the anhydride group of MA-g-PP reacts with the hydroxyl group of sisal fibers forming an ester linkage at the interface. Furthermore, the high molecular weight MA-g-PP has more flexible PP chains, which are able to diffuse into the matrix leading to interchain entanglements, thereby contributing to the mechanical continuity of the systems. Gassan and Bledzki [36] have reported similar behaviour for jute and flax reinforced PP composites. However, increase in the MA-g-PP content to 7 wt% resulted in the decrease of mechanical strength of composites. This is due to self-entanglement among the compatibilizer chains rather than with polymer matrix resulting slippage. Similar results are also indicated by Biswal et al. in their work on "Influence of Organically Modified Nanoclay on the Performance of Pineapple Leaf Fiber-Reinforced Polypropylene Nanocomposites" [7].

3.2.3. Effect of Surface Treated Sisal Fiber on Mechanical Properties of RPP/SF/MA-g-PP Composites. The different chemical modifications of natural fibers aimed at improving the adhesion with a polymer matrix were performed by a number of researchers [7, 15, 19, 24, 27, 33]. Some examples of chemical modification of fiber surface such as Mercerization, Acetylation, Silane, Strontium titanate, GMA and O-hydroxybenzene diazonium chloride treatments are represented in our current study. Different chemical treatments of SF intrinsically increase the interacting ability of the fiber with the polymer matrix which results improved mechanical properties as represented in Figure 5.

NaOH Treated SF. Mercerization of SF results in an improvement in interfacial debonding of fibers with RPP, which is probably due to the additional sites created for

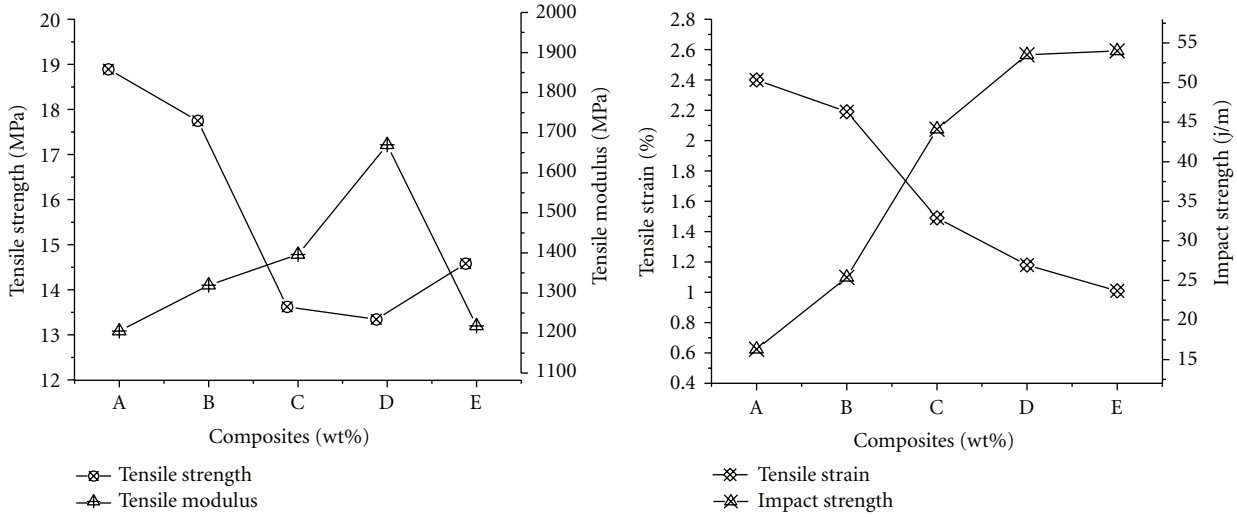

Figure 3: Mechanical properties of RPP/SF composites at a different wt% fiber loading whereas A: RPP, B: RPP/SF (90/10), C: RPP/SF (80/20), D: RPP/SF (70/30) and E: RPP/SF (60/40).

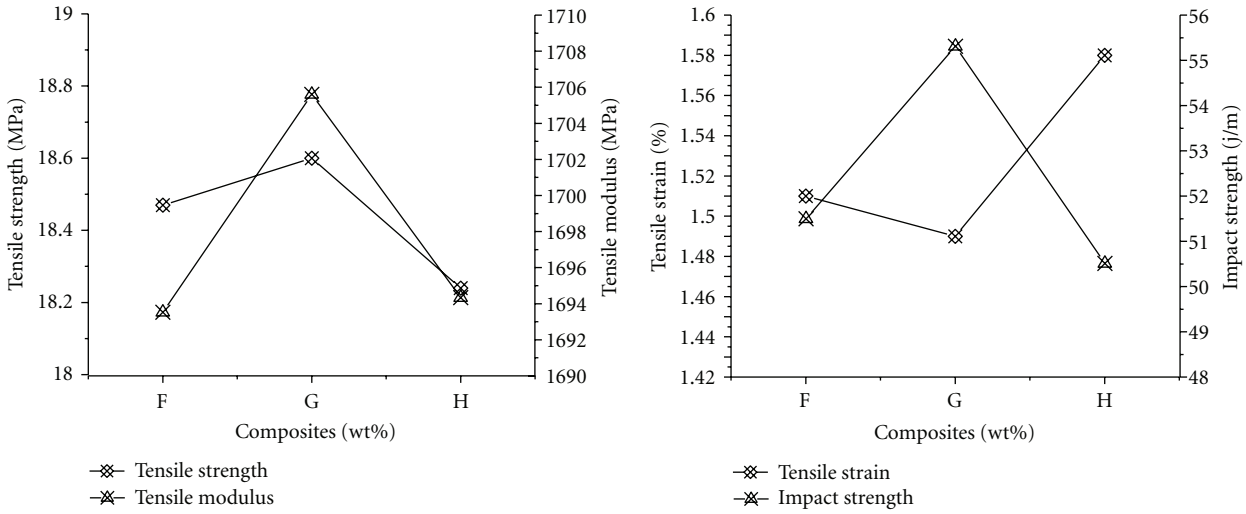

Figure 4: Mechanical properties of RPP/SF/MA-g-PP composites at different wt% of MA-g-PP loading whereas F: RPP/SF/MA-g-PP (67/30/3), G: RPP/SF/MA-g-PP (65/30/5) and H: RPP/SF/MA-g-PP (63/30/7).

mechanical interlocking [25]. This treatment increases the tensile strength 5.5%, tensile modulus 32.02%, and impact strength 72.75% as compared to RPP. Mercerization also provides better fiber surface adhesion characteristics by removing natural and artificial impurities, thus producing better surface topography.

Acetylated SF. Incorporation of acetylated SF (Acty-SF) into RPP indicates improvement of 0.21% in tensile strength, 28.93% in tensile modulus, and 65.64% in impact strength as compared to RPP. This improvement in tensile strength is due to the loss of hemicelluloses from the fiber surface [25] and tensile modulus due to the cross-linking reaction during melt mixing [24], whereas impact strength increases due to the minimum interfacial debonding according to Mishra et al. [37].

Silane Treated SF. Silane treated SF significantly increased the tensile strength, tensile modulus, and impact strength to 10.97%, 31.61%, and 78.72%, respectively as compared to RPP. This is due to that the ethoxy group of the silane reacts with the carbonyl group of the cellulosic fiber in ethanol media which further interact with RPP through hydrogen and covalent bonds. The sulphur atom present in silane can also impart polarity in the system to enhance the interaction with the RPP matrix. Thus it forms a bridge between fiber and matrix, enhancing the interfacial interaction between them [24–26]. Furthermore it can also be explained by

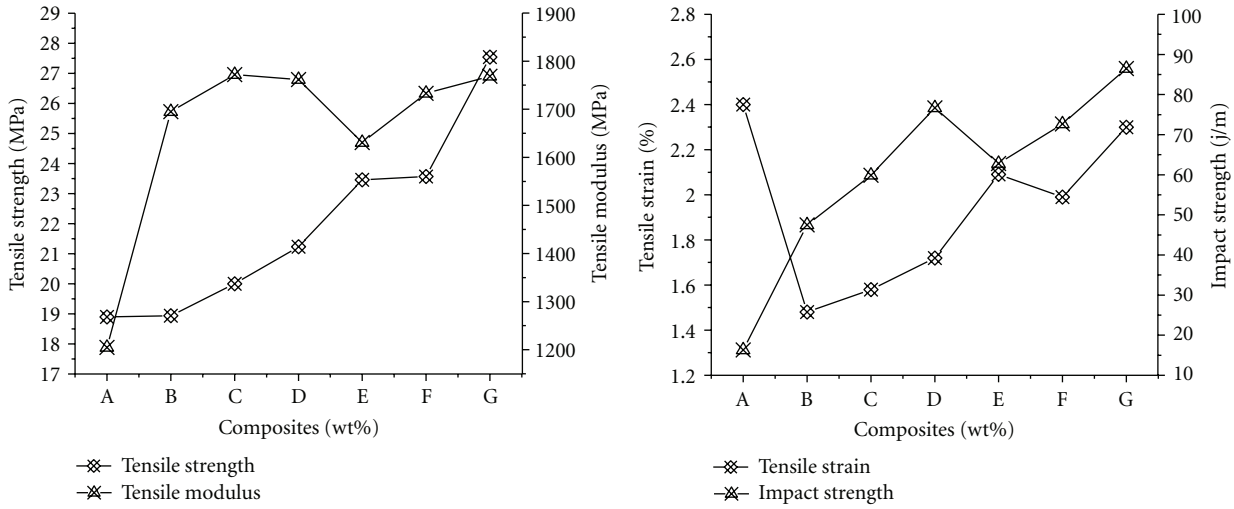

Figure 5: Mechanical properties of RPP/SF/MA-g-PP composites at ratio (65/30/5) whereas A: RPP, B: RPP/Acty-SF/MA-g-PP, C: RPP/NaOH-SF/MA-g-PP, D: RPP/Si-SF/MA-g-PP, E: RPP/$SrTiO_3$-SF/MA-g-PP, F: RPP/GMA-SF/MA-g-PP and G: RPP/OBDC-SF/MA-g-PP.

increased nucleation ability as a result of silane surface treatment yielding smaller and better crystals in a transcrystalline interphase region improving the bonding capability between the fiber and matrix.

$SrTiO_3$ Treated SF. The improvement in tensile strength, tensile modulus, and impact strength is found to be 19.43%, 26.12%, and 74.03% with the addition of $SrTiO_3$ treated SF. These results indicate improved bond durability and increased interaction between fiber and polymer matrix. This is also responsible for the hardening of fiber morphology and decreased elasticity [20].

GMA Treated SF. GMA treated SF indicates the improvement of tensile strength to 19.81%, tensile modulus to 30.48%, and impact strength to 77.55% respectively. This improvement is probably due to the effect of interfacial interactions in the presence of compatibilizer. The interactions between the epoxy groups grafted on fiber and the hydroxyl group on cellulose fibers are enhanced as the compatibilizer ratio increased [26].

OBDC Treated SF. Mechanical results due to OBDC treated fiber indicate improvement in tensile strength, tensile modulus and impact strength to 31.37%, 31.88%, and 81.13%, respectively. This indicates that interfacial bonding between the fiber and matrix has significantly improved upon chemical treatment leading to increased stress transfer efficiency from the matrix to the fiber. This further confirms the capability of the fiber to absorb energy that can stop crack propagation [15, 24, 25].

3.3. Thermal Analysis

3.3.1. Differential Scanning Calorimetry (DSC). The DSC heating and cooling thermograms of RPP, RPP/SF, and RPP/untreated and treated SF/MA-g-PP composites are depicted in Table 1 and Figure 6. The glass transition temperature (T_g), crystalline temperature (T_c), and melting temperature (T_m) of all samples are listed in Table 1. RPP shows a T_g value of -12.18°C, which is decreased to about -14.23°C with the incorporation of untreated SF. This indicates the plasticization effect occurs with the incorporation of natural fiber. Plasticization due to untreated fiber increased the chain mobility and free volume of the matrix chains by loose packing of fiber within the matrix confirms the improper surface interaction. This interaction can be further enhanced by addition of compatibilizer (MA-g-PP) and surface treatment of SF. In case of RPP/Si-SF/MA-g-PP composites, T_g of RPP increased from -12.18°C to -3.91°C. This confirms efficient adhesion between fiber and matrix upon treatment with silane. RPP/GMA-SF and RPP/OBDC-SF composites with MA-g-PP also an increase of -3.36°C and -4.48°C due to the poor adhesion and moisture absorption effect by GMA and OBDC surface treated fiber, respectively [15, 27].

The crystalline temperature (T_c) of RPP, RPP/SF, and RPP/untreated and treated SF/MA-g-PP are represented in Table 1. The results indicate that the T_c of RPP/SF with and without MA-g-PP and treated SF (Silane, GMA, OBDC) was slightly increased as compared with RPP. This may be due to the reorganization of amorphous domains in to crystalline regions with increased macromolecular flexibility and mobility at higher temperature [7–9].

Melting temperature (T_m) of RPP was observed around 167.8°C whereas its RPP/SF decreased to 165.83°C due to loss of chain alignment and conformational purity of RPP matrix during melt process with SF. This indicates the formation of crystallites with different sizes and/or perfection of ordering [38]. The melting transition has been enhanced by addition of MA-g-PP and surface treated SF as compared with RPP/SF composites. The improved interfacial interaction of fiber with polymer matrix leads

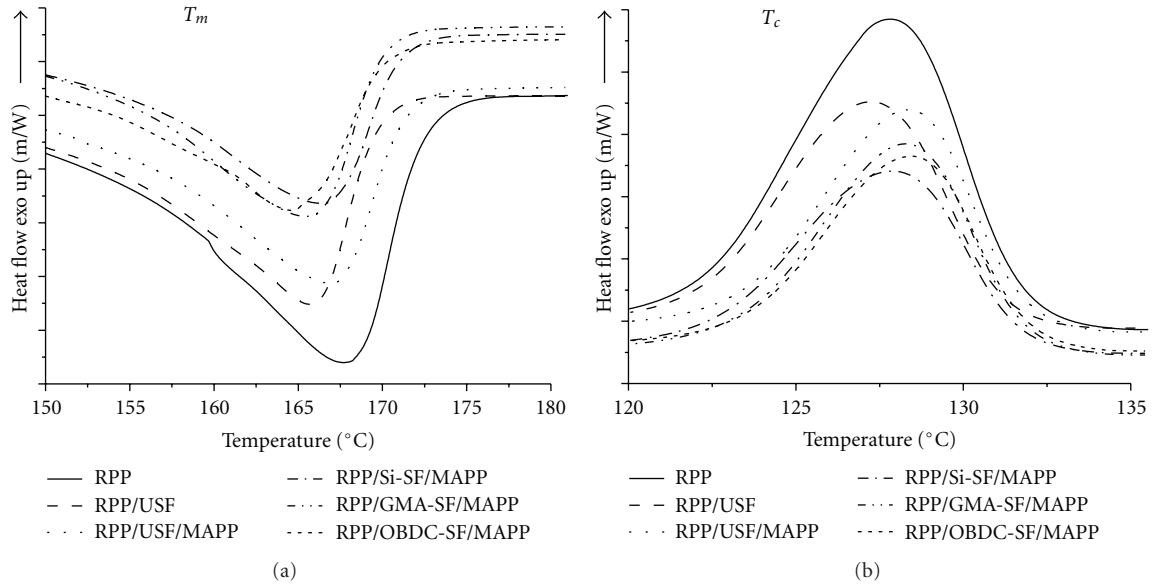

Figure 6: DSC graph temperature versus exothermic heat flow for (a) melting temperature (T_m) and (b) crystalline temperature (T_c).

to the enhancement in melting temperatures due to the addition of MA-g-PP and surface treated fiber [7].

3.3.2. Thermogravimetric Analysis (TGA). The thermal stability of RPP, RPP/SF, RPP/SF/MA-g-PP (65/30/5), and RPP/SF (Silane and GMA and OBDC treated SF)/MA-g-PP (65/30/5) composites were investigated using TGA and DTG curve as represented in Table 2 and Figure 7. It is evident that the thermal degradation of RPP started at 356°C with the final degradation temperature of 460°C. It also can be seen that the weight loss of RPP occurred in a one-step degradation process from 356°C to 450°C. The mass loss of RPP 234.2°C continues very slowly at temperature below 401.5°C. Above 400.6°C this process takes place very rapidly and the residue amount is almost zero at 460°C. On the other hand the thermal degradation of RPP/SF composites occurred in two-step degradation process. This result is also confirmed from DTG curve as represented in Figure 7. Addition of SF up to 30 wt% decreases its thermal stability as compared to RPP. This may be due to the lower decomposition temperature of SF present in the composites [32].

However RPP/SF composites with MA-g-PP exhibited increased thermal stability with an initial degradation temperature of 246.8°C and final degradation temperature of 412.5°C. This is probably due to dehydration from cellulose unit and thermal cleavage of glycosidic linkage by transglycosylation and scission of C–O and C–C bonds. At 436.5°C, RPP got completely decomposed, whereas in the composites a charred residue of carbonaceous product of 2.13% was left [7]. The RPP/SF composites with treated SF such as silane, GMA, and OBDC indicate higher thermal stability. Treated Silane is found to be increased to about 362.6°C and 472.5°C in initial and final degradation temperature. This behaviour is probably due to the increase in molecular weight by cross-linking reaction between matrix and fiber or molecular chain extension of the matrix itself, whereas GMA and OBDC are found to be increased in 363.4°C and 494.3°C in initial temperature and 379.2°C and 512.8°C in final degradation temperature. This is due to better surface adhesion towards the polymer matrix [15].

Table 1: Glass transition, melting, and crystallization properties of RPP/SF composites.

Sample	T_g (°C)	T_m (°C)	T_c (°C)
RPP	−12.18	167.86	128.18
RPP/SF (70/30)	−14.23	165.83	127.42
RPP/SF/MA-g-PP (65/30/5)	−5.66	166.85	128.28
RPP/Si-SF/MA-g-PP (65/30/5)	−3.91	166.32	128.87
RPP/GMA-SF/MA-g-PP (65/30/5)	−3.36	165.54	128.29
RPP/OBDC-SF/MA-g-PP (65/30/5)	−4.48	166.49	128.44

3.3.3. Heat Deflection Temperature (HDT). Heat deflection temperature (HDT) of RPP and RPP/SF composites was investigated using HDT analysis, which is depicted in Figure 8. The HDT values of RPP are found to be lesser with the addition of 30 wt% of SF and 5 wt% of MA-g-PP, whereas with the incorporation of treated fiber in RPP/SF composites show a significant increase in thermal stability to about 25°C–42°C. RPP/Si-SF/MA-g-PP, RPP/GMA-SF/MA-g-PP, and RPP/OBDC-SF/MA-g-PP composites indicate improved HDT to about 3.35%, 6.7%, and 14.77% as compared to RPP, respectively. The HDT value depends on the modulus and glass-transition temperature of a material. The modulus-temperature relationship plays a critical role in determining the HDT. Thus the improvement in the HDT values for

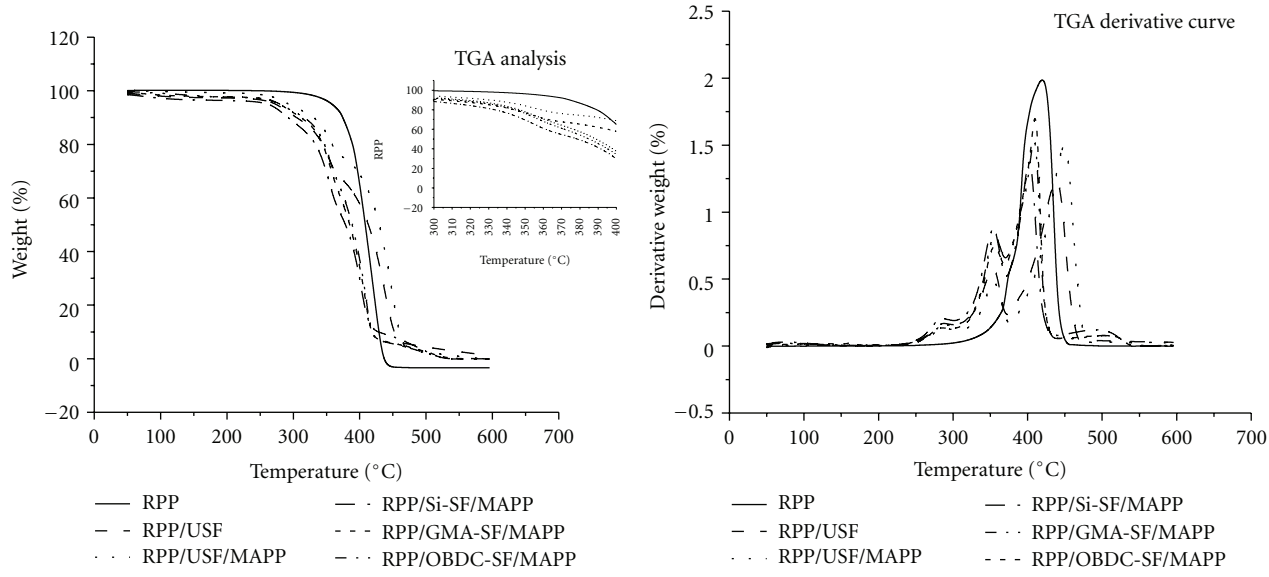

Figure 7: TGA and DTG analysis curve for thermal analysis.

Table 2: Thermogravimetric analysis (TGA).

Sample	Initial degradation temperature (°C)	Maximum degradation temperature 1 (°C)	Maximum degradation temperature 2 (°C)	Final degradation temperature (°C)
RPP	356	419.17	—	460
RPP/SF (70/30)	234.20	401.53	436.54	412.5
RPP/SF/MA-g-PP (65/30/5)	246.74	403.53	443.30	425.7
RPP/Si-SF/MA-g-PP (65/30/5)	362.13	399.57	446.95	472.6
RPP/GMA-SF/MA-g-PP (65/30/5)	363.67	400.68	451.41	494.3
RPP/OBDC-SF/MA-g-PP (65/30/5)	379.44	397.15	456.48	512.8

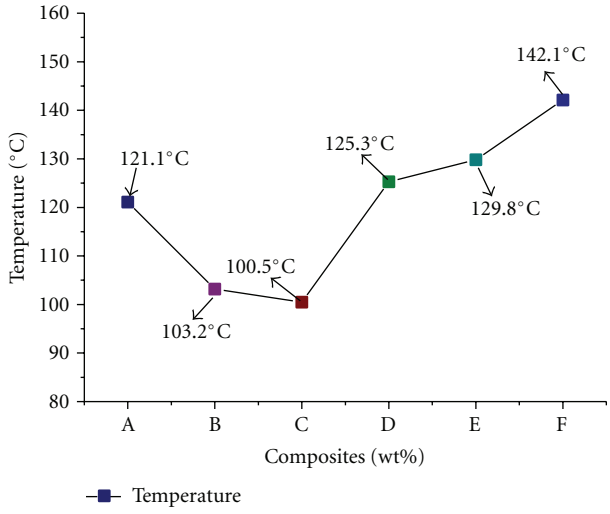

Figure 8: HDT graph where A: RPP, B: RPP/SF (70/30), C: RPP/SF/MA-g-PP (65/30/5), D: RPP/Si-SF/MA-g-PP (65/30/5), E: RPP/GMA-SF/MA-g-PP (65/30/5), and F: RPP/OBDC-SF/MA-g-PP.

the RPP/SF composites approches towards higher modulus values at elevated temperature as discussed earlier in case of mechanical properties [27].

3.4. Flammability Study. The burning rate of all the systems was investigated through horizontal burning test using UL-94 standards. All the systems burned up to 100 mm marks. Burning rates of RPP and RPP/SF composites measured by horizontal burning test are represented in Table 3 and Figure 9. The composites with the loading of 30 wt% of SF showed lower burning rate than that of the RPP. This indicated the lower sensitivity of sisal fiber filled RPP composites, to the flame. On the other hand the burning rate of the RPP/SF composites compatibilized with MA-g-PP was slightly decreased as compared to that of the uncompatibilized composites and was even less than that of RPP. This revealed the addition of compatibilizer help to reduce the burning rate of the RPP. Among the composites filled with treated fibers, the RPP/Si-SF/MA-g-PP showed the lowest rate of burning as it decreased by 16% and 7.42% as compared with RPP and RPP/SF composites, respectively. Therefore among all the systems

Table 3: Rate of burning properties of RPP/SF composites.

Sample	Rate of burning (mm/min.)	SD	Burning behaviour
RPP	10.00	0.43	Drips and ignites cotton, high flame, no residue, do not produce smoke
RPP/SF (70/30)	9.26	0.11	Slow dripping, ignites cotton, less spreading flame, residue remains, produce smoke
RPP/SF/MA-g-PP (65/30/5)	9.47	0.35	Drips in a slower rate, ignites cotton, less spreading flame, residue gray colour, produce smoke
RPP/Si-SF/MA-g-PP (65/30/5)	8.62	1.22	Very less dripping, do not ignite cotton, very less flame spreading, less smoke produced
RPP/GMA-SF/MA-g-PP (65/30/5)	9.31	0.41	Very less dripping, do not ignite cotton, very less spreading flame, high smoke production
RPP/OBDC-SF/MA-g-PP (65/30/5)	9.76	0.30	Do not drip, do not ignite cotton, high flame spread, large amount of residue, high smoke production

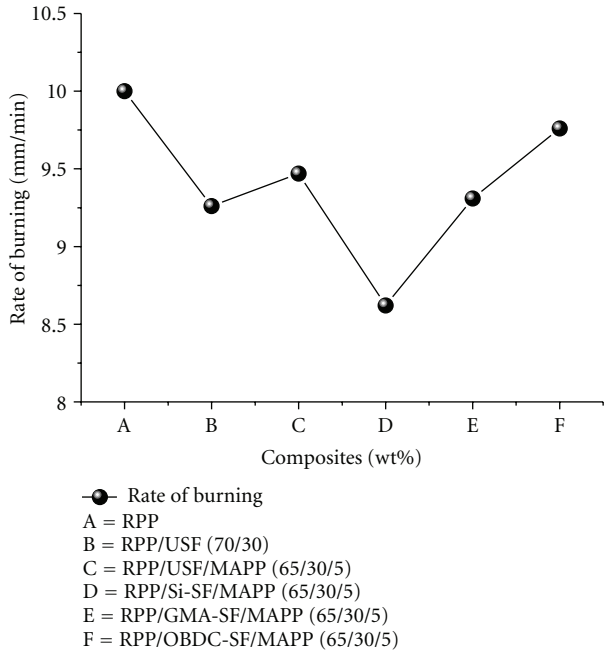

Figure 9: Rate of horizontal burning.

RPP/Si-SF/MA-g-PP composite showed the highest stability towards flame [39].

3.5. Morphological Study (SEM). The surface morphology of fractured RPP/SF composites reflects the reason about higher mechanical properties. The Morphological impact fractured surface of RPP/SF (70/30), RPP/SF/MA-g-PP (65/30/5), RPP/Si-SF/MA-g-PP (65/30/5), RPP/GMA-SF/MA-g-PP (65/30/5), and RPP/OBDC-SF/MA-g-PP (65/30/5) composites and treated sisal fiber shown in Figure 10, SEM images of RPP/SF, RPP/SF/MA-g-PP implies poor interfacial bonding between the matrix and the untreated fiber. On the other hand chemically treated SF composites show almost no sign of fiber agglomeration and microvoids in the fractured surface of the composites. These results suggest that interfacial adhesion between the chemically treated SF and RPP matrix has become much more favorable upon treatment of the fiber with Silane, GMA and OBDC [7]. In general, fiber treatments can significantly improve adhesion at the former interface and also lead to ingress of the matrix into the fibers, obstructing pullout of the cells. This further confirms the removal of wax, oils and other low molar mass impurities which make the fiber surface rougher towards better adhesion with the matrix. The micrographs show that the untreated fibres are covered with a layer, whose composition is probably mainly waxy substances, as has been reported also previously [15–32]. It can be seen that the layer is not evenly distributed along the fibre surface, but its thickness varies from point to point. As seen in SEM images the surface of the treated fiber became smoother as compared to that of untreated fiber. Removal of the waxy and oil substances on the surface of lignocellulosic materials and replacement of surface hydroxyl groups by acetyl and propionyl groups could explain smoothening of the fibre surface after treatments [40].

4. Conclusions

In this present study the mechanical, thermal, flammability, and morphological properties of the RPP/SF (untreated and treated) with and without compatibilizer composites have been investigated. RPP/SF composites were prepared using melt compounding techniques. Composites prepared at 30 wt% of fiber loading with 5% MA-g-PP showed optimum mechanical performance. Incorporation of treated sisal fiber such as silane and GMA and OBDC additionally increases the mechanical and thermal properties of PP matrix. Thermal degradation temperature of RPP/SF composites shows higher values as indicated by TGA and HDT analysis. DSC study shows higher T_g and T_c as compared to RPP indicating increased macromolecular flexibility and mobility. The flammability of RPP/SF composites studied by horizontal burning (UL-94) method shows the decrease level of burning rate of RPP/SF composites due to the presence of flammable sisal fiber. The morphological observations by SEM indicate efficient removal of cementing agents from

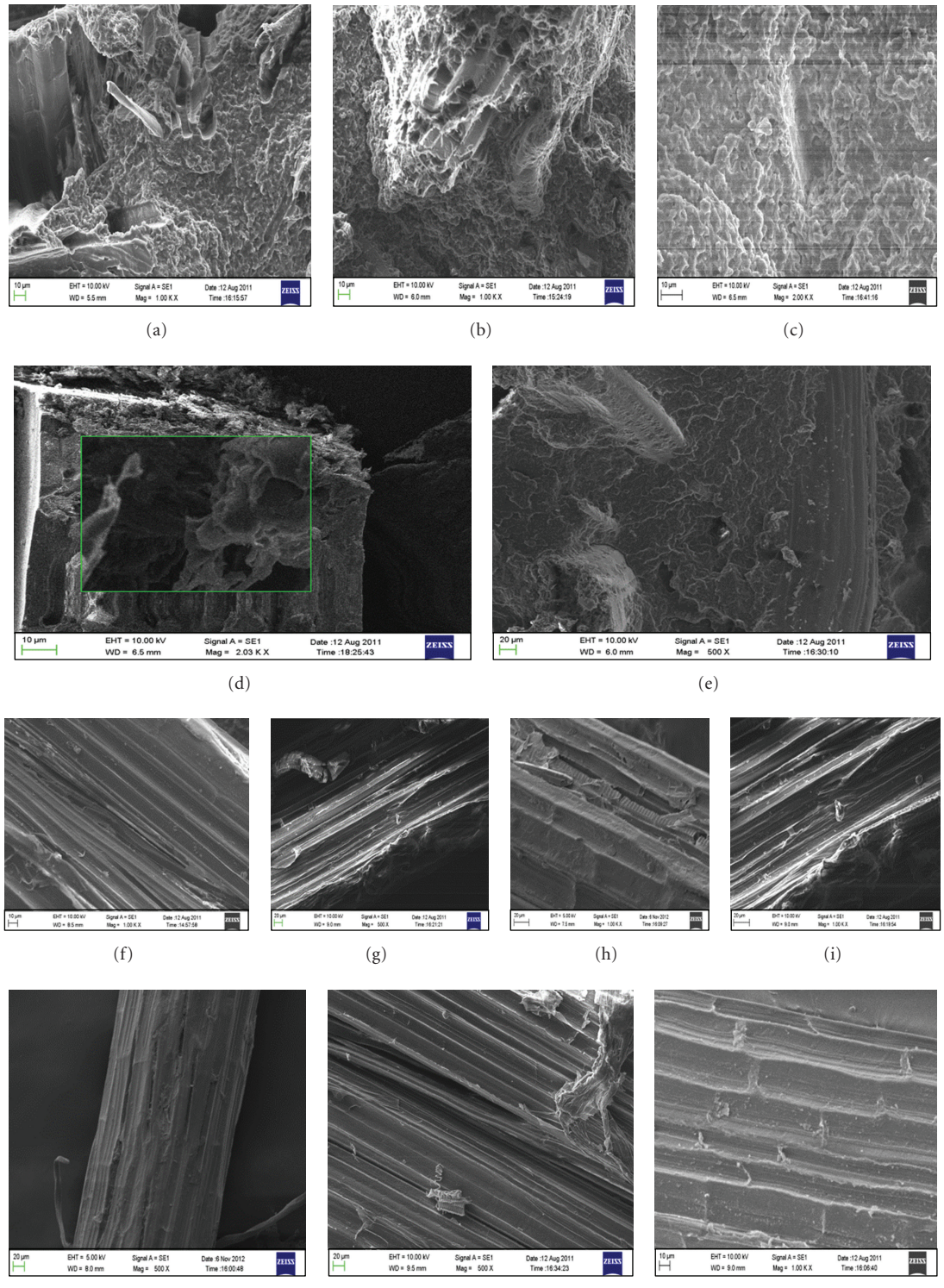

Figure 10: SEM image of impact fractured RPP/SF composites, untreated and treated sisal fiber, whereas (a) RPP/SF, (b) RPP/SF/MA-g-PP, (c) RPP/Si-SF/MA-g-PP, (d) RPP/GMA-SF/MA-g-PP, and (e) RPP/OBDC-SF/MA-g-PP, (f) untreated SF, (g) NaOH-SF, (h) Acetylated SF, (i) Si-SF, (j) $SrTiO_3$-SF, (k) GMA-SF, and (l) OBDC-SF.

raw sisal fibers enhances the fiber adhesion properties with matrix due to surface treatment. Thus RPP/SF composites with balanced mechanical and thermal properties can be achieved at an optimal concentration of treated SF and compatibilizer with RPP matrix.

References

[1] M. Q. Zhang, M. Z. Rong, and X. Lu, "Fully biodegradable natural fiber composites from renewable resources: all-plant fiber composites," *Composites Science and Technology*, vol. 65, no. 15-16, pp. 2514–2525, 2005.

[2] A. K. Bledzki, V. E. Sperber, and O. Faruk, "Natural and wood fibre reinforcement in polymers," *Rapra Review Reports*, vol. 13, p. 152, 2002.

[3] G. Pritchard, "Two technologies merge: wood plastic composites," *Plastics, Additives and Compounding*, vol. 6, no. 4, pp. 18–21, 2004.

[4] S. Mishra, A. K. Mohanty, L. T. Drzal, M. Misra, and G. Hinrichsen, "A review on pineapple leaf fibers, sisal fibers and their biocomposites," *Macromolecular Materials and Engineering*, vol. 289, no. 11, pp. 955–974, 2004.

[5] E. Sinha and S. K. Rout, *Bulletin of Material Science*, vol. 32, pp. 65–67, 2009.

[6] F. Khan and S. R. Ahmad, "Chemical modification and spectroscopic analysis of jute fibre," *Polymer Degradation and Stability*, vol. 52, no. 3, pp. 335–340, 1996.

[7] M. Biswal, S. Mohanty, and S. K. Nayak, "Influence of organically modified nanoclay on the performance of pineapple leaf fiber-reinforced polypropylene nanocomposites," *Journal of Applied Polymer Science*, vol. 114, no. 6, pp. 4091–4103, 2009.

[8] A. C. N. Singleton, C. A. Baillie, P. W. R. Beaumont, and T. Peijs, "On the mechanical properties, deformation and fracture of a natural fibre/recycled polymer composite," *Composites Part B*, vol. 34, no. 6, pp. 519–526, 2003.

[9] N. E. Zafeiropoulos, C. A. Baillie, and F. L. Matthews, *Advanced Composite*, vol. 10, pp. 291–295, 2001.

[10] H. L. Bos and A. M. Donald, "In situ ESEM study of the deformation of elementary flax fibres," *Journal of Materials Science*, vol. 34, no. 13, pp. 3029–3034, 1999.

[11] C. R. Reddy, A. P. Sardashti, and L. C. Simon, "Preparation and characterization of polypropylene-wheat straw-clay composites," *Composites Science and Technology*, vol. 70, no. 12, pp. 1674–1680, 2010.

[12] A. K. Bledzki and J. Gassan, "Composites reinforced with cellulose based fibres," *Progress in Polymer Science*, vol. 24, no. 2, pp. 221–274, 1999.

[13] M. Sain, P. Suhara, S. Law, and A. Bouilloux, "Interface modification and mechanical properties of natural fiber-polyolefin composite products," *Journal of Reinforced Plastics and Composites*, vol. 24, no. 2, pp. 121–130, 2005.

[14] S. Panthapulakkal and M. Sain, "Studies on the water absorption properties of short hemp-glass fiber hybrid polypropylene composites," *Journal of Composite Materials*, vol. 41, no. 15, pp. 1871–1883, 2007.

[15] N. Islam, R. Rahman, M.. Haque, and M. Huque, *Composites*, vol. 41, pp. 192–198, 2010.

[16] S. Spoljaric, A. Genovese, and R. A. Shanks, "Polypropylene-microcrystalline cellulose composites with enhanced compatibility and properties," *Composites Part A*, vol. 40, no. 6-7, pp. 791–799, 2009.

[17] Z. Demjen, B. Pukanszky, and J. Nagy, *Composites*, vol. 29, pp. 323–329, 1998.

[18] A. P. Mathew, K. Oksman, and M. Sain, "Mechanical properties of biodegradable composites from poly lactic acid (PLA) and microcrystalline cellulose (MCC)," *Journal of Applied Polymer Science*, vol. 97, no. 5, pp. 2014–2025, 2005.

[19] A. Terenzi, J. M. Kenny, and S. E. Barbosa, "Natural fiber suspensions in thermoplastic polymers. I. analysis of fiber damage during processing," *Journal of Applied Polymer Science*, vol. 103, no. 4, pp. 2501–2506, 2007.

[20] A. Leão and S. Paulo, *Plástico Industrial*, vol. 229, pp. 214–229, 2001.

[21] R. Kohler and K. Nebel, *Macromolecules*, vol. 244, pp. 97–106, 2006.

[22] A. K. Bledzki and J. Gassan, "Natural fiber reinforced plastics," in *Handbook of Engineering Polymeric Materials*, N. P. Cheremisinoff, Ed., chapter 52, p. 787, Marcel Dekker, New York, NY, USA, 1997.

[23] G. Marsh, "Next step for automotive materials," *Materials Today*, vol. 6, no. 4, pp. 36–43, 2003.

[24] M. S. Sreekala, M. G. Kumaran, S. Joseph, M. Jacob, and S. Thomas, "Oil palm fibre reinforced phenol formaldehyde composites: influence of fibre surface modifications on the mechanical performance," *Applied Composite Materials*, vol. 7, no. 5-6, pp. 295–329, 2000.

[25] D. Nabi Saheb and J. P. Jog, "Natural fiber polymer composites: a review," *Advances in Polymer Technology*, vol. 18, no. 4, pp. 351–363, 1999.

[26] T. J. Keener, R. K. Stuart, and T. K. Brown, "Maleated coupling agents for natural fibre composites," *Composites Part A*, vol. 35, no. 3, pp. 357–362, 2004.

[27] M. Pracella, D. Chionna, I. Anguillesi, Z. Kulinski, and E. Piorkowska, "Functionalization, compatibilization and properties of polypropylene composites with Hemp fibres," *Composites Science and Technology*, vol. 66, no. 13, pp. 2218–2230, 2006.

[28] S. K. Garkhail, R. W. H. Heijenrath, and T. Peijs, "Mechanical properties of natural-fibre-mat-reinforced thermoplastics based on flax fibres and polypropylene," *Applied Composite Materials*, vol. 7, no. 5-6, pp. 351–372, 2000.

[29] J. Gassan and A. K. Bledzki, "Possibilities to improve the properties of natural fiber reinforced plastics by fiber modification—jute polypropylene composites," *Applied Composite Materials*, vol. 7, no. 5-6, pp. 373–385, 2000.

[30] K. Oksman, "Mechanical properties of natural fibre mat reinforced thermoplastic," *Applied Composite Materials*, vol. 7, no. 5-6, pp. 403–414, 2000.

[31] P. R. Hornsby, E. Hinrichsen, and K. Tarverdi, "Preparation and properties of polypropylene composites reinforced with wheat and flax straw fibres: part II Analysis of composite microstructure and mechanical properties," *Journal of Materials Science*, vol. 32, no. 4, pp. 1009–1015, 1997.

[32] R. Krishnamoorti, R. A. Vaia, and E. P. Giannelis, "Structure and dynamics of polymer-layered silicate nanocomposites," *Chemistry of Materials*, vol. 8, no. 8, pp. 1728–1734, 1996.

[33] M. Zenkiewicz and M. Kurcok, "Effects of compatibilizers and electron radiation on thermomechanical properties of composites consisting of five recycled polymers," *Polymer Testing*, vol. 27, no. 4, pp. 420–427, 2008.

[34] G. Cantero, A. Arbelaiz, F. Mugika, A. Valea, and I. Mondragon, "Mechanical behavior of wood/polypropylene composites: effects of fibre treatments and ageing processes,"

Journal of Reinforced Plastics and Composites, vol. 22, no. 1, pp. 37–50, 2003.

[35] S. Kalia, B. S. Kaith, and I. Kaur, "Pretreatments of natural fibers and their application as reinforcing material in polymer composites-a review," *Polymer Engineering and Science*, vol. 49, no. 7, pp. 1253–1272, 2009.

[36] J. Gassan and A. K. Bledzki, "The influence of fiber-surface treatment on the mechanical properties of jute-polypropylene composites," *Composites Part A*, vol. 28, no. 12, pp. 1001–1005, 1997.

[37] S. Mishra, A. K. Mohanty, L. T. Drzal et al., "Studies on mechanical performance of biofibre/glass reinforced polyester hybrid composites," *Composites Science and Technology*, vol. 63, no. 10, pp. 1377–1385, 2003.

[38] P. S. Mukherjee and K. G. Satyanarayana, "Structure and properties of some vegetable fibres—part 1 Sisal fibre," *Journal of Materials Science*, vol. 19, no. 12, pp. 3925–3934, 1984.

[39] M. Sain, S. H. Park, F. Suhara, and S. Law, "Flame retardant and mechanical properties of natural fibre-PP composites containing magnesium hydroxide," *Polymer Degradation and Stability*, vol. 83, no. 2, pp. 363–367, 2004.

[40] M. Z. Rong, M. Q. Zhang, Y. Liu, G. C. Yang, and H. M. Zeng, "The effect of fiber treatment on the mechanical properties of unidirectional sisal-reinforced epoxy composites," *Composites Science and Technology*, vol. 61, no. 10, pp. 1437–1447, 2001.

Hindawi Publishing Corporation
Advances in Mechanical Engineering
Volume 2012, Article ID 141248, 6 pages
doi:10.1155/2012/141248

Research Article

Effect of Red Mud and Copper Slag Particles on Physical and Mechanical Properties of Bamboo-Fiber-Reinforced Epoxy Composites

Sandhyarani Biswas,[1] Amar Patnaik,[2] and Ritesh Kaundal[2]

[1] *Department of Mechanical Engineering, NIT, Rourkela 769008, India*
[2] *Department of Mechanical Engineering, NIT, Hamirpur 177005, India*

Correspondence should be addressed to Sandhyarani Biswas, biswas.sandhya@gmail.com

Received 26 April 2012; Revised 20 October 2012; Accepted 3 November 2012

Academic Editor: Mohamed S. Aly-Hassan

In the present work, a series of bamboo-fiber-reinforced epoxy composites are fabricated by using red mud and copper slag particles as filler materials. A filler plays an important role in determining the properties and behavior of particulate composites. The effects of these two fillers on the mechanical properties of bamboo-epoxy composites are investigated. Comparative analysis shows that with the incorporation of these fillers, the tensile strength of the composites increases significantly, whereas the flexural strength and impact strength decrease with increase in filler content (red mud and copper slag fillers) in the epoxy-bamboo fiber composites. The density and hardness are also affected by the type and content of filler particles. It is found that the addition of copper slag filler improves the hardness of the bamboo-epoxy composites, whereas the addition of red mud filler reduces the hardness value of bamboo-epoxy composites. The study reveals that the addition of copper slag filler in bamboo-epoxy composites shows better physical and mechanical properties as compared to the red-mud-filled composites.

1. Introduction

In the recent years, for making the low-cost engineering materials the use of natural fibers in polymers composites has brought forth a lot of interest. The new environmental legislation as well as consumer demands has pressured manufacturing industries (especially automotive, packaging and construction) to search new materials that can replace the conventional nonrenewable reinforcing materials such as glass fibre, carbon fiber, and so forth [1]. The advantages of natural fibers over the traditional glass fibers are low density, good specific strength and modulus, economical viability, enhanced energy recovery, and good biodegradability [2]. There are also some disadvantages of natural fiber-reinforced polymer composites such as the incompatibility between the hydrophilic natural fibres and hydrophobic thermoplastic and thermoset matrices requiring appropriate use of physical and chemical treatments to enhance the adhesion between fibre and the matrix [3]. Generally the cellulosic fibers, like henequen, sisal, coconut fiber (coir), jute, palm, bamboo, wood, paper in their natural condition, and several waste cellulosic products such as shell flour, wood flour, and pulp have been used as reinforcement materials in different thermosetting and thermoplastic resins [4–11].

Being a conventional construction material since ancient times, bamboo fiber is a good campaigner for use as a natural fiber in composite materials. The reason that many studies focus on bamboo is because it is an abundant natural resource in Asia, and its overall mechanical properties are comparable to those of wood. Bamboo is a naturally occurring composite material, which grows abundantly in most of the tropical countries. This is one of the oldest building materials used by human kind. The attractive physical and mechanical properties that can be obtained with bamboo-fiber- reinforced composites, such as high specific modulus, strength, and thermal stability, have been well documented in the literature. Jain et al. [12] have compared the Bamboo fiber reinforced epoxy composites $(BFRP)_{epoxy}$

with Bamboo-fiber-reinforced unsaturated polyester composites. $(BFRP)_{USP}$ in terms of their cost and mechanical strength. Jindal [13] has observed that tensile strength of bamboo-fiber-reinforced plastic (BFRP) composite is comparatively equivalent to that of the mild steel, whereas their density is only 12% of that of the mild steel. Hence, the BFRP composites can be extremely useful in structural applications. Takagi and Ichihara [14] have studied the effect of fiber content and fiber length on mechanical properties of bamboo-fiber-reinforced green composites (BFGC). Fiber length up to 15 mm has given positive effect on tensile strength and flexural strength.

In the fiber-reinforced polymer composites, fillers play an important role. The addition of particulate fillers has shown a great promise and has been a subject of considerable interest due to the improvement in performance of polymers and their composites in industrial and structural applications due to the addition of fillers. Filler materials are used in composite materials to reduce material costs, to improve mechanical properties to some extent, and in some cases to improve processability. They also increase the properties like hardness and abrasion resistance and reduce the shrinkage. The physical and mechanical characteristics can further be modified by adding a solid filler phase to the matrix body during the composite preparation. Biswas and Satapathy [15] study the effect of red mud filler particles on the epoxy-bamboo fiber composites and epoxy-glass fiber composites. Also Biswas et al. [16] studied the effect of ceramic fillers on mechanical properties of bamboo-fiber-reinforced epoxy composites and results show that the addition of ceramic fillers in bamboo-fiber-reinforced epoxy composites enhanced the mechanical properties of the composites. Although a great deal of work has been published on the effect of various types and content of fillers on polymer composites, the potential of ceramic-rich industrial wastes for such use in polymeric matrices has rarely been explored. Industrial development over the last decades has generated huge amounts of toxic and hazardous inorganic waste like, fly ash, cement by pass dust, copper slag, red mud, and so forth, which contain appreciable amounts of hazardous elements.

Production of alumina from bauxite by the Bayer's process is associated with the generation of red mud as the major waste material in alumina industries worldwide. Depending upon the quality of bauxite, the quantity of red mud generated varies from 55 to 65% of the bauxite processed [17]. The enormous quantity of red mud discharged by these industries poses an environmental and economical problem. Red mud, as the name suggests, is brick red in colour and slimy having average particle size of about 80–100 μm. It comprises of the iron, titanium, and the silica part of the parent ore along with other minor constituents. Depending on the source, these residues have a wide range of composition: Fe_2O_3 20–60%, Al_2O_3 10–30%, SiO_2 2–20%, Na_2O_2 10%, CaO 2–8%, and TiO_2 traces 2–8%. Copper slag is produced during matte smelting and conversion steps in the pyro-metallurgical production of copper. During matte smelting, two separate liquid phases, copper-rich matte (sulphides) and slag (oxides) are formed. It has been estimated that for every tonne of refined copper produced, about 2.2 tonne of slag is generated and every year, approximately 24.6 million tonne of slag is generated in copper production worldwide. Slag containing <0.8% copper is either discarded as waste or sold as products with properties similar to those of natural basalt (crystalline) or obsidian (amorphous). Copper slag having average particle size of about 80–100 μm. The composition of the copper slag is as follows: Fe_2O_3 35.3%, SiO_2 36.6%, CaO 10%, Al_2O_3 8.1%, CuO 0.37%, MgO 4.38%, Na_2O 0.47%, K_2O 3.45%, PbO 0.12%, Zn 0.97%, and Cu 0.24%. The objectives of this study were to investigate the physical and mechanical properties of particulate (red mud and copper slag) filled epoxy-bamboo fiber hybrid composites and present the comparison between the effect of red mud and copper slag filler on bamboo-epoxy composites.

2. Preparation of Composites

The filler composites of four different compositions are prepared for this study. Bamboo fiber was collected from local supplier and is used as the common reinforcing phase in all the four compositions. The bamboo fiber has an elastic modulus 1.9 GPa and possesses a density of 1.32 g/cm^3. Epoxy resin (Elastic modulus 3.42 GPa, density 1.36 g/cm^3), manufactured by Ciba Geigy and locally supplied by Northern Polymers Ltd. New Delhi, India, is the matrix material. Here the red mud and copper slag are used as filler materials. The composites are made by conventional hand lay-up technique. The low temperature curing epoxy resin and corresponding hardener (HY951) are mixed in a ratio of 10 : 1 by weight as recommended. After that red mud and copper slag fillers are mixed in the epoxy resin before the bamboo fiber is reinforced in the matrix, the composites are prepared in two different sets. In first set, the red mud, (0, 5, 10, and 15 wt.%) is used as filler materials and mixed in the epoxy resin before the bamboo fiber is reinforced in the matrix. In second set, copper slag (0, 5, 10, and 15 wt.%) is used as a filler materials and mixed in the epoxy resin before the bamboo fiber is reinforced in the matrix. For all the composition, bamboo fiber-loading (weight fraction of bamboo fiber in the composite) is kept fixed, that is, 45 wt.% of bamboo fiber. The castings are put under load for about 24 h for proper curing at room temperature. Specimens of suitable dimension are cut using a diamond cutter for physical, mechanical characterization, and erosion testing.

3. Physical and Mechanical Characterization

3.1. Density. The theoretical density of the composite materials in terms of weight fraction can easily be calculated as in the following equation given by Agarwal and Broutman [18]:

$$\rho_{ct} = \frac{1}{\left(W_f/\rho_f\right) + \left(W_m/\rho_m\right)}. \quad (1)$$

In this equation, W and ρ represent the weight fraction and density of the fiber and matrix materials. Equation (1) is suitable only for two phase composite materials, but in the present investigation the composites consist of three

Table 1: Density and void fraction of red mud filled short epoxy-bamboo fiber composites.

Designation	Composition	Theoretical density (g/cm^3)	Experimental density (g/cm^3)	Voids fraction (%)
EBR-1	Epoxy + 45 wt.% Bamboo fiber + 0 wt.% red mud	1.17	1.15	1.71
EBR-2	Epoxy + 45 wt.% Bamboo fiber + 5 wt.% red mud	1.21	1.18	2.48
EBR-3	Epoxy + 45 wt.% Bamboo fiber + 10 wt.% red mud	1.23	1.17	4.88
EBR-4	Epoxy + 45 wt.% Bamboo fiber + 15 wt.% red mud	1.25	1.16	7.20

EBR: Red mud filled Bamboo fiber reinforced Epoxy composites.

Table 2: Density and void fraction of copper slag filled short epoxy-bamboo fiber composites.

Designation	Composition	Theoretical density (g/cm^3)	Experimental density (g/cm^3)	Voids fraction (%)
EBC-1	Epoxy + 45 wt.% Bamboo fiber + 0 wt.% copper slag	1.17	1.15	1.71
EBC-2	Epoxy + 45 wt.% Bamboo fiber + 5 wt.% copper slag	1.27	1.21	4.72
EBC-3	Epoxy + 45 wt.% Bamboo fiber + 10 wt.% copper slag	1.34	1.25	6.72
EBC-4	Epoxy + 45 wt.% Bamboo fiber + 15 wt.% copper slag	1.49	1.38	7.38

components, that is, matrix, fiber and particulate filler. Therefore, the theoretical density of the theses composites can be calculated easily by using the following modified form of (1) written as

$$\rho_{ct} = \frac{1}{\left(W_f/\rho_f\right) + \left(W_m/\rho_m\right) + \left(W_p/\rho_p\right)}, \quad (2)$$

where the suffix "ρ" indicates the particulate filler materials.

Whereas the actual density (ρ_{ce}) of the composites can be determined experimentally by using simple water immersion technique. The volume fraction of voids (V_v) in the composites is calculated using the following equation:

$$V_v = \frac{\rho_{ct} - \rho_{ct}}{\rho_{ct}}. \quad (3)$$

3.2. Micro-Hardness. Micro-hardness measurement is done using a micro-hardness tester equipped with a square-based pyramidal (angle 136° between opposite faces) diamond indenter by applying a load of 10 N.

3.3. Tensile Test. The tensile test is performed on flat specimens. During the tensile test, a uniaxial load is applied through both ends of the specimen. The ASTM standard test method for tensile properties of fiber resin composites has the designation D 3039-76. The length of the test section should be 200 mm. The tensile test is performed in the universal testing machine (UTM) Instron 1195, and results are analyzed to calculate the tensile strength of composite samples.

3.4. Flexural Strength. The flexural strength is calculated by three point bend test, and the data is recorded during the test. The flexural strength (F.S) of any composite specimen is determined using the following equation. The test is conducted as per ASTM standard (D2344-84) using the same universal testing machine (UTM)

$$\text{F.S} = \frac{3PL}{2bt^2}, \quad (4)$$

where P is maximum load, b the width of specimen and t the thickness of specimen, and L the span length of the sample.

3.5. Impact Test. Low velocity instrumented impact tests are carried out on composite specimens. The tests are done as per ASTM D 256 using an impact tester. The pendulum impact testing machine ascertains the notch impact strength of the material by shattering the V notched (45°) specimen with a pendulum hammer, measuring the spent energy, and relating it to the cross section of the specimen. The standard specimen for ASTM D 256 is 60 mm × 10 mm × 4 mm and the depth under the notch is 2 mm.

4. Results and Discussions

4.1. Effect of Filler Content on Void Faction of Particulate Filled Epoxy-Bamboo Fiber Composites. Determining the properties of the composites, density is the most important factor. Density generally depends upon the relative proportion of the matrix and the reinforcing materials. The theoretical and measured densities along with the corresponding volume fraction of voids for red mud filled and copper filled epoxy-bamboo fiber composites are presented in Tables 1 and 2. It is noticed that the density calculated theoretically using (1) is not in agreement with the experimental calculated density value. Therefore, the difference between the theoretical and experimental density value is the measure of the voids and pores present in the composites.

It is seen from Tables 1 and 2 that the volume fraction of voids increases with increasing the filler concentration in the epoxy-bamboo fiber composites. In case of 0 wt.% red mud and copper slag filled epoxy-bamboo fiber composite, the volume fraction of voids is less. However, with the addition

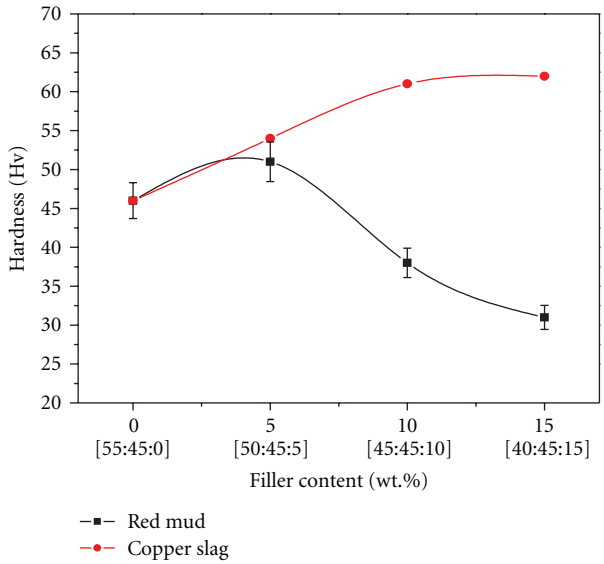

Figure 1: Variation of Micro-hardness with red mud and copper slag filler percentage.

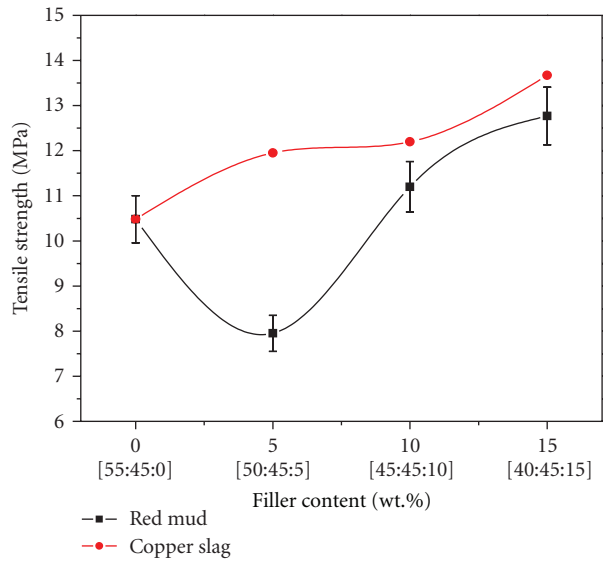

Figure 2: Variation of Tensile strength with red mud and copper slag filler percentage.

of filler materials, more voids are found in the composites. As the filler content increases from 5 wt.% to 15 wt.%, the volume fraction of voids is also found to be increasing proportionately. The composites filled with 15 wt.% of red mud and copper slag filled epoxy-bamboo fiber composites showd the maximum volume fraction of voids as compare to the others composites. Hence, based up on the above analysis, it is clearly demonstrated that with increase in filler concentration the void content of the composites goes on increasing. On comparison of red mud and copper slag filled epoxy-bamboo fiber composites, it is seen that the composites filled copper slag filler shows the higher values of voids as compared to the red mud filled composites. This is due to the higher density of the copper slag fillers as compared to the red mud filler.

The mechanical performance of the composites is generally influenced by the presence of voids, and the estimation of the quality of the composites is based upon the knowledge of void contents in the composites. The air-filled cavities formed inside the composite is known as porosity, and it is, often unavoidable part in all the composites during the fabrication process. The void may be originated during the mixing and integration of two or more different material parts. Higher void contents usually mean lower fatigue resistance, greater susceptibility to water penetration, and weathering [18]. It is understandable that a good composite should have fewer voids. However, presence of void is unavoidable in composite making particularly through hand-lay-up route.

4.2. Effect of Filler Content on Hardness of Particulate Filled Epoxy-Bamboo Fiber Composites. Surface hardness of the composites is considered as one of the most important factors that govern the nature and properties of the composites. The measured hardness values of both the red mud and copper slag filled and unfilled epoxy-bamboo fiber composites are shown in Figure 1. It is seen that in case of red mud filled composites, the hardness value decreases with increase in the filler contents.

Whereas in case of copper slag, the hardness value increases with increases in the fillers contents. In case of hardness test, a compression or pressing stress is in action. So the matrix phase and the solid filler phase would press together and touch each other more significantly. Thus the interface can transfer pressure more effectively although the interfacial bond may be poor.

4.3. Effect of Filler Content on Tensile Strength of Particulate Filled Epoxy-Bamboo Fiber Composites. Tensile properties of red mud and copper slag filled epoxy-bamboo fiber composites were studied. Tensile strength of the bamboo-epoxy filled with red mud and copper slag filler content ranged from 0 wt.% to 15 wt.% is shown in Figure 2. It is seen that the tensile strength of all the composites increases with increase in the both the fillers contents.

However, the composite filled with 5 wt.% of red mud filler contents shows the lower tensile strength value as compared to 0 wt.% of red mud filled epoxy-bamboo fiber composite. The decreased in tensile strength with 5 wt.% of red mud filler content is due to the poor adhesion between the fiber, filler, and the matrix, because without proper adhesion at higher loads reinforcements promote void formation. The particle loading and particle size, the particle, fiber and matrix interfacial adhesion significantly affects the strength of the composites. The effective stress transfer is the most important factor, which leads to the strength of composites materials. When the bonding between the particles and matrix is poor, the stress transfer at the particle/polymer interface is insufficient. Therefore, discontinuity in the form of debonding exists because of non-adherence of particle to polymer. Due to this (debonding),

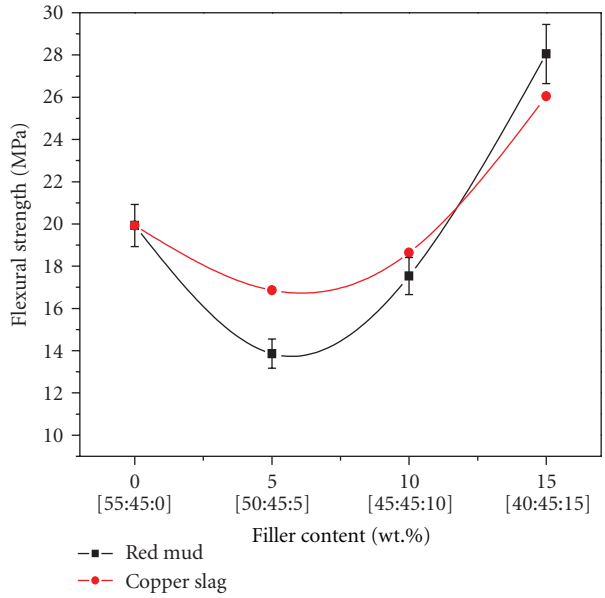

Figure 3: Variation of Flexural strength with red mud and copper slag filler percentage.

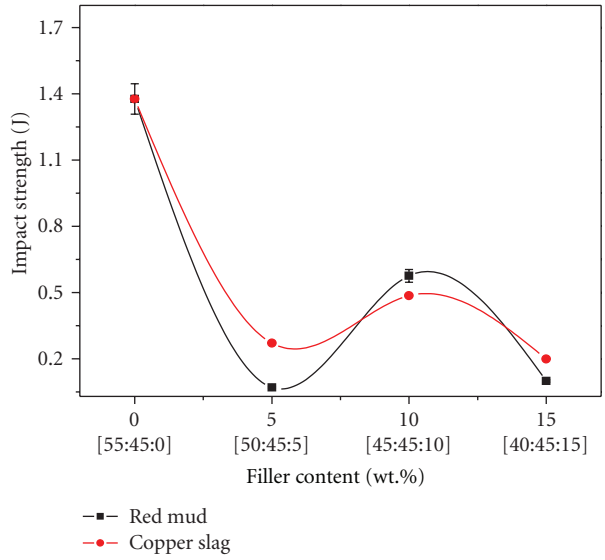

Figure 4: Variation of Impact Strength with red mud and copper slag filler percentage.

the particle cannot carry any load and the composite strength decreases with increasing particle loading [19]. However, for composites containing well-bonded particles, addition of particles to a polymer will lead to an increase in strength of the composites. So due to the good bonding of red mud and copper slag fillers particles with matrix, the tensile strength of all the composites increases with increases in the both the fillers contents.

4.4. Effect of Filler Content on Flexural Strength of Particulate Filled Epoxy-Bamboo Fiber Composites. Figure 3 shows the flexural strength of red mud and copper slag filled epoxy-bamboo fiber composites obtained experimentally from three bend tests.

It is observed that the epoxy-bamboo fiber composites filled with 5 wt.% and 10 wt.% of red mud and copper slag particles have the lower value of flexural strength as compared to the 0 wt.% of red mud and copper slag filled epoxy-bamboo fiber composites, whereas the composite filled with 15 wt.% of red mud and copper slag particles shows the higher value of flexural strength as compared to the 0 wt.% of red mud and copper slag filled bamboo-epoxy composites. This increase in the flexural strength may be related to the presence of red mud and copper slag particulates located at the interface of the fiber and matrix. The reduction in the flexural strengths of the composites with filler content is probably caused by an incompatibility of the particulates and the epoxy matrix, leading to poor interfacial bonding. The lower values of flexural properties may also be attributed to fiber-to-fiber interaction, voids, and dispersion problems. Also it is observed that the cooper slag filled composites show the better flexural strength as compare to the red mud filled bamboo epoxy composites.

4.5. Effect of Filler Content on Impact Strength of Particulate Filled Epoxy-Bamboo Fiber Composites. The ability of a material to resist breaking under a sudden loading or the ability of material to withstand the fracture under the action of high speed stress is known as the impact strength. In the polymer materials, the impact strength is the most widely specified mechanical property [20]. The impact performance of particulate filled fiber-reinforced composites depends on many factors like the nature of the constituent, the filler, fiber, matrix interface, the fabrication, geometry of the composite, and the test conditions. The impact failure of a composite occurs by factors like matrix fracture, and fibre/matrix debonding. The applied load transferred by shear to fibres may exceed the fibre/matrix interfacial bond strength and debonding occurs. When the stress level exceeds the fibre strength, fibre fracture occurs, which involves energy dissipation [21].

Figure 4 shows the impact strength of both the red mud and copper slag filled epoxy-bamboo fiber composites. The value of impact strength shows a reduction with the addition of both the red mud and copper slag in epoxy-bamboo fiber composites. It is seen that with the increase in the both the filler contents, the impact strength of all the composites decreases. Increased filler contents in the matrix resulted in composites becoming stiffer and harder. This will reduce the composite's resilience and toughness and lead to lower impact strength.

5. Conclusions

This study shows that successful fabrication of epoxy-bamboo fiber composites filled with red mud and copper sag particles is possible. Addition of these fillers modifies the physical (density and hardness) and mechanical properties

(tensile, flexural, and impact strength) of the bamboo-epoxy composites. The tensile strength of both the red mud and copper slag filled composites increases with increase in the filler contents, whereas the flexural strength and impact strength of both the filled composites decrease with increase in the fillers filler contents. The micro-hardness and density of the composites are also greatly influenced by the type and content of fillers. In case of micro-hardness, with the addition of copper slag fillers the hardness value of epoxy-bamboo fiber composites increases, whereas with the addition of red mud filler the hardness value decreases with increase in the filler contents. Hence, while fabricating a composite of specific requirements, there is a need for the choice of appropriate filler material and for optimizing its content in the composite system.

Acknowledgment

The corresponding author is grateful to Department of Science and Technology, Govrnment of India for providing the financial support for this research work under the Research Project Ref. no. SR/FT/ET-026/2009.

References

[1] A. K. Bledzki and J. Gassan, "Composites reinforced with cellulose based fibres," *Progress in Polymer Science*, vol. 24, no. 2, pp. 221–274, 1999.

[2] J. Bolton, "The potential of plant fibres as crops for industrial use," *Outlook on Agriculture*, vol. 24, no. 2, pp. 85–89, 1995.

[3] J. Gassan and V. S. Gutowski, "Effects of corona discharge and UV treatment on the properties of jute-fibre expoxy composites," *Composites Science and Technology*, vol. 60, no. 15, pp. 2857–2863, 2000.

[4] H. Belmares, A. Barrera, E. Castillo et al., "New composite materials from natural hard fibres," *Industrial & Engineering Chemistry Product Research and Development*, vol. 20, pp. 555–561, 1981.

[5] C. A. Cruz-Ramos, E. M. Saenz, E. C. Bautista, M. D. Simposium, and N.-D Polimeros, Universidad Nacional Autonoma de Mexico, D.F., vol. 153, 1982.

[6] M. N. Casaurang-Martinez, S. R. Peraza-Sanchez, and C. A. Cruz-Ramos, "Dissolving-grade pulps from henequen fiber," *Cellulose Chemistry and Technology*, vol. 24, pp. 629–683, 1990.

[7] M. N. Cazaurang-Martinez, P. J. Herrera-Franco, P. I. Gonzalez-Chi, and M. Aguilar-Vega, "Physical and mechanical properties of henequen fibers," *Journal of Applied Polymer Science*, vol. 43, no. 4, pp. 749–756, 1991.

[8] S. Jain, R. Kumar, and U. C. Jindal, "Mechanical behaviour of bamboo and bamboo composite," *Journal of Materials Science*, vol. 27, no. 17, pp. 4598–4604, 1992.

[9] S. Varghese, B. Kuriakose, and S. Thomas, "Stress relaxation in short sisal-fiber-reinforced natural rubber composites," *Journal of Applied Polymer Science*, vol. 53, no. 8, pp. 1051–1060, 1994.

[10] G. Ahlblad, A. Kron, and B. Stenberg, "Effects of plasma treatment on mechanical properties of rubber/cellulose fibre composites," *Polymer International*, vol. 33, no. 1, pp. 103–109, 1994.

[11] V. G. Geethamma, R. Joseph, and S. Thomas, "Short coir fiber-reinforced natural rubber composites: effects of fiber length, orientation and alkali treatment," *Journal of Applied Polymer Science*, vol. 55, pp. 583–594, 1995.

[12] S. Jain, U. C. Jindal, and R. Kumar, "Development and fracture mechanism of the bamboo/polyester resin composite," *Journal of Materials Science Letters*, vol. 12, no. 8, pp. 558–560, 1993.

[13] U. C. Jindal, "Development and testing of bamboo fibers reinforced plastic Composites," *Journal of Composite Materials*, vol. 20, no. 1, pp. 19–29, 1986.

[14] H. Takagi and Y. Ichihara, "Effect of fiber length on mechanical properties of "green" composites using a starch-based resin and short bamboo fibers," *JSME International Journal A*, vol. 47, no. 4, pp. 551–555, 2004.

[15] S. Biswas and A. Satapathy, "A comparative study on erosion characteristics of red mud filled bamboo-epoxy and glass-epoxy composites," *Materials and Design*, vol. 31, no. 4, pp. 1752–1767, 2010.

[16] S. Biswas, A. Satapathy, and A. Patnaik, "Effect of ceramic fillers on mechanical properties of bamboo fiber reinforced epoxy composites: a comparative study," *Advanced Materials Research*, vol. 123–125, pp. 1031–1034, 2010.

[17] B. K. Mahapatra, M. B. S. Rao, R. B. Rao, and A. K. Paul, *Characteristics of Red Mud Generated at NALCO Refinery*, Light Metals, Damanjodi, India.

[18] B. D. Agarwal and L. J. Broutman, *Analysis and Performance of Fiber Composites*, John Wiley and Sons, 2nd edition, 1990.

[19] S. Y. Fu, X. Q. Feng, B. Lauke, and Y. W. Mai, "Effects of particle size, particle/matrix interface adhesion and particle loading on mechanical properties of particulate-polymer composites," *Composites Part B*, vol. 39, no. 6, pp. 933–961, 2008.

[20] S. J. Park and J. S. Jin, "Effect of silane coupling agent on interphase and performance of glass fibers/unsaturated polyester composites," *Journal of Colloid and Interface Science*, vol. 242, no. 1, pp. 174–179, 2001.

[21] J. L. Thomason and M. A. Vlung, "The influence of fibre length and concentration on the properties of glass fibre reinforced polypropylene: (7) interface strength and fibre strain in injection moulded long fibre PP at high fibre content," *Composites A*, vol. 28, pp. 277–288, 1997.